Distributed cooperative control for DC microgrids

Sifeddine Benahmed

École doctorale IAEM Lorraine
Commission de mention Automatique, Traitement du Signal et des Images, Génie Informatique
Université de Lorraine

Distributed Cooperative Control for DC Microgrids

THÈSE

présentée et soutenue publiquement le 16 Février 2020

pour l'obtention du

Doctorat de l'Université de Lorraine

Spécialité Automatique, Traitement du Signal et des Images, Génie Informatique

par

Sifeddine BENAHMED

Composition du jury

Rapporteurs :	C. ALONSO	Professeur, Université Toulouse III - Paul Sabatier, LAAS
	M. GHANES	Professeur, Centrale Nantes, LS2N
Examinateurs :	I. PRODAN	Maître de Conf., Institut Polytechnique de Grenoble, LCIS
	P. RIEDINGER	Professeur, Université de Lorraine, CRAN (Directeur de thèse)
	S. PIERFEDERICI	Professeur, Université de Lorraine, LEMTA (Co-directeur de thèse)

Centre de Recherche en Automatique de Nancy
UMR 7039 CNRS – Université de Lorraine
2, avenue de la forêt de Haye 54516 Vandœuvre-lès-Nancy
Tél.+33 (0)3 83 59 59 59 Fax +33 (0)3 83 59 56 44

Contents

List of Figures

Acronyms

MG	- Microgrids.
DC	- Direct Current.
AC	- Alternating Current.
PCC	- Point of Common Coupling.
CS	- Current Sharing.
VR	- Voltage Regulation.
AVR	- Average Voltage Regulation.
SB	- State-of-charge Balancing.
DGU	- Distributed Generation Unit.
SU	- Storage Unit.
HIL	- Hardware-In-the-Loop.
MAS	- Multi-Agent Systems.

List of Symbols

$\mathbb{R}$	-	the set of real numbers.
$\mathbb{R}_{>0}$	-	the set of positive real numbers.
$\otimes$	-	the Kronecker product of two matrices.
$\mathbf{I}_n$	-	identity matrix of the size $(n \times n)$.
A^T	-	transpose of a matrix A.
$\mathbb{1}_n$	-	vector of dimension n with all components equal 1.
$\mathbb{0}_{m\times p}$	-	zero matrix of the size $(m \times p)$.
$\emptyset$	-	empty set.
$\mathcal{K}er(A)$	-	kernel of a matrix A.
$(A)_{[i_1,i_2]\times[j_1,j_2]}$	-	submatrix formed by the entries (i, j) of A between range $i_1 \leq i \leq i_2$ and $j_1 \leq j \leq j_2$.
$(x_1, x_2, \cdots, x_n)$	-	a column vector as an n-tuple whose entries x_i can be also column vectors or equivalently $(x_1, x_2, \cdots, x_n) = \begin{bmatrix} x_1^T & x_2^T & \cdots & x_n^T \end{bmatrix}^T$.
$diag(A_1, ..., A_n)$	-	block diagonal matrix having the matrices A_1 to A_n on the diagonal and 0 every where else.

Résumé en Français

Motivation

Au cours des dernières années, les systèmes électriques traditionnels connaissent une transition rapide vers un nouveau concept appelé *SmartGrids*. En général, un système électrique traditionnel comprend la production, la transmission, la distribution et la consommation où le flux d'énergie est unidirectionnel, des producteurs aux consommateurs. Cependant, ce concept actuel est confronté aux problèmes de pollution de l'environnement en raison de l'utilisation massive de ressources en combustibles fossiles, et l'augmentation constante de la demande d'énergie qui nécessite d'énormes investissements. En outre, l'incertitude de la demande d'énergie est, traditionnellement, gérée en ajustant l'offre. Néanmoins, en raison de l'émergence massive de ressources énergétiques renouvelables de nature volatile et imprévisible, comme les panneaux solaires et les éoliennes, l'incertitude du côté de la production doit également être traitée.

Ces défis, pour lesquels les systèmes électriques existants ne sont plus suffisamment adaptés, conduisent au développement du smartgrid, un paradigme plus flexible, plus écologique et bidirectionnel dans lequel un consommateur peut également être un producteur et vice versa. En outre, ce nouveau concept se caractérise par une vaste intégration des technologies modernes de l'information et de la communication permettant une meilleure coordination entre la production et l'utilisateur final.

Les micro-réseaux (microgrid) représentent l'un des composants clés efficaces et durables des réseaux électriques intelligents. En règle générale, un micro-réseau est un groupe de plusieurs alimentations électriques, systèmes de stockage et charges interconnectés par des lignes électriques. Un microgrid est principalement composées d'unités de production distribuées (DGU), d'unités de stockage (SU), de charges électrique, de

convertisseurs électroniques de puissance et d'unités de contrôle. Les microgrids peuvent être divisés en trois types, à savoir les microgrids à courant continu (DC), à courant alternatif (AC) et les microgrids hybrides DC/AC. Les microgrids DC ont suscité un intérêt croissant au sein des communautés de contrôle automatique et d'ingénierie électrique. Cet intérêt croissant est dû à leur efficacité, leur simplicité et leur large gamme d'applicabilité. En fait, la plupart des systèmes de stockage, des ressources énergétiques renouvelables et des charges modernes, par exemple les ordinateurs portables, les tablettes, les téléphones, etc. sont par nature à courant continu.

Un microgrid peut être situé dans différents endroits, par exemple dans des petites maisons, des quartiers intelligents, des îles, etc. En outre, les microgrids peuvent fonctionner en mode connecté au réseau ou en mode autonome (déconnecté). Cette capacité des microgrid à fonctionner de manière autonome offre la possibilité d'électrifier des zones isolées sans avoir besoin de grandes lignes de transmission.

Les problèmes de commande des Microgrids

Lors de la conception de systèmes de contrôle pour les microgrids DC autonomes, plusieurs défis opérationnels doivent être relevés afin de garantir la fiabilité et les avantages de la génération distribuée. [1]. Dans cette section, nous présentons quelques défis liés aux microgrids DC que nous considérons dans cette thèse.

- **Profil de charge inconnu :** La coordination entre les différentes DGU pour maintenir l'équilibre entre la demande et l'offre est nécessaire pour un fonctionnement économique et résilient des des microgrids DC. Cependant, sous les incertitudes du profil de charge et l'intermittence de plusieurs ressources énergétiques dans le microgrid (par exemple, les panneaux photovoltaïques), l'équilibre entre la demande et l'offre devient plus difficile [2].

- **Problèmes de stabilité:** Un microgrid stable doit être capable de maintenir l'alimentation électrique de la charge sans dynamique indésirable (par exemple, oscillations de tension ou de flux de puissance). Les microgrids DC peuvent être sensibles aux problèmes de stabilité à grand signal et à petit signal. La stabilité des grands signaux fait référence à la capacité du système à résister à des perturbations très importantes, telles que des changements brusques de la demande de puissance ou des défauts dans le système. La stabilité des petits signaux se réfère à la stabilité du système sous de petites perturbations, par exemple le bruit et les changements de paramètres [3].

- **Partage du courant (CS):** Il s'agit d'une caractéristique hautement souhaitable pour le maintien du bon fonctionnement des microgrids. Elle vise à partager, de manière proportionnelle, la demande de courant entre les différents DGU, en tenant compte de leur capacité de puissance. En d'autres termes, les DGU doivent être capables de partager correctement les courants de charge en fonction de leur capacité de génération. De plus, le CS permet d'éviter les situations où un DGU ne peut pas fournir le courant demandé pour sa charge locale et peut être amenée à délivrer au-delà de son courant maximum, ce qui peut détériorer l'unité et causer des dommages au système [4], [5].

- **Régulation de tension moyenne (AVR):** La régulation de la tension est également l'un des paramètres de qualité importants de l'alimentation en courant continu. Une condition nécessaire au bon fonctionnement du microgrid est que les tensions restent proches de leurs valeurs nominales, quelle que soit la perturbation. En effet, une déviation incontrôlée de la tension par rapport à sa référence peut provoquer une défaillance de la charge puisque celle-ci a été conçue pour être alimentée avec une tension de niveau nominal. Réaliser le CS et la régulation de la tension est une tâche ardue et généralement impossible car le CS nécessite une déviation des tensions par rapport à leurs valeurs de référence. Par conséquent, une alternative consiste à fournir une régulation de tension moyenne (AVR), c'est-à-dire que la valeur moyenne des tensions aux points de couplage communc (PCC) est égale à la moyenne de leurs références [6], [7].

- **Equilibrage des états de charge (SB):** Pour un microgrid doté d'unités de stockage (SU), un déséquilibre de l'état de charge entre ces unités peut affecter leur durée de vie en provoquant un phénomène de surcharge ou de surdécharge, une surchauffe, une détérioration, etc. [8]. Lorsque le SB est assuré entre les SU, le SU dont l'état de charge est le plus faible absorbera plus de puissance que les autres pendant le cycle de charge et, par conséquent, celui dont l'état de charge est le plus élevé fournira plus de puissance que les autres pendant le cycle de décharge [9]. Cela permet de prolonger la durée de vie des batteries et de les maintenir dans un bon état de fonctionnement. Notez qu'un équilibrage de l'état de charge est également nécessaire entre les cellules de batterie connectées en série qui composent le SU. Ce dernier est effectué par le système de gestion de la batterie (BMS), qui sort du cadre de ce manuscrit.

Noter que les microgrids peuvent confronter d'autres types de défis qui sortent du cadre de cette thèse, comme les problèmes de cyber-sécurité, d'optimisation des coûts énergétiques, de transition entre les modes de fonctionnement autonomes et connecté, etc.

Techniques de Contrôle des Microgrids

Pour préserver les avantages des microgrids, les défis déjà mentionnés doivent être relevés par des stratégies de contrôle efficaces qui tiennent compte de la complexité du système et exploitent les capteurs et les actionneurs largement distribués. En fonction de leur échelle temporelle, les techniques de contrôle des microgrids peuvent être classées en trois niveaux de contrôle, à savoir le contrôle primaire, secondaire et tertiaire. Dans chacun de ces niveaux, le contrôleur peut être mis en œuvre de manière centralisée, décentralisée et distribuée.

Dans les techniques centralisées, une seule unité centrale contrôle tous les éléments du microgrid. Malgré les avantages de ces techniques en termes d'observabilité et de contrôlabilité élevées, elles présentent de nombreux inconvénients tels que le point de défaillance unique (c'est-à-dire que toute défaillance de l'unité centrale entraîne l'arrêt de l'ensemble du microgrids et la nécessité d'une communication étendue entre le contrôleur central et les unités contrôlées. En outre, la centralisation des données peut poser des problèmes de confidentialité et de sécurité. Par conséquent, cette architecture de contrôle convient aux microgrids de petite taille où les informations à transmettre sont limitées [4].

Dans les techniques décentralisées, les composants du microgrid sont contrôlés par des contrôleurs indépendants sans avoir besoin de communiquer entre eux. Bien que ces techniques présentent une excellente fiabilité et flexibilité, elles souffrent de plusieurs inconvénients tels qu'une mauvaise réponse transitoire et une dépendance à la charge nécessitant un contrôle secondaire. De plus, en raison du fort couplage entre les différents composants du microgrid, un niveau minimum de coordination est nécessaire. Ceci ne peut être atteint en utilisant uniquement des variables locales, ce qui rend impossible une approche entièrement décentralisée.

Les architectures distribuées comprennent un schéma dans lequel chaque élément du microgrid possède son propre contrôleur et échange des informations avec les autres éléments du système via un réseau de communication afin d'atteindre des objectifs communs de manière coopérative. Les stratégies les plus connues de cette technique sont les architectures de contrôle basées sur le consensus et sur les systèmes multi-agents [10], [11]. Ces derniers sont utilisées pour réduire le problème centralisé à plusieurs sous-problèmes locaux. Ainsi, les composants du microgrid peuvent être considérés comme des agents qui interagissent entre eux et appliquent un algorithme de contrôle distribué afin d'atteindre les objectifs globaux souhaités, ce qui apporte plus de flexibilité, d'extensibilité et de fiabilité au microgrid.

Pour revenir aux niveaux de contrôle, le contrôle primaire est la première couche et la plus rapide du schéma

de contrôle hiérarchique [12]. Il se compose de deux parties principales, la première est appelée boucle interne et concerne le contrôle des convertisseurs de puissance (par exemple, les convertisseurs DC/DC) afin de fournir une interface contrôlable entre les charges et les sources [13], [14]. La seconde partie est responsable du contrôle de la tension locale et du courant local. En outre, un partage de courant préliminaire peut également être réalisé à ce niveau.

Le contrôle secondaire, également appelé niveau de gestion, est utilisé pour la gestion de la qualité de l'énergie délivrée aux consommateurs et l'amélioration des objectifs du contrôle primaire [11], [15], [16], [17], [18], [19], [20], [21]. L'implémentation de la commande secondaire peut se faire de manière centralisée [20], [21], de manière distribuée avec un réseau communication complet (c'est-à-dire, deux unités quelconques sont directement connectées) [15], [18] ou avec une communication voisin-voisin seulement (c'est-à-dire un réseau de communication creux) [6], [7], [17], [19], [22], [23].

Le niveau de contrôle tertiaire est le niveau le plus élevé et sa dynamique est la plus lente. Il est utilisé à plusieurs fins : coordination entre plusieurs microgrid, optimisation du coût de l'énergie, coordination avec le gestionnaire du réseau de distribution et la gestion de l'énergie des éléments de stockage à long terme [1], [24], [12].

Objectives et Contributions

L'objectif de ce travail est de développer une nouvelle approche de contrôle distribué aux niveaux primaire et secondaire pour les microgrids DC en mode de fonctionnement autonomes assurant un partage de courant proportionnel entre les unités de production, une régulation de la tension moyenne des lignes et un équilibrage simultané des états de charge des éléments de stockage. La méthodologie de contrôle proposée est basée sur la séparation entre les problèmes du partage du courant et la régulation de la tension moyenne d'une part et le problème de l'équilibrage des état de charge d'autre part ; les principaux outils sont : le consensus dans les systèmes multi-agents, la passivité, la commande par retour d'état, les actions intégrales distribuées, la stabilité de Lyapunov et les inégalités matricielles linéaires, etc.

La nouveauté dans ce travail est l'utilisation de trois actions intégrales distribuées de type consensus pour atteindre *simultanément* les trois objectifs considérés même en cas de perturbations constantes. Nous montrons qu'à l'intérieur de l'ensemble des équilibres, les objectifs de contrôle sont atteints. La preuve de la

Convergence Exponentielle Globale (CEG) vers cet ensemble est fournie, sous l'hypothèse que tous les DGU (respectivement, tous les SU) ont les mêmes valeurs de paramètres physique, malgré la variation inconnue de la charge et les conditions initiales du microgrid et de l'état du contrôleur. De plus, l'équilibrage des état de charge est réalisé en utilisant une stratégie leader-suiveur qui donne la possibilité d'une surveillance de haut niveau (contrôleur tertiaire) en ajustant la référence d'état de charge envoyée au leader. Les contrôleurs n'ont besoin d'aucune information sur la topologie du réseau électrique, ni sur les paramètres et les courants des lignes électriques. La topologie du réseau de communication n'a pas besoin d'être la même que la topologie du microgrid. En outre, l'approche de contrôle proposée est basée sur les inégalités linéaires matricielles, ce qui la rend intéressante sur le plan numérique. En outre, le contrôleur proposé est robuste en cas de perturbations constantes à l'entrée de commande. Enfin, nous fournissons une simulation Matlab/Simulink et des tests Hardware-in-the-Loop (HIL) en temps réel dont les résultats montrent l'efficacité des contrôleurs proposés.

Plan de la thèse

Chapitre 1: Préliminaires

Le chapitre 1 fournit les préliminaires nécessaires aux développements présentés dans cette thèse. Tout d'abord, nous présentons des définitions générales des microgrids et les trois propriétés principales sur lesquelles ils s'appuient, à savoir : l'interconnexion et la distribution, la coopération et la commande et enfin une certaine indépendance du reste du réseau. Puis, nous présentons les différents types de microgrids avec un accent particulier sur les microgrids DC et leurs défis. Ensuite, un aperçu des techniques de contrôle existantes pour surmonter les défis liés aux microgrids DC est donné. Ensuite, nous rappelons quelques définitions de la théorie des graphes et du consensus dans les systèmes multi-agents linéaires. Nous soulignons le fait que plusieurs défis des microgrids DC peuvent être représentés comme des problèmes de consensus des systèmes multi-agents. Enfin, nous rappelons quelques résultats fondamentaux de la stabilité, de la passivité et des techniques d'analyse de stabilité des systèmes à paramètres variants.

Chapitre 2: Commande distribuée pour le partage du courant, la régulation de la tension moyenne et l'équilibrage des états de charge

Ce chapitre contient les principaux résultats théoriques de la thèse. Nous présentons la méthodologie de contrôle proposée pour atteindre les objectives de contrôle considérés pour les microgrids DC composés de DGU, de SU, de lignes électriques résistives-inductives et de charges. Ce chapitre est divisé en quatre parties. Dans la première partie, nous présentons le modèle du microgrid considéré. Ensuite, dans la deuxième partie, nous considérons le problème du CS et de AVR pour un microgrid composé uniquement de DGU, de lignes électriques résistives et de charges. Pour atteindre les objectifs de contrôle, le modèle est augmenté de deux actions intégrales distribuées de type consensus. Un changement de variable est proposé pour transformer le système en plusieurs sous-systèmes découplés (DGU augmenté d'actions intégrales locales). Nous montrons que s'il existe un gain unique de retour d'état qui stabilise les sous-systèmes sous une condition de passivité, la CEG du modèle nominal est assurée. À la fin de cette partie, nous donnons une formulation LMI pour la conception du gain du contrôleur.

Dans la troisième partie, on considère un microgrid composé uniquement de SU avec des lignes électriques et des charges résistives où le problème de SB est étudié. Pour atteindre les objectifs de contrôle, un algorithme de consensus leader-follower est proposé. Les étapes de conception des contrôleurs sont similaires à celles de la partie précédente.

Dans la dernière partie du chapitre, nous montrons que les contrôleurs conçus dans les parties précédentes peuvent être utilisés pour atteindre les trois objectifs de contrôle en même temps pour un microgrid comprenant à la fois des DGU et des SU et même des lignes électriques résistives-inductives.

Le schéma global du contrôleur proposé est illustré dans la Fig. 1. Il se compose de deux modules, le premier module comprend deux actions intégrales distribuées pour garantir le CS et l'AVR. Chaque contrôleur local reçoit la référence de tension V_i^{ref} et, de ses voisins, les courant pondérés (par unité[1]) $\omega_j I_j$ et les variables de commande $\omega_j \gamma_j$. Il génère ensuite deux variables de commande ϕ_i et γ_i. Ces deux variables, avec le courant local I_i et la tension locale V_i, définiront l'état augmenté du DGU i. Ensuite, l'état augmenté est multiplié par un gain de de retour d'état $\mathcal{K}$ pour générer le contrôleur local u_i^d.

Le deuxième module comprend une action intégrale distribuée pour assurer le SB. L'état de charge est estimé localement. Chaque contrôleur local reçoit de ses voisins l'état de charge Soc_j et génère une variable de

[1] les poids ω_i peut être défini comme l'inverse du courant nominal du DGU i

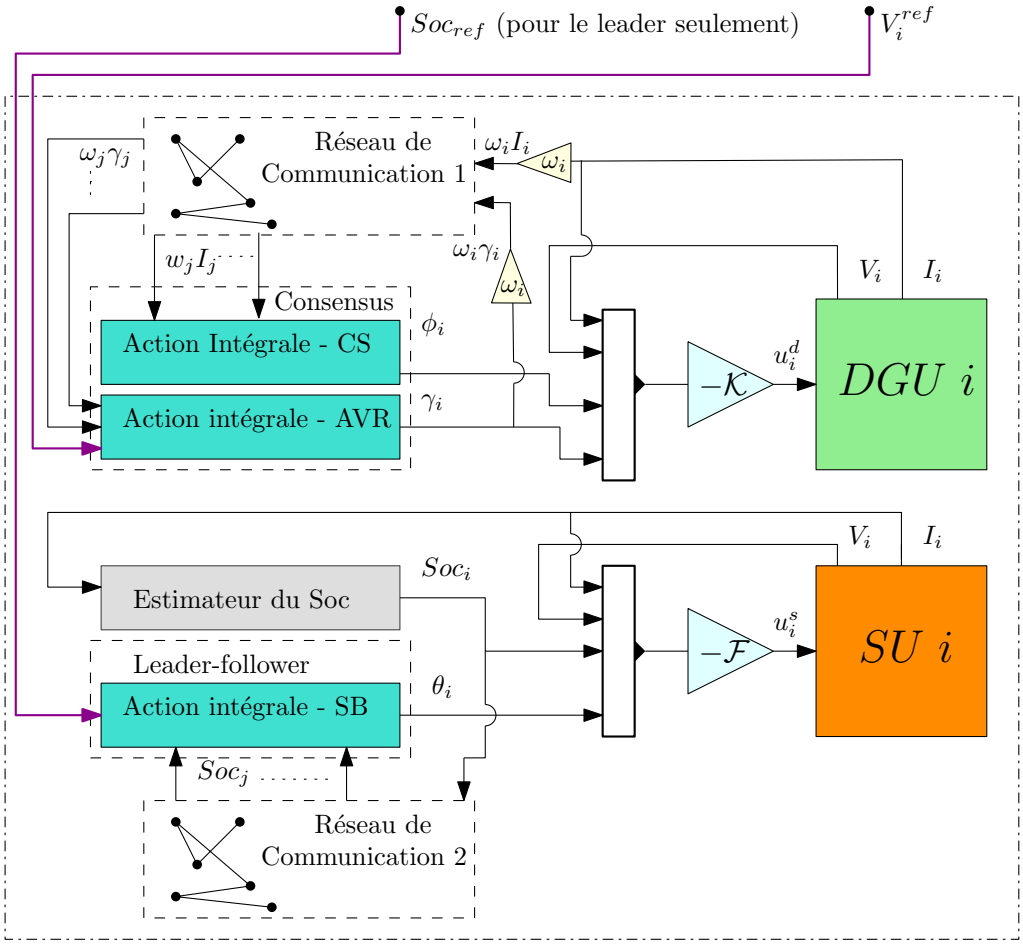

Figure 1: Structure de la commande distribuée proposée.

contrôle θ_i. Il convient de noter que si le SU i est le leader, son contrôleur local recevra également le Soc_{ref} d'un moniteur de haut niveau (par exemple, un contrôleur tertiaire). La variable de contrôle θ_i ainsi que le courant local I_i, la tension V_i et l'état de charge Soc_i définiront l'état augmenté de SU i. Ensuite, l'état augmenté est multiplié par un gain de retour d'état $\mathcal{F}$ pour générer le contrôleur local u_i^s.

Chapitre 3: Étude de Cas: Simulation Matlab et mise en œuvre des tests HIL en temps réel

Dans le chapitre 3, l'approche de commande distribuée proposée au chapitre précédent est évaluée. Le microgrid considéré est composé de trois DGU, trois SU, des lignes électriques résistives-inductives et des charges. Plusieurs scénarios sont envisagés et mis en œuvre dans Matlab/Simulink et dans un plateforme Hardware-In-the-Loop (HIL) en temps réel (Fig. 2).

Les résultats de de chacun de ces scénarios montrent que la méthodologie de contrôle proposée permet un

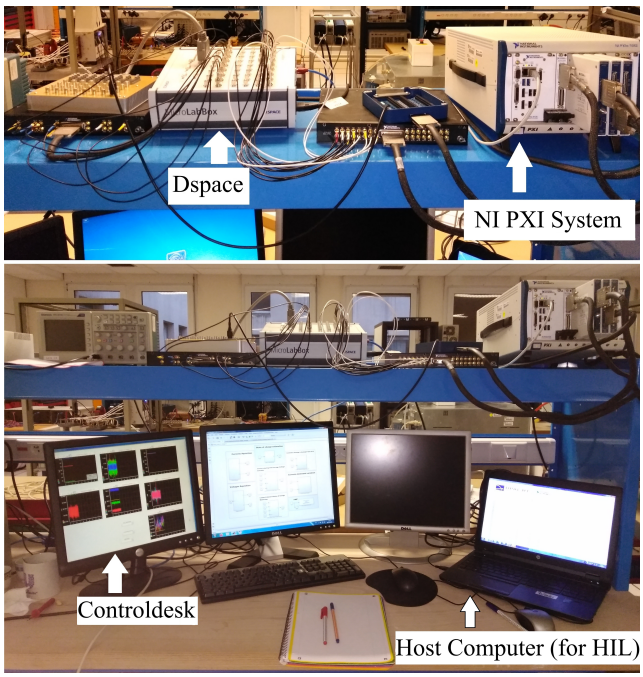

Figure 2: Plateforme expérimentale utilisé pour les tests HIL.

partage précis du courant, une régulation de la tension moyenne et un équilibrage de l'état de charge, même dans le cas de lignes électriques résistives ou résistives-inductives, d'agents ayant des valeurs de paramètres identiques ou différentes, de variations de la demande de courant et des références, etc. Les résultats montrent également que si aucune référence d'état de charge n'est définie par l'utilisateur (ou si le leader perd la référence des états de charge en raison d'un problème de communication), l'état de charge convergera vers la moyenne de leurs valeurs initiales, ce qui offre une plus grande flexibilité pour l'équilibrage de l'état de charge.

Chapitre 4: Conclusion et Perspectives

Dans ce chapitre, nous présentons les conclusions générales de la thèse et nous énonçons ses contributions. En outre, nous proposons diverses extensions possibles du travail de recherche présenté dans cette thèse. Par exemple, cette approche peut être appliquée pour des microgrid AC en considérant une transformation dq et que le microgrid est déjà synchronisés [25]. Même si les tests HIL ont montré que les contrôleurs proposés fonctionnent dans le cas où les DGU et les SU ont des valeurs de paramètres physiques différentes, il pourrait être intéressant de considérer l'assouplissement des hypothèses 2.2 et 2.4 dans la preuve de la convergence globale. Une autre amélioration possible de l'approche de contrôle proposée peut être l'utilisation

d'observateurs pour estimer la valeur de la tension locale ou du courant local plutôt que de la mesurer. Du côté de la charge, il peut être intéressant de considérer les charges à puissance constante (CPL) dans la preuve de convergence globale. La fonctionnalité plug-and-play des microgrids DC avec l'approche proposée peut également être une extension intéressante de ce travail. En ce qui concerne le réseau de communication, d'autres questions peuvent également être considérées comme le retard de transmission, la topologie variante et l'optimisation du coût de communication [26]. Enfin, d'autres tests peuvent être réalisés en appliquant l'approche de contrôle proposée sur un prototype réel de microgrids DC.

Introduction

Nowadays, conventional power systems are undergoing a rapid transition towards a new concept known as *SmartGrids*. Generally, a traditional power system includes generation, transmission, distribution and loads where the flow of energy is unidirectional, from producers to consumers. However, this actual concept faces the problems of environmental pollution because of the massive use of fossil fuel resources, and the ever-increasing energy demand requiring huge investment. Moreover, the uncertainty of energy demand is, traditionally, managed by adjusting the supply. Nevertheless, because of the massive emergence of renewable energy resources of a volatile and unpredictable nature, such as solar panels and wind turbines, the uncertainty on the production side needs to be addressed as well.

These challenges, for which the existing power systems are no longer sufficiently adapted, are leading to the development of smartgrid, a more flexible, eco-friendly and bi-directional paradigm in which a consumer can also be a producer and vice versa. Moreover, this new concept is characterized by the vast integration of modern information and communication technologies allowing for better coordination between the generation and the end user.

Microgrids (MGs) represent one of the efficient and sustainable key components of smartgrids. Generally, a MG is a cluster of several interconnected power supplies, storage systems and loads interconnected through power lines. A MG can be located in different places e.g., small houses, smart neighborhoods, islands, etc. Moreover, MGs can operate in grid-connected mode or in standalone (autonomous) modes. This ability of MGs to operate autonomously gives the possibility to electrify isolated areas with no needs for large transmission lines. However, the issues of stability, energy management, power sharing, voltage regulation, cyber-security, energy cost optimization, etc. are more critical for islanded MGs.

To preserve the advantages of MGs, these challenges should be addressed with effective control strategies that take into account the complexity of the system and exploit the widely distributed sensors and actuators. Because of the single point of failure and the needs for extensive communication, centralized control approaches are no more adapted to the distributed nature of modern power systems. Multi-agent systems can be used to tackle these issues by reducing the centralized problem to several local sub-problems. Hence, the components of the MG can be considered as agents that interact between each other and apply a distributed control algorithm in order to achieve the desired global objectives providing more flexibility, expandability and reliability for the MG.

Furthermore, MGs can be divided into three types, namely Direct Current (DC), Alternating Current (AC), and DC/AC microgrids. DC-MGs have received an increasing interest within the automatic control and electrical engineering communities. This growing interest is due to its efficiency, simplicity and wide range of applicability. In fact, most storage systems, renewable energy resources and modern loads, e.g. laptops, tablets, computers, etc. are inherently DC.

The purpose of the present work is to develop a novel distributed control approach for islanded DC-MGs to *provably* achieve Current Sharing (CS), Average Voltage Regulation (AVR) and State-of-charge Balancing (SCB) *at the same time*. Resolving these issues is critical for the safe and reliable operation of the MG. The proposed control methodology is based on the separation between the CS and AVR problems on one side and the SB problem on the other; the main tools are: consensus in multi-agent systems, passivity, state feedback, distributed integral actions, Lyapunov stability and Linear Matrix Inequalities (LMIs).

Structure of the thesis

The thesis is structured as follows.

Chapter 1. The first chapter presents the concept of Microgrid, its definition, importance and challenges with an overview of the existing control techniques of DC-MGs. It contains a presentation of the concept of consensus in linear multi-agent systems with some mathematical preliminaries required for a good understanding of the manuscript.

Chapter 2. The second chapter presents the theoretical contributions of the thesis where the design of the proposed distributed controllers is detailed. The chapter is divided into four parts. In the first part,

the dynamic model of the studied DC-MG with a meshed topology is presented. The considered power network is composed of Distributed Generation Units (DGUs), Storage Units (SUs), loads and power lines. The second part is dedicated to the problems of CS and AVR for a DC-MG composed of only DGUs with resistive power lines and loads. The third part addresses the problem of SB for a DC-MG that includes only SUs with resistive power lines and loads through a leader-follower approach. The fourth part combines the results in the previous parts to achieve simultaneously CS, AVR, and SB for a DC-MG that includes both DGUs and SUs; first, by considering resistive power lines and then resistive-inductive power lines.

Chapter 3. In the third chapter, a case study is considered, and the proposed control approach is tested in different scenarios with Matlab/Simulink simulations and real-time digital Hardware-In-the-Loop (HIL) experiments.

Chapter 4. The fourth chapter presents the conclusions of the thesis and some suggestions for future research.

ULHyS Project

This thesis is part of Université de Lorraine Hydrogen Sciences and technologies (ULHyS) project, which is one of the impact projects of the Lorraine Université d'Excellence (LUE) initiative. ULHyS aims at reinforcing the excellence of basic and applied research by connecting several actors in the hydrogen sector. It seeks to introduce education programs at master level in energy carrier management focusing specifically on hydrogen. Moreover, ULHyS is composed of 10 laboratories and over 50 researchers presenting a high level in their respective disciplines. ULHyS is organized into 5 interconnected thematic Work-Packages (WPs) to cover the entire supply chain, from hydrogen production methods to the end user, the impact on the local economy and territorial deployment (Fig. 3). This work is part of WP 3 that concerns Microgrids, Multi-source, Multi-vector with a special focus on the control of DC-MGs.

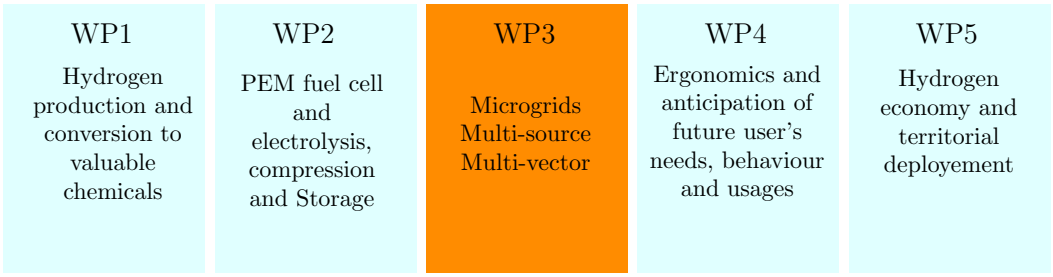

Figure 3: ULHyS work-packages.

Publications

The research carried out during this PhD has inspired and given rise to the following publications

International journal

- S. Benahmed, P. Riedinger, S. Pierfederici. Distributed Control for States-of-charge Balancing, Current sharing and Average Voltage Regulation in DC Microgirds, *IEEE Transactions on Smart Grid* - submitted - under review.

International conferences

- S. Benahmed, P. Riedinger, S. Pierfederici. Distributed Static State feedback control for Current Sharing and Average Voltage Regulation in DC Microgrids. *24th International Symposium on Mathematical Theory of Networks and Systems* (MTNS), 24-28 August 2020, (reported to 2021 because of the pandemic Covid-19), Cambridge, UK - Accepted.
- S. Benahmed, P. Riedinger, S. Pierfederici. Distributed Cooperative Control for DC Microgrids, *International Conference on NETwork Games, Control and Optimisation* (NetGcoop), 18-20 March 2020 (reported to 2021 because of the pandemic Covid-19), Corsica, France - Accepted.

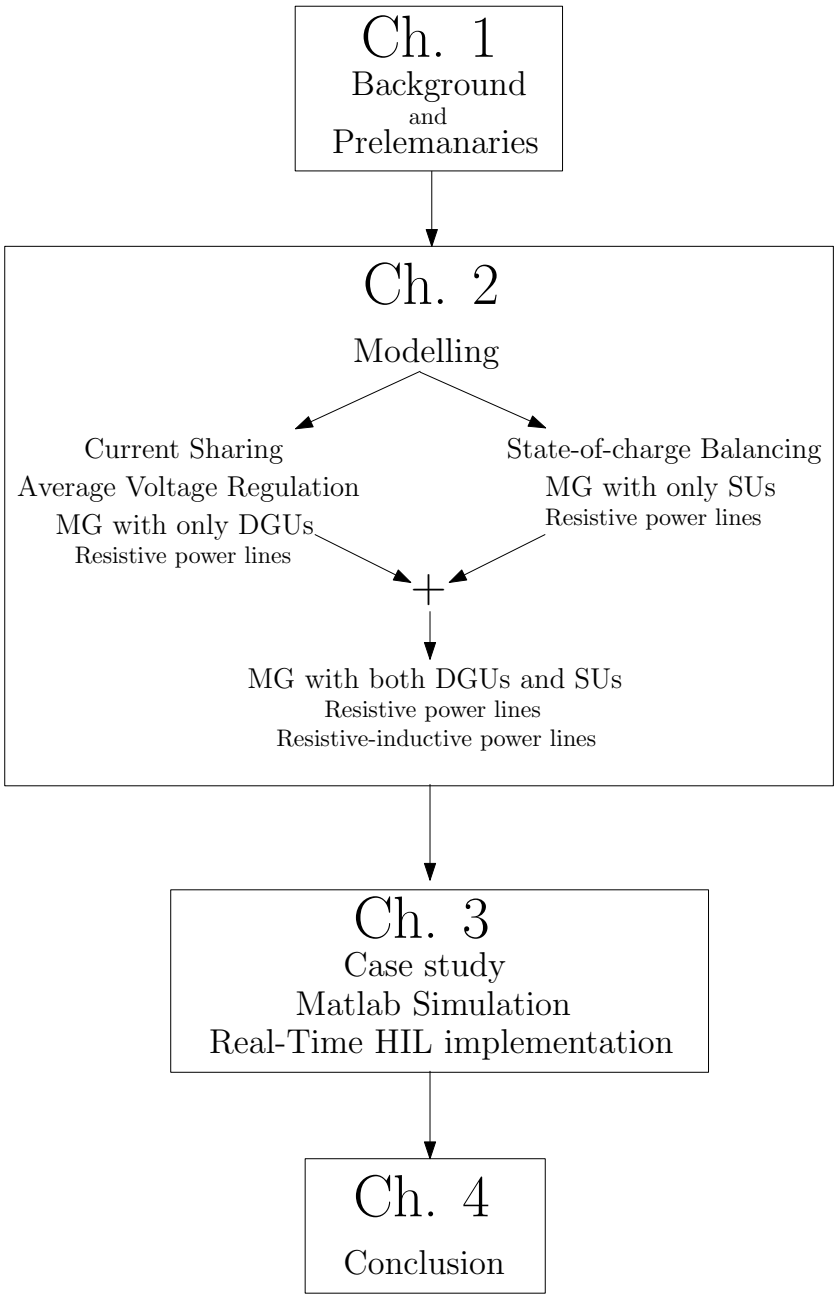

Figure 4: Structure of the thesis.

Chapter 1

Background and Preliminaries

Contents

This chapter provides the preliminaries needed for the further developments presented in this thesis. First, general definitions of Microgrids (MGs) and their concept are provided with a particular focus on Direct Current (DC) MGs and their challenges. Next, an overview of the existing control techniques to overcome the challenges related to DC-MGs is given. Then, we recall some definitions of graph theory and consensus in linear multi-agent systems. In Section 1.5, we emphasize the fact that several challenges in DC-MGs can be represented as consensus problems of multi-agent systems. Finally, some fundamental results of stability, passivity and linear parameter-varying techniques are recalled.

1.1 Microgrids

Several definitions of MGs exist in the literature, one of them is given by the U.S. Department of Energy's Microgrid Initiative

Definition 1.1. **[27]** A microgrid is a group of interconnected loads and distributed energy resources within clearly defined electrical boundaries that acts as a single controllable entity with respect to the grid. A microgrid can connect and disconnect from the grid to enable it to operate in both grid-connected or island mode (Fig. 1.1).

Another definition from [28] and [29] is as follows

Definition 1.2. A microgrid is a cluster of several interconnected power supplies, loads and energy storage system which coordinate between each-other to reliably provide energy, it can be connected to the main-grid or operates independently.

In these two definitions, one can remark that they include three main points:

- interconnection and distribution,
- cooperation and control and
- independence from the main-grid.

These three points make microgrids one of the critical components of modern power systems. Interconnection and distribution properties give the ability to simplify the integration of renewable and eco-friendly

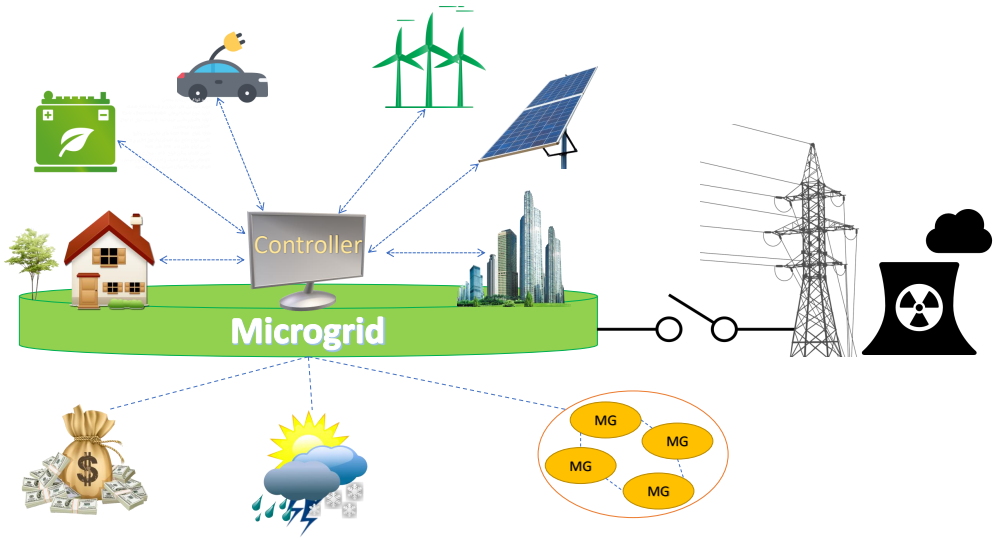

Figure 1.1: Microgrids.

power generation technologies with almost zero emissions. Cooperation between these sources can largely reduce the energy cost per unit and bring a flourishing market that can enhance the local economy and creates more local jobs [30]. Finally, independence from the main-grid allows providing energy for isolated places. A MG can be installed in several places starting from a small building to a smart neighborhood, from urban places to islands and even in elevators, air-crafts and ships [31], [32], [33], [34].

1.1.1 Components

MGs are mainly composed of Distributed Generation Units (DGUs), Storage Units (SUs), loads, power electronic converter and control units.

- DGUs : They can be various types of renewable energy, e.g., fuel cell, photovoltaic (PV) and wind turbines; or thermal energy sources e.g., natural gas or biogas. In this thesis, we consider that the DGU is composed of the energy source with its connection interface to the grid i.e. power-electronic converters, filters, etc.
- SUs: They can provide broad benefits to MGs and include all of the hydrogen, chemical, gravitational, flywheel and heat storage technologies. They can perform multiple functions, e.g., decreasing losses and increasing reliability, providing backup power for the MG and playing a crucial role in cost optimization. Storage can be combined with non-dispatchable renewable energy sources (e.g., wind

turbines and PV panels) to turn them into dispatchable units enabling a large-scale of their integration. SUs are used to maintain power balance between generation and demand, peak-shaving and helping to maintain power quality by contributing additional energy at peak hours and absorbing energy at off-peak hours [35]. Usually, a SU is composed of several battery cells and is connected to the MG through a power-electronics bidirectional interfacing converter.

- Loads: They represent the elements that consume energy in the grid, e.g., single devices, electrical vehicles, lighting, heating system, etc. Some of the loads are controllable allowing to manage the energy demand in the MG [36].

- Power electronic converters: They are used for four types of power conversion, i.e., (1) DC to DC, (2) AC to DC, (3) DC to AC and (4) AC to AC.
  DC to DC converters are used to step-up or step-down a DC voltage (e.g., boost and buck converters). AC to DC converters (e.g., rectifiers) are used to supply DC loads, such as DC motors, using AC power supply. DC to AC conversion is ensured by inverters, it gives the possibility to supply AC loads using DC sources, such as batteries. An example of AC to AC converters is back-to-back converters used to connect wind turbines to the power grid.
  Power electronics converters are mainly composed of linear passive elements such as resistances, inductors and capacitors and nonlinear passive elements (switches) such as diodes, MOSFET, Thyristors, etc. Some of the switches can be controlled (e.g, Thyristors) and others are not (e.g., diodes). The controllable ones represent the control input of the power electronic converters. The switches can be either *on* or *off* and their switching frequency can be very high giving a fast time response for the converter. The use of power electronic converters has enhanced the integration of renewable energy. However, they can cause serious problems notably the injection of harmonics [37], [38].

- Control units: They constitute the control system of the MG components. The control algorithms can be implemented in several electronic solutions as microcontrollers and programmable logic controllers.

1.1.2 Types of Microgrids

MGs can be classified into three types based on the nature of the output voltage fed to the load. There are (i) DC-MG, (ii) AC-MG and (iii) AC/DC hybrid MG.
In AC-MGs, the components are interconnected through AC power lines. DGUs and SUs are connected to the AC power line via an inverter (see Fig. 1.2). Since the components are interconnected via AC power lines, no

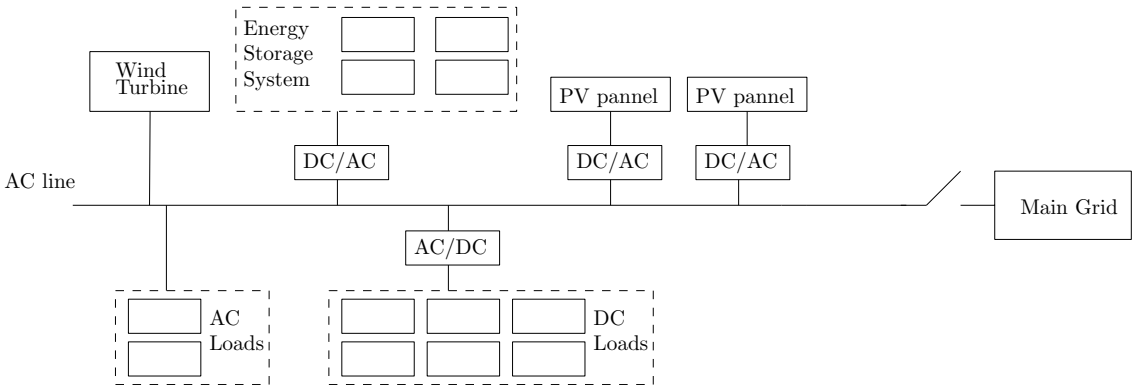

Figure 1.2: Structure of an AC-MG with single power line.

inverter is required to supply AC loads [39]. However, most storage systems, renewable energy resources and modern loads (e.g., laptops, tablets, computers, etc.) are inherently DC requiring more integrated inverters [40], [41].

In DC-MGs, the components are interconnected through DC power lines (see Fig. 1.3). Therefore, DC-MGs are more natural interfaces to many types of renewable energy resources and energy storage systems. They have received increasing interest in the power system control engineering community due to its efficiency, simplicity and a wide range of applicability [42].

In AC/DC hybrid MGs, the components are interconnected through DC and AC power lines. The AC and

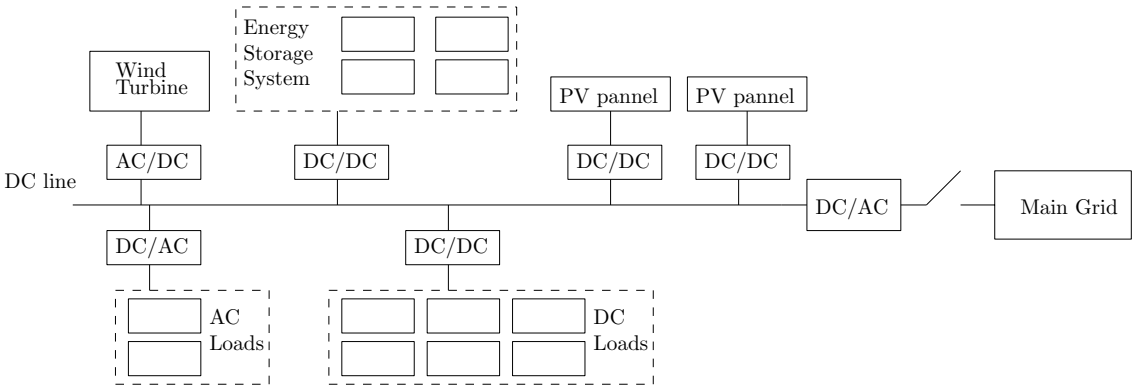

Figure 1.3: Structure of a DC-MG with single power line.

DC lines are linked through AC/DC converter (see Fig. 1.4). Finally, as we can see in Figs. 1.2-1.4, a MG can be disconnected/connected to the main-grid depending of its mode of operation.

In this thesis, we consider a DC-MG composed of DGUs, SUs, power lines and loads.

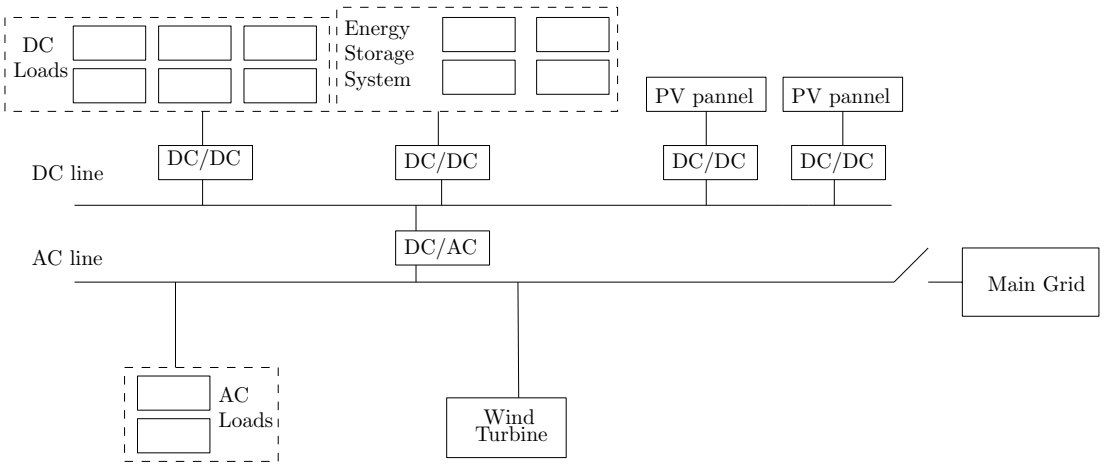

Figure 1.4: Structure of an AC/DC hybrid MG.

1.1.3 Operation Modes

MGs can have two modes of operation either grid-connected or island mode. In Grid-connected operation mode, the MG is connected to the main-grid and can exchange energy with it. The grid-connected mode is further divided into power-matched operation when there is no exchange of energy between the MG and the main-grid and power-mismatched operation when there is an exchange of energy between the MG and the main-grid.

In island mode, the MG is disconnected from the main-grid and operates autonomously. In this mode, the local demand is only supplied by the local generation which is generally small. MGs in island mode have more challenging control issues. In this thesis, we consider a DC-MG operating in island mode.

1.1.4 Examples of Microgrids Project

One of the first villages in Europe to be totally using MG is Hoogkerk, a suburb of the Groningen city in the north of the Netherlands (Fig. 1.5). The Hoogkerk MG includes 25 interconnected houses and is part of the SmartHouse/SmartGrid project (see this Video).

In France, the Grenoble city has already launched several projects for energy self-sufficient districts or buildings such as the LearningGrid project launched by Schneider Electric and the Grenoble CCT[1]. This project was installed on the campus of the industrial school IMT[2] in Grenoble and aims to reduce the campus'

[1] Chambre de Commerce et d'Industrie
[2] Institut des Métiers et Techniques

electrical energy consumption by 30% [43].

Figure 1.5: A smart-district in the Hoogkerk village, the Netherlands [44].

A low-voltage DC-MG project has also been developed in the ADREAM building of the LAAS[3] laboratory in Toulouse, France (Fig. 1.6). The building is 1200 m^2 and includes PV panels, energy storage system, more than 7000 sensors, etc. The objective of this project is to transform the ADERAM building to a net-zero emission one [31].

Figure 1.6: ADREAM building developed in the LAAS-CNRS laboratory [31].

Another example is the Kythnos MG project located in the Kythnos island in the Aegean sea, close to Athens, Grace. The project is part of the European Microgrids program «More microgrids» where the objective was to test centralized and decentralized control strategies in island mode. It is a village-scale autonomous MG, composed of a low-voltage network, solar PV generation, battery storage, a backup generator and power lines supplying 12 houses. Communication cables are used to serve monitoring and control requirements [45].

[3]Laboratoire d'analyse et d'architecture des systèmes

1.2 DC-MG Challenges

When designing control systems for MGs, several operational challenges need to be addressed so as to guarantee the reliability and the benefits of distributed generation [1]. In this section, we will present some DC-MGs challenges where some of them will be studied in this thesis.

- Bi-directional power flows: Initially, distributed generators are designed for unidirectional power flows. However, in DC-MGs, DGUs can operate at low voltage levels. This might cause power flows in the reverse direction and leads to undesirable power flows patterns. Hence, bi-directional power flows in MGs requires new technical strategies, protecting devices and control techniques [1].

- Transition between island and grid-connected operation modes: The ability to operate in both island and grid-connected modes is one of the desirable features of MGs. Fast islanding detection is required to ensure a smooth transition between these two modes and to adjust the control strategy accordingly - since different control strategies might be used for each mode of operation [46].

- Cyber-security: Control system networks implemented for MGs may have cyber vulnerabilities allowing an attacker to jeopardize the confidentiality, stability, or availability of the MG [47], [48].

- Unknown load profile: Coordination between the several DGUs to maintain the balance between demand and supply in DC-MGs is required for the economical and resilient operation of DC-MGs. However, under the uncertainties in the load profile (current demand) and the intermittency of several energy resources in the MG (e.g., PV panels), demand-supply balance becomes more challenging [2].

- Stability issues: A stable DC-MG must be able to maintain the power supply to the load without undesirable dynamics (e.g. voltage or power flow oscillations). DC-MG may be susceptible to large-signal and small-signal stability concerns. Large signal stability refers to the ability of the system to withstand larger disturbances such as step changes in the power demand or faults in the system. Small signal stability refers to the stability of the system under small disturbances, e.g., noise and parameter changes [3].

- Current Sharing (CS): It is a highly desirable feature for maintaining the proper operation of DC-MGs. It aims to share, proportionally, the current demand between the different DGUs, taking into consideration their power capacity. In other words, DGUs must be able to distribute (share) correctly the load currents according to given constants, e.g., their rated currents. Moreover, CS helps to avoid

situations where a DGU cannot provide the requested current for its local load and might be led to deliver beyond its maximum rated current (overloading), which can spoil the unit and cause system damage [4], [5].

- Average Voltage Regulation (AVR): Voltage Regulation is also one of the important quality parameters in DC-MG supply. A necessary condition for proper operation of the MG is that voltages remain close to their nominal values under any perturbation. Indeed, uncontrolled deviation of the voltage from its reference can cause failure to the load device since the latter was designed to be supplied with a nominal level voltage. Achieving CS and voltage regulation is an arduous and generally impossible task as CS requires voltages deviation from their reference values. Therefore, an alternative is to provide an Average Voltage Regulation (AVR), i.e., the average value of voltages at the points of common coupling is equal to the average of their references [6], [7].

- State-of-charge Balancing (SB): For a MG with Storage Units (SUs), unbalanced state-of-charges can affect the life of the batteries by causing over-charge or over-discharge phenomenon, overheating, deterioration, etc. [8]. When the SB is ensured between the SUs, the SU with lower state-of-charge will absorb more power than the others during the charging cycle and accordingly, the one with higher state-of-charge will provide more power than the others during the discharging cycle [9]. This will prolong the batteries' life and maintain them in a good functional state. Note that a state-of-charge balancing is also required between the series-connected battery cells that compose the SU. The latter is performed by the Battery Management System (BMS), which is out of the scope of this manuscript.

In this thesis, the following challenges will be considered: (i) current sharing and (ii) average voltage regulation between the DGUs, (iii) state-of-charge balancing between the SUs, (iv) stability and (v) unknown load profile.

1.3 Literature Review of DC Microgrids Control

To overcome the aforementioned challenges, different control schemes for DC-MG have been proposed in the literature. Generally speaking, they can be categorized into three levels of control (hierarchies): primary, secondary and tertiary control (Fig. 1.7). At each of these levels, the controller can be implemented in several ways, centralized, decentralized and distributed architecture (Fig. 1.8).

In centralized techniques (Fig. 1.8-(a)), a central unit controls all elements of the MG. Despite the advantages of these techniques in terms of high observability and controllability, they suffer from many drawbacks like the single point of failure (i.e., any failure of the central unit will cause the breakdown of the whole MG) and the need for extensive communication between the central controller and the controlled units. Also, data centralization can introduce confidentiality and security issues [49]. Therefore, this control architecture is suitable for small size DC-MGs where the information to be transmitted is limited [4].

In decentralized techniques (Fig. 1.8-(b)), the components of the MG are controlled by independent controllers without the need to communicate with each other. Although these techniques have excellent reliability and flexibility, they suffer from several disadvantages such as poor transient response and load dependence requiring secondary control. Moreover, due to the strong coupling between the different components of the MG, a minimum level of coordination is required. This cannot be achieved by using only local variables, making a fully decentralized approach not possible.

The distributed architectures include a scheme in which, each element of the MG has its own controller and exchanges information with other elements of the grid over a communication network to cooperatively achieve common objectives (Fig. 1.8-(c)). The most known strategies of this technique are consensus-based and agent-based control architectures [10], [11].

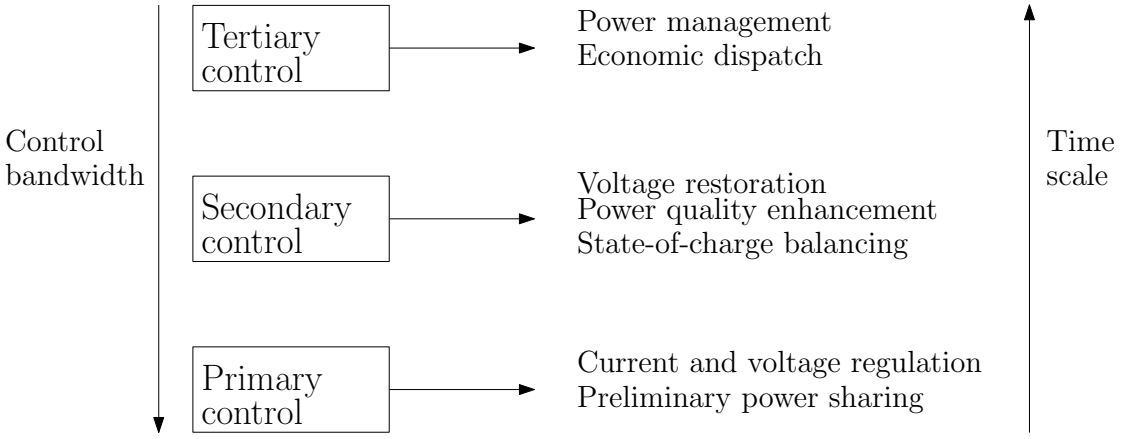

Figure 1.7: Illustration of the DC-MG control hierarchy (inspired from [24]).

Primary control. Going back to the control levels, primary control is the first and fastest layer in the hierarchical control scheme [12]. It consists of two main parts, the first part is called inner-loop and concerns the control of power electronic converters (e.g., DC/DC converters) to provide a controllable interface between loads and sources [13], [14]. The second part is responsible for local voltage and local current control. Moreover, a preliminary CS can also be achieved at this level.

In [50] and [51], a master-slave control approach is used to achieve CS among parallel converter system. In this method, one converter is selected as the master to stabilize the DC bus voltage, while all the other converters become slaves. The master module has both current and voltage loops. However, the slave modules have only the current loop. Then, the output signal of the voltage loop in the master converter is used as a reference for the current loop of all the slave modules so as to reach CS among the slaves and balance the load current. The main disadvantage of this control strategy is the fact that it is less flexible and expandable since it is centralized.

To overcome the drawbacks of the master-slave control, other techniques are used at the primary level such as *droop control*. In droop-controlled DC- MG, the CS is achieved by linearly reducing the local output voltage of the DGU as the local output current increases. This strategy is decentralized since it does not require any communication between the controllers. Even if droop-control has been widely applied on DC power networks [52], [53], [54], it has several limitations. In [55], it is shown that if the power line resistance is not negligible, the efficiency of the droop control is reduced, and the CS accuracy is degraded. To overcome this problem, the value of the droop coefficients can be increased so the power line resistance becomes negligible. However, this approach is not always efficient since for low voltage DC-MG the power lines are mostly resistive and the CS accuracy will still be degraded. Moreover, by increasing the droop coefficient, the voltage deviation will also increase. A detailed explanation of the conventional droop control method and its drawbacks can be found in [53] and Section 2 of [15].

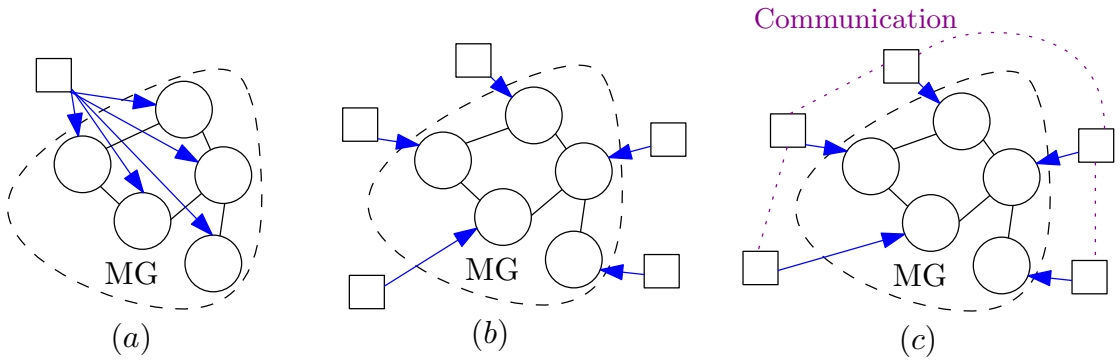

Figure 1.8: Illustration of the three main control architectures in MGs. From the left, centralized, decentralized and distributed control (○ element of the MG and □ controller).

Several modified droop-control characteristics have been proposed in [56], [57], [58] to resolve the trade-off between the accuracy of CS and the voltage deviation. Most of these approaches are based on the idea of

increasing the droop coefficient when load increases to achieve better CS at high-load operation mode and tighter voltage regulation at low-load operation mode. In [58], linear and nonlinear droop characteristics (control laws) are combined, and conditions of switching between them are defined based on the operation mode. The main inconvenience of this technique is when we are near the point of switching between the droop-control laws (i.e., linear and nonlinear characteristics), because of sensor errors, the switch can not take place exactly at the desired point. Hence, one DGU can operate with nonlinear droop-control and another DGU with linear one that will not ensure the accuracy of the CS.
Moreover, [56] presents an investigation of the different nonlinear droop control methods proposed in the literature. Even if the use of nonlinear droop techniques can reduce the impact of the CS accuracy degradation and voltage deviation, the complexity of the MG requires more cooperative techniques.

Secondary control. Also called management level, is used for energy management and enhancing the objectives of primary control [11], [15], [16], [17], [18], [19], [20], [21]. The implementation of the secondary control can be done in a centralized fashion [20], [21], distributed fashion with all-to-all communication (i.e., any two units are directly connected) [15], [18] or with a neighbor-to-neighbor communication (i.e., a sparse communication network) [6], [7], [17], [19], [22], [23].
In [15], a distributed secondary control is proposed where the primary level is ensured by droop control. First, local controllers are implemented for each element of the MG (i.e., DGUs in closed-loop with droop control). Each controller receives information from all the other DGUs using a low bandwidth communication network. Then the output of each local controller is used as a voltage-shifting term to adjust the voltage set-point of the droop mechanism. This helps to reduce the voltage deviation and improve the current sharing accuracy. Even if this approach is distributed (since all the calculations are done locally), the use of an all-to-all communication network still a serious drawback since any failure in a communication link between two units will influence the whole control system.
In [17], a consensus-based [4] approach is proposed where each agent (unit) exchanges information with only its neighbors. Then, the collected information will be used to update the control variables of the agent. Each local controller generates two correction terms that are sent to the droop mechanism. The first term is used to rectify the voltage deviation while the second one is used to ensure the CS accuracy.

SB is also considered in the secondary level [9], [59], [60], [61], [62], [63], [64]. In [9], a centralized technique based on droop control is proposed to balance the state-of-charge where the central controller computes the average of all the state-of-charge and generates a voltage shifting term. This correction term

[4]The consensus techniques will be detailed in Section 1.5.

is then sent to the local droop-control to adjust the voltage setpoint of the interfacing converter of the SUs. In [59], the SB is achieved through a decentralized droop-based method by adjusting the droop coefficient using only the local state-of-charge. However, only the discharge operation mode was taken into account. In [60], a similar approach is proposed but this time, both charge and discharge process were considered. In [62], a consensus-based observer is proposed to estimate the average of the state-of-charge. Then, the difference between the local state-of-charge and the average one is sent to the local control. The output of the latter is used as a voltage shifting term that will be added to the local droop control to balance the state-of-charge. Even if this control paradigm uses a sparse communication network for data exchange, the global convergence is not proved. In fact, stability is analyzed through a centralized method, i.e., the root locus.

In [7], [22], [65], only voltage stabilization is taken into account but with proof of global stability. In [23], a sliding-mode approach is proposed by designing a manifold that couples CS and AVR with global stability assurance. However, proper initialization of the controller is needed. In [6], a control approach, in an ad-hoc manner, is proposed with global convergence independently of the MG parameters and the initial conditions but only CS and AVR were considered.

Tertiary control. Also known as the grid level control, is the highest level in the control hierarchy and has the slowest dynamics. It is used for several purposes: coordination and optimal operation between several MGs (cluster of MGs), to carry out the power flow in grid-connected mode, optimization of the system efficiency such as optimal pricing, coordination with the distribution system operator and long-term energy storage management [1], [24], [12].

1.3.1 Contribution of the thesis

- In this thesis, we propose a new distributed control methodology in the primary and the secondary levels for a more general DC-MG model including not only DGUs but also SUs interconnected through *resistive-inductive* power lines, and where the control objectives are CS, AVR and SB.

- The novelty in this work is the use of three consensus-like distributed integral actions to achieve *simultaneously* the three aforementioned objectives. We show that inside the set of equilibria, SCB, CS and AVR objectives are achieved. The proof of the *global exponential convergence* to this set is provided despite the unknown variation of the load and the initial conditions of the MG and the controller state.

- The consensus algorithm that we propose to achieve AVR at the equilibrium is a new modified version

of [66] and its dynamics are considered in the proof of convergence, which is not the case in [61] where the consensus algorithm used to compute the average voltage is assumed to converge for a voltage step variation.

- Also, the SB is achieved using a leader-follower strategy that gives the ability for high-level monitoring by adjusting the state-of-charge reference sent to the leader.
- The controllers do not need any information about the topology of the power network, neither the parameters and currents of the power lines. The topology of the communication network does not need to be the same as the topology of the DC-MG.
- Furthermore, the proposed control approach is LMI-based, which makes it attractive numerically.
- Finally, we provide Matlab/Simulink simulation and real-time Hardware-in-the-loop (HIL) implementation tests where the results show the effectiveness of the proposed controllers.

In the next part of this chapter, we will recall fundamental definitions and results of some mathematical tools needed for the modeling and control of DC-MGs.

1.4 Graph Theory

Usually, graph theory is used to describe the structural properties (topology) of a network. It gives an abstraction of how the information is exchanged between agents in a network. This high-level description is done in terms of objects referred to as vertices and edges. In this section, we recall some definitions and properties from [67] and [68].

A finite graph $\mathcal{G}$ is composed of a finite set of elements that we call the *vertex set* and denote it by $\mathcal{V}$. The vertices represent the elements of the graph; the set $\mathcal{V}$ can be represented as

$$\mathcal{V} = \{1, 2, \cdots, n\}.$$

The interconnection between the vertices is described by a subset of $\mathcal{V} \times \mathcal{V}$ called the edges set; denoted by $\mathcal{E}$.

Definition 1.3. (Neighborhood) The neighborhood $\mathcal{N}_i \subseteq \mathcal{V}$ of the vertex i is defined by the set $\{j \in \mathcal{V} \mid (i, j) \in \mathcal{E}\}$.

Definition 1.4. (Undirected Graph) A graph $\mathcal{G}$ is undirected if for all $i,\ j \in \mathcal{V}$,

$$(i,j) \in \mathcal{E} \implies (j,i) \in \mathcal{E}.$$

Otherwise the graph is directed.

Remark 1.1. All the graphs considered in this thesis are assumed to be without self loops, i.e., $(i,i) \notin \mathcal{E}$

Example 1.1. Fig. 1.9 shows an example of a graph where the vertex set is $\mathcal{V} = \{1,2,3,4,5\}$ and the adjacency set is $\mathcal{E} = \{(1,2),(1,3),(2,3),(2,4),(2,5)\}$.

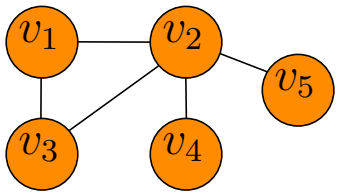

Figure 1.9: Example of an undirected graph with 5 vertices and 5 edges.

Two vertices are neighbors (adjacent) if there is at least one edge between them.

Definition 1.5. (Connected Graph) A graph $\mathcal{G}$ is *connected* if for every pair of vertices there is a sequence of distinct vertices $i_0, \cdots, i_m$ that relate it such that for $k = 0, 1, \cdots, m-1$, the vertices i_k and i_{k+1} are adjacent; if not, the graph $\mathcal{G}$ is *disconnected*.

For example the graph in Fig. 1.9 is connected and the graph in Fig. 1.10 is disconnected.

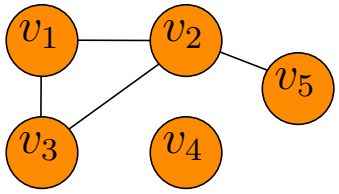

Figure 1.10: Example of an undirected graph with 5 vertices and 5 edges.

Graphs can be presented not only by graphical representation but also using matrices. For an undirected graph $\mathcal{G}$, the degree of a given vertex $i \in \mathcal{V}$ is the cardinality of the neighborhood set $\mathcal{N}_i$, that is, it is equal to the number of vertices that are adjacent to the vertex i. Thus, for the graph in Fig. 1.9, the degrees of the

vertices are

$$d(1) = 2,\ d(2) = 4,\ d(3) = 2,\ d(4) = 1,\ d(5) = 1.$$

Definition 1.6. (Degree Matrix) The degree matrix $\mathcal{D} \in \mathbb{R}^{n\times n}$ of a graph $\mathcal{G}$ with n vertices, is the diagonal matrix, containing the vertex-degrees of $\mathcal{G}$ on the diagonal, that is,

$$\mathcal{D} = \begin{pmatrix} d(1) & 0 & \cdots & 0 \\ 0 & d(2) & \cdots & 0 \\ \vdots & \vdots & \ddots & \vdots \\ 0 & 0 & \cdots & d(n) \end{pmatrix}. \tag{1.1}$$

For example the degree matrix of the graph in Fig. 1.9 is

$$\mathcal{D} = \begin{pmatrix} 2 & 0 & 0 & 0 & 0 \\ 0 & 4 & 0 & 0 & 0 \\ 0 & 0 & 2 & 0 & 0 \\ 0 & 0 & 0 & 1 & 0 \\ 0 & 0 & 0 & 0 & 1 \end{pmatrix}. \tag{1.2}$$

Definition 1.7. (Adjacency Matrix) The adjacency matrix $\mathcal{A} \in \mathbb{R}^{n\times n}$ is the symmetric matrix encoding the adjacency relationship in the graph $\mathcal{G}$, that is,

$$\mathcal{A}_{ij} = \begin{cases} 1 & if\ (i,j) \in \mathcal{E}, \\ 0 & otherwise. \end{cases} \tag{1.3}$$

Going back to the example in Fig. 1.9, the corresponding adjacency matrix is

$$\mathcal{A} = \begin{pmatrix} 0 & 1 & 1 & 0 & 0 \\ 1 & 0 & 1 & 1 & 1 \\ 1 & 1 & 0 & 0 & 0 \\ 0 & 1 & 0 & 0 & 0 \\ 0 & 1 & 0 & 0 & 0 \end{pmatrix}. \tag{1.4}$$

Definition 1.8. (Graph Laplacian Matrix) An important matrix representation of a graph is the *graph*

Laplacian matrix $\mathcal{L}$ defined as

$$\mathcal{L} = \mathcal{D} - \mathcal{A}. \tag{1.5}$$

The laplcian matrix of the graph in Fig. 1.9 is

$$\mathcal{L} = \begin{pmatrix} 2 & -1 & -1 & 0 & 0 \\ -1 & 4 & -1 & -1 & -1 \\ -1 & -1 & 2 & 0 & 0 \\ 0 & -1 & 0 & 1 & 0 \\ 0 & -1 & 0 & 0 & 1 \end{pmatrix}. \tag{1.6}$$

Remark 1.2. Let $\mathbb{1} \in \mathbb{R}^{n\times 1}$ be the vector of all ones, i.e.,

$$\mathbb{1} = \begin{bmatrix} 1 \\ \vdots \\ 1 \end{bmatrix}.$$

Note that by construction, for every connected undirected graph $\mathcal{G}$, the vector of all ones is the eigenvector associated with the zero eigenvalue of $\mathcal{L}$, i.e.:

$$\mathbb{1} \in Ker(\mathcal{L}). \tag{1.7}$$

Now we can define a graph as

Definition 1.9. (Graph) A graph is a triple $(\mathcal{V}, \mathcal{E}, \mathcal{L})$, where $\mathcal{V} = \{1, 2, ..., n\}$ is the node set, $\mathcal{E} \subseteq \mathcal{V} \times \mathcal{V}$ is the edge set and $\mathcal{L} \in \mathbb{R}^{n\times n}$ is the Laplacian matrix.

Remark 1.3. The following properties will be used in the rest of the thesis:

- The Laplacian matrix of an undirected graph is symmetric and positive semidefinite. Thus, its eigenvalues are real and can be ordered as follows:

$$\lambda_1(\mathcal{L}) = 0 \leq \lambda_2(\mathcal{L}) \leq \cdots \leq \lambda_n(\mathcal{L}). \tag{1.8}$$

- The graph $\mathcal{G}$ is connected if and only if $\lambda_2(\mathcal{L}) > 0$.

- If for a given $X \in \mathbb{R}^n$, we have $\mathcal{L}X = 0$, implies $X = \alpha \mathbb{1}_n$, with $\alpha \in \mathbb{R}$.
- There exists an orthonormal matrix $T \in \mathbb{R}^{n \times n}$ that verifies $T^\top T = TT^\top = \mathbf{I}_n$ such that:

$$T^\top L T = diag(\lambda_1(\mathcal{L}), \lambda_2(\mathcal{L}), \cdots, \lambda_n(\mathcal{L})).$$

1.5 Consensus in Linear Multi-Agent Systems

A Multi-Agent System (MAS) consists of a set of dynamical systems that we call agents, interacting with each other to form a network. Agents can have the same dynamical system (i.e., homogeneous MAS) or a possibly different one to another (i.e., heterogeneous MAS). Several problems and approaches of MAS are inspired by nature e.g., flocking of birds, schooling of fishes, the swarm of bacteria, etc. (see Fig. 1.11),[5] and have many applications in several fields as in MGs [69].

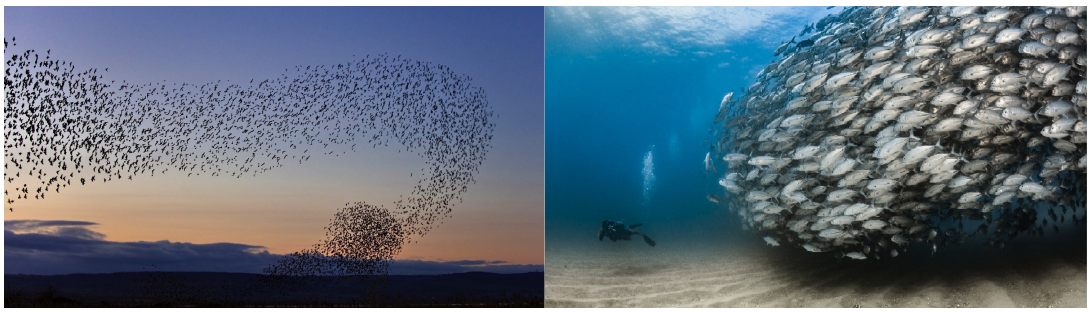

Figure 1.11: Collective behaviours of animals, from the left: flocking of birds and schooling of fishes [70].

MAS has become an essential tool for understanding inter-elemental interactions in MGs. Indeed, DGUs and SUs can be considered as agents that interact with each other through physical coupling (power lines). Moreover, due to the distributed nature of the generation in MGs, agents (DGUs or SUs) could have a partial representation of the power network, e.g., a SU knows only its state-of-charge and may receive information about the state-of-charge of some other SUs, but it does not know what is happening in the whole network. Therefore, several decisions can be made locally and coordination between the agents is needed to achieve an agreement regarding a certain quantity of interest, i.e., *a consensus*. This requires a certain level of autonomy for the agents and a certain rule of interaction that specifies how information is exchanged between the agents, i.e., *a consensus algorithm*. The latter introduces another type of interaction, the soft coupling

[5] For more examples, with animation, about the collective behavior in nature and its application, the reader is invited to see the following videos: Video 1, and Video 2)

(communication links), making the analysis of the system more complicated [71].

Our interest here is to present the formulation of some consensus problems of MAS. This will be useful when formulating the considered control problems in Chapter 2. Moreover, we aim to highlight the difficulties associated with the analysis of stability and the design of distributed control laws for DC-MGs.

The most commonly used models to study MAS are decoupled single integrator and double integrator models [72]. However, in DC-MGs, agents may be governed by more commonly coupled inherent linear dynamics. Consider a physical linear MAS represented by a connected and undirected graph $\mathcal{G}^{phy} = (\mathcal{V}, \mathcal{E}^{phy}, \mathcal{L}^{phy})$ composed of N linear systems interconnected with static physical coupling of the form:

$$\begin{aligned} \dot{x}_i &= Ax_i + B_u u_i - B_z \sum_{j \in \mathcal{N}_i^{phy}} \alpha_{ij}(z_i - z_j), \\ z_i &= Mx_i, \end{aligned} \tag{1.9}$$

with $x_i \in \mathbb{R}^n$,$u_i \in \mathbb{R}^m$, $z_i \in \mathbb{R}^q$, $\alpha_{ij} \in \mathbb{R}$ and A, B_u, B_z, M are matrices of appropriate dimensions and $\mathcal{N}_i^{phy}$ is the set of neighbors of the agent i with respect to $\mathcal{G}^{phy}$. The term $B_z \sum_{j \in \mathcal{N}_i^{phy}} \alpha_{ij}(z_i - z_j)$ represents the physical coupling between the agents.

Let us consider that there exist certain output variables of interest for which the agents wants to reach an agreement. These variables can be defined as follows

$$y_i = Cx_i, \ i \in \mathcal{V}, \tag{1.10}$$

for simplicity we consider y_i as scalar i.e., $y_i \in \mathbb{R}$ and $C \in \mathbb{R}^{1 \times n}$.

Let us assume that agents can exchange the value of the variable of interest through a communication network represented by a connected and undirected graph $\mathcal{G}^{com} = (\mathcal{V}, \mathcal{E}^{com}, \mathcal{L}^{com})$ whose topology is not necessarily the same as that of the physical network, i.e. $\mathcal{L}^{com} \neq \mathcal{L}^{phy}$ (e.g., Fig. 1.12). Let $\mathcal{N}_i^{com}$ be the set of neighbors of agent i with respect to $\mathcal{G}^{com}$. Each agent $i \in \mathcal{V}$ receives the following measurements:

- Internal state measurement x_i.
- External state measurements (relative to other agents) $y_j, \ j \in \mathcal{N}_i^c$.

Agents can achieve several types of agreement on the output variables of interest (1.10) such as, weighted output consensus, leader-follower consensus and output averaging.

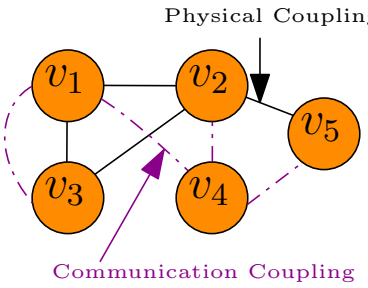

Figure 1.12: An illustration of MAS with physical and communication coupling.

1.5.1 Weighted Output Consensus Problem

Before presenting the weighted output consensus problem, we need to recall the following definitions

Definition 1.10. (Invariant set) A set $\Omega \subseteq \mathbb{R}^n$ is invariant, with respect to a dynamical system $\dot{x} = f(x)$, if for every trajectory x,

$$x(t) \in \Omega \implies x(\tau) \in \Omega \; for \; all \; \tau \geq t. \tag{1.11}$$

Definition 1.11. (Convergence to a set) If $d(x, y)$ denotes a distance in a metric space, the distance of a point x to a set S is defined by:

$$d(x, S) = \inf_{y \in S} d(x, y).$$

A trajectory $x(\cdot)$ is said to converge asymptotically to a set S if

$$\lim_{t \to +\infty} d(x(t), S) = 0.$$

Let us associate to each agent i a weight parameter $\omega_i \in \mathbb{R}_{>0}$. The weighted output consensus of MAS (1.9) means designing a distributed control laws $u_i, \; i \in \mathcal{V}$, (i.e., a consensus algorithm) based on the local information obtained by each agent, such that all the agents reach an agreement on the output variables of interest (1.10) by negotiating with their neighbors. For DC-MGs, these variables might represent currents.

Definition 1.12. (Weighted output consensus) The state of system (1.9) converges to a weighted output consensus if it converges to an invariant set $\mathcal{A}$ (the agreement set) with reference to (1.9), defined equivalently as

- $\mathcal{A} = \{y = (y_1, \cdots, y_N) \in \mathbb{R}^N : \omega_i y_i = \omega_j y_j, \forall (i, j) \in \mathcal{V} \times \mathcal{V}\}$.
- $\mathcal{A} = \{y = (y_1, \cdots, y_N) \in \mathbb{R}^N : \mathcal{L}^{com} W y = 0, W = diag(\omega_1, \cdots, \omega_N).\}$

- $\mathcal{A} = \{y = (y_1, \cdots, y_N) \in \mathbb{R}^N : y = \beta W^{-1}\mathbb{1}_N, \beta \in \mathbb{R}\}$.

Remark 1.4. The weights $\omega_i,\ i \in \mathcal{V}$ in Definitions 1.12 and 1.14 can be used to give to some agents more influence (weight) on the result of the agreement than other agents in the same graph. In the context of DC-MGs, the weights can be related to the generation capacity or rated current of the DGUs .

1.5.2 Leader-follower Consensus Problem

The leader-follower consensus of the MAS (1.9) means to design a distributed control laws $u_i,\ i \in \mathcal{V}$, (i.e., a leader-follower algorithm) based on the local information obtained by each agent, such that the values of the output variables of interest (1.10) converge to a common value defined by one agent (called leader) by negotiating with their neighbors. For DC-MGs, these variables might represent the state-of-charge.

Definition 1.13. (Leader-follower consensus problem) The state of system (1.9) converges to a leader-follower consensus if it converges to an invariant set $\mathcal{A}$ with reference to (1.9), defined equivalently as

- $\mathcal{A} = \{y = (y_1, \cdots, y_N) \in \mathbb{R}^N : y_i = y_j = y_{i_l}, \forall (i,j) \in \mathcal{V} \times \mathcal{V},\ i_l \text{ is the index of the leader}\}$.
- $\mathcal{A} = \{y = (y_1, \cdots, y_N) \in \mathbb{R}^N : y = y_{i_l}\mathbb{1}_N\}$.

1.5.3 Output Averaging Problem

Consider that each output variable of interest (1.10) has its reference y_{ref_i} for which we associate a weight parameter $\omega_i \in \mathbb{R}_{>0}$. The output averaging consensus problem of the MAS (1.9) means to design a distributed control laws $u_i,\ i \in \mathcal{V}$, (i.e., an output averaging algorithm) based on the local information obtained by each agent, such that the weighted average value of the output variables of interest (1.10) of all the agents converge to the weighted average value of their references by negotiating with their neighbors. For a MG, these variables might represent the voltages at the points of common coupling.

Definition 1.14. (Output averaging problem) The output averaging problem of system (1.9) is solved if the state of the system converges to an invariant set $\mathcal{A}$ with reference to (1.9), defined equivalently as

- $\mathcal{A} = \{y = (y_1, \cdots, y_N) \in \mathbb{R}^N : \frac{1}{N}\sum_{i\in\mathcal{V}} \omega_i y_i = \frac{1}{N}\sum_{i\in\mathcal{V}} \omega_i y_i^{ref},\ \forall (i,j) \in \mathcal{V} \times \mathcal{V}\}$.
- $\mathcal{A} = \{y = (y_1, \cdots, y_N) \in \mathbb{R}^N : \mathbb{1}_N^\top W y = \mathbb{1}_N^\top W y_{ref_i},\ W = diag(\omega_1, \cdots, \omega_N)\}$.

To summarize this part of the chapter, several objectives in DC-MGs can be formulated as a weighted output consensus problem, leader-follower problem and output averaging problem. Among the difficulties when controlling a DC-MG in a distributed fashion and analyzing its stability are the existence of physical coupling (power lines) and the availability of only partial information (no agent has access to the overall state of the MG).

1.6 Stability and Passivity of Interconnected Linear Systems

In this section, some basic definitions of stability of Linear Time-Invariant (LTI) systems are presented. Moreover, we provide two application examples to show how Linear Parameter-Varying (LPV) techniques and passivity are useful for the stability analysis of linear MAS.

1.6.1 Lyapunov Stability

When studying the properties of a dynamical control system, one of the important questions is whether the system is stable or not. The most useful method for studying the stability of a control system is the theory introduced by the russian mathematician and engineer *Alexandr Mikhailovich Lyapunov* in the late 19th century [73], [74].
Consider the following autonomous LTI system:

$$\dot{x}(t) = Ax(t). \tag{1.12}$$

We call x^e an equilibrium point of (1.12) if $Ax^e = 0$. The stability (in the sense of Lyapunov) means that solutions that start nearby an equilibrium point remain close enough to it. Moreover, an equilibrium point is unstable if it is not stable.

Definition 1.15. An equilibrium point x^e of system (1.12) is said to be stable if for all $\epsilon > 0$, there exists $\delta > 0$, such that

$$||x(0) - x^e|| < \delta \implies ||x(t) - x^e|| < \epsilon, \ \ \forall t > 0.$$

Asymptotic stability means that solutions that start close enough to equilibrium point not only remain close enough but also eventually converge to it.

Definition 1.16. x^e is asymptotically stable, if it is stable and there exists $\delta > 0$, such that

$$||x(0) - x^e|| < \delta \implies \lim_{t \to +\infty} x(t) = x^e.$$

Exponential stability is a form of asymptotic stability which requires an exponential rate of convergence.

Definition 1.17. x^e is exponentially stable if there exist three positive real constants $\alpha,\ \beta$ and γ such that

$$||x(0) - x^e|| \leq \alpha,\ ||x(t) - x^e|| \leq \beta ||x(0) - x^e|| e^{-\gamma t}.$$

Definitions 1.15-1.17 give information about local stability, i.e., when the system starts nearby its equilibrium point. The following definition gives information in the case where the trajectory of the system can start from any point in $\mathbb{R}^n$.

Definition 1.18. (Global stability) x^e is globally asymptotically (exponentially) stable if it is stable and for any initial condition $x(0) \in \mathbb{R}^n$,

$$\lim_{t \to +\infty} x(t) = x^e,\ (\exists \beta, \gamma \in \mathbb{R}_{>0},\ ||x(t) - x^e|| \leq \beta ||x(0) - x^e|| e^{-\gamma t},\ \forall t > 0).$$

The stability of an equilibrium point can be ascertained by testing the rate of change of the system's energy, i.e. if the total energy of the system is continuously dissipating, then the system tends to return to its equilibrium. Lyapunov's direct method is a generalization of this idea. It gives sufficient conditions for the stability of an equilibrium point by constructing an "energy-like" scalar function for the system and examining its time variation [73].

Note that by shifting the origin of system (1.12), we can assume that the equilibrium point of interest occurs at $x^e = 0$. If several equilibrium points exist, one needs to analyze the stability of each of them by appropriately shifting the origin.

Theorem 1. *Consider system* (1.12) *with* $x^e = 0$ *as equilibrium point and* $V(x) : x \in \mathbb{R}^n \to \mathbb{R}$ *a scalar function called Lyapunov function.*

- x^e *is stable if* $V(x)$ *is positive definite and* $-\dot{V}(x)$ *is positive semidefinite*[6].

[6] See Definition A.2 in the appendix for the definition of positive and positive semidefinite functions.

- *x^e is asymptotically stable if $V(x)$ is positive definite and $-\dot{V}(x)$ is positive definite.*

It is noteworthy that one can look at $V(x)$ as a generalized energy function and $-\dot{V}(x)$ as the corresponding generalized dissipation function.

Remark 1.5. The notions of exponential and asymptotic stability are equivalent for linear time-invariant systems.

Usually, for an LTI system, a standard Lyapunov function candidate is the quadratic function of its state, e.g., $V(x) = x^\top Px$ where P is a symmetric positive definite matrix.

Theorem 2. *The equilibrium point x^e of system (1.12) is asymptotically stable if and only if, for all $Q = Q^\top > 0$, there exists a matrix $P = P^\top > 0$ such that*

$$A^\top P + PA + Q \leq 0. \tag{1.13}$$

Equation (1.13) is called Lyapunov equation.

The analysis of stability becomes more challenging when considering systems with nonlinear dynamics such as LPV systems.

1.6.2 Stability of Linear Parameter-Varying System

Consider an autonomous LPV system [75]:

$$\dot{x} = A(\theta)x, \tag{1.14}$$

where the matrix A depends on the vector of the varying parameters $\theta = [\theta_1, \cdots, \theta_k]$, with

$$\underline{\theta_i} \leq \theta_i \leq \bar{\theta}_i, \quad 1 \leq i \leq k. \tag{1.15}$$

Generally, when no information is given about the dependence of the matrix A on θ, the condition of stability in Theorem 2 should be verified for each value of the parameters θ_i, $1 \leq i \leq k$, which results an infinite number of LMI to verify.

A polytop is a convex[7] set limited by a finite number of points called *vertices* (Fig. 1.13).

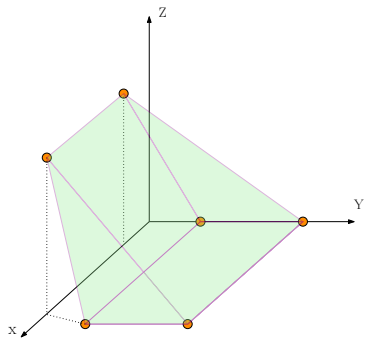

Figure 1.13: A 3-dimensional convex polytop.

For polytopic LPV system, the matrix A is a linear convex combination of several matrices: A_1^p, ..., A_m^p, i.e.,

$$A(\theta) = \sum_{i=1}^{m} \alpha_i A_i^p, \quad \alpha_i \in [0\ 1],\ \sum_{i=1}^{m} \alpha_i = 1,$$

such that there exists a function $f : \mathbb{R}^k \to \mathbb{R}^m$ mapping every value of the vector of parameters θ to a unique value of the vector of coefficients $\alpha = [\alpha_1, \cdots, \alpha_m]$. Moreover, $A_i^p,\ 1 \leq i \leq m$, are the value of the matrix $A(\theta)$ at the vertex i of the polytop.

In case of polytopic LPV system, it is sufficient that the conditions of stability are verified at the vertices of the polytop, with a common Lyapunov function, to be verified inside the whole polytop.

Theorem 3. *If there exist $P = P^\top > 0$, $Q = Q^\top > 0$ such that:*

$$A_i^{pT} P + P A_i^p + Q \leq 0,\ \ 1 \leq i \leq m. \tag{1.16}$$

Then for all the values of the vector θ that respect (1.15), the following LMI condition is verified:

$$A(\theta)^\top P + P A(\theta) + Q \leq 0. \tag{1.17}$$

[7] A set E is convex if and only if

$$\forall x_1,\ x_2 \in E,\ \xi \in [0\ 1] \implies \xi x_1 + (1-\xi) x_2 \in E.$$

Example 1.2. Consider the following polytopic LPV system:

$$\dot{x} = \begin{bmatrix} -\theta_1 & 0.3 \\ \theta_1 + 2 & -2 \end{bmatrix} x, \tag{1.18}$$

where $x \in \mathbb{R}^2$ and $1 \leq \theta_1 \leq 2$. Thus, the polytop is a straight line that has two vertices, i.e.,

$$A(\theta) = \alpha_1 A_1^p + \alpha_2 A_2^p, \text{ where } 0 \leq \alpha_1, \alpha_2 \leq 1, \ \alpha_1 + \alpha_2 = 1,$$

and

$$A_1^p = \begin{bmatrix} -1 & 0.3 \\ 3 & -2 \end{bmatrix}, \ A_2^p = \begin{bmatrix} -2 & 0.3 \\ 4 & -2 \end{bmatrix}.$$

If there exist $P = P^\top > 0, Q = Q^\top > 0$ such that:

$$A_1^{p\top} P + P A_1^p + Q \leq 0, \tag{1.19}$$

$$A_2^{p\top} P + P A_2^p + Q \leq 0, \tag{1.20}$$

then System (1.18) is asymptotically stable for all values of $\theta_1 \in [1\ 2]$.

The result in Theorem 3 can be useful when studying the stability of heterogeneous linear MAS. To illustrate this utility, consider the following decoupled MAS:

$$\dot{x}_i = A_i x_i, \tag{1.21}$$

where $x_i \in \mathbb{R}^2$ and

$$A_i = \begin{bmatrix} \alpha_i & a_{12} \\ a_{21} & a_{22} \end{bmatrix}, \tag{1.22}$$

and where the elements a_{12}, a_{21}, and a_{22} have the same values for all the agents and the value of α_i can change from an agent to another within a certain interval, i.e.,

$$\underline{\alpha} \leq \alpha_i \leq \bar{\alpha}, \ 1 \leq i \leq n.$$

One can conclude about the stability of all the agents by only analyzing the stability of two agents (corresponding to $\alpha_i = \bar{\alpha}$ and $\alpha_i = \underline{\alpha}$, respectively) with a common Lyapunov function. In another words, the

MAS (1.21) can be seen as an LPV system and the agents corresponding to the maximum and minimum values of α_i as the vertices of the polytop. However, this technique does not handle the case when there is an interconnection between the agents.

When studying interconnected systems as MGs, the analysis of stability becomes more complex. The question is, does there exist any property that gives us the possibility to conclude about the stability of a whole system by analyzing its interconnected components separately. Here comes the utility of passivity.

1.6.3 Passivity

Passivity is part of a broader and general theory of dissipativeness [76]. It is a notion directly related to energy that was first introduced in circuit analysis and since then has been successfully applied in various fields, such as stability [77].

Consider the following linear minimal-realization time-invariant system:

$$\begin{aligned} \dot{x} &= Ax + Bu, \\ y &= Cx, \end{aligned} \tag{1.23}$$

where the input u and the output y have the same dimension.

Definition 1.19. [74] Consider a continuously differentiable positive semidefinite function $S(x)$, system (1.23) is said to be

- passive if $u^\top y \geq \dot{S} = \dfrac{\delta S}{\delta x} f(x,u),\ \forall (x,u) \in \mathbb{R}^n \times \mathbb{R}^p$.
- strictly passive if there exists a positive definite function $\phi(x)$ such that $u^\top y \geq \dot{S} + \phi(x),\ \forall (x,u) \in \mathbb{R}^n \times \mathbb{R}^p$.
- lossless if $u^\top y = \dot{S},\ \forall (x,u) \in \mathbb{R}^n \times \mathbb{R}^p$.

The function $S(x)$ is called Storage function.

Note that the main point of passivity is that *"The feedback interconnection of passive system yields a passive system"*. The following lemmas show two algebraic characterizations of the strict passivity property of System (1.23) [74].

Lemma 1.1. System (1.23) is said to be strictly passive if and only if there exist matrices $P = P^\top > 0$ and $Q = Q^\top > 0$ such that

$$A^\top P + PA + Q \leq 0, \tag{1.24}$$

$$PB = C^\top. \tag{1.25}$$

Lemma 1.2. System (1.23) is said to be strictly passive if and only if there exist matrices $P = P^\top > 0$ and $Q = Q^\top > 0$ such that

$$\begin{bmatrix} A^T P + PA + Q & PB - C^T \\ B^T P - C & 0 \end{bmatrix} \leq 0. \tag{1.26}$$

The following example illustrates the utility of passivity for interconnected systems.

Example 1.3. Consider a coupled MAS composed of two agents whose dynamics are as follows:

$$\begin{aligned} \dot{x}_1 &= A_1 x_1 + B_1(y_2 - y_1), \\ y_1 &= C_1 x_1, \end{aligned} \tag{1.27}$$

and

$$\begin{aligned} \dot{x}_2 &= A_2 x_2 + B_2(y_1 - y_2), \\ y_2 &= C_2 x_2, \end{aligned} \tag{1.28}$$

where the matrices A_1, A_2, B_1, B_2, C_1 and C_2 are of appropriate dimension. The overall system is represented by a connected and undirected graph $\mathcal{G} = (\mathcal{V}, \mathcal{E}, \mathcal{L})$, where $\mathcal{V} = \{1, 2\}$, $\mathcal{E} = \{(1, 2)\}$ and

$$\mathcal{L} = \begin{bmatrix} 1 & -1 \\ -1 & 1 \end{bmatrix}.$$

The overall dynamics can be written as follows

$$\dot{x} = Ax - B\mathcal{L}y, \tag{1.29}$$

where $x = [x_1\ x_2]^\top$, $y = [y_1\ y_2]^\top$, $A = diag(A_1, A_2)$ and $B = diag(B_1, B_2)$.

Let us consider that systems (1.27) and (1.28) are strictly passive, i.e., there exist symmetric positive definite

matrices P_1, P_2, Q_1, Q_2 such that

$$\begin{aligned} A_1^\top P_1 + P_1 A_1 + Q_1 \leq 0, \\ P_1 B_1 = C_1^\top, \end{aligned} \tag{1.30}$$

and

$$\begin{aligned} A_2^\top P_2 + P_2 A_2 + Q_2 \leq 0, \\ P_2 B_2 = C_2^\top. \end{aligned} \tag{1.31}$$

Now, we will show how by ensuring the strict passivity of each agent separately, we can conclude about the stability of the whole system. The stability of System (1.29) can then be guaranteed by considering the following Lyapunov function:

$$V(x) = \frac{1}{2} \begin{bmatrix} x_1 & x_2 \end{bmatrix} \begin{bmatrix} P_1 & 0 \\ 0 & P_2 \end{bmatrix} \begin{bmatrix} x_1 \\ x_2 \end{bmatrix}. \tag{1.32}$$

Indeed, by derivation of $V(x)$ along the trajectories and using the conditions of passivity (1.30) and (1.31), we get:

$$\dot{V}(x) = x^\top P A x - x^\top P B \mathcal{L} y, \tag{1.33}$$

$$= x_1^\top P_1 A_1 x_1 + x_2^\top P_2 A_2 x_2 - x^\top P B \mathcal{L} C x, \tag{1.34}$$

$$\leq \underbrace{-x_1^\top Q_1 x_1 - x_2^\top Q_2 x_2}_{<0} \underbrace{-x^\top C^\top \mathcal{L} C x}_{\leq 0}. \tag{1.35}$$

Since, the graph $\mathcal{G}$ is connected and undirected, $\mathcal{L}$ is positive semidefinite and $x^\top C^\top \mathcal{L} C x \geq 0$. Hence, we can conclude that,

$$\dot{V}(x) < 0, \quad x \neq 0. \tag{1.36}$$

Thus, System (1.29) is asymptotically stable.

1.7 Conclusion

MGs represent the future of power systems. They are mainly composed of distributed generation units, storage units, loads and power lines. They can be classified into three categories: DC, AC and DC-AC MGs and have two operation modes, grid-connected and island modes. Moreover, several challenges of DC-MGs have been addressed in the literature using several control architectures. Depending on their time scale, they can be categorized into three control levels, namely primary, secondary and tertiary control. In each of these

levels, the control can be implemented in a centralized, decentralized and distributed manner. Graph theory as well as consensus dynamics, stability, passivity, etc., are essential tools for studying DC-MG. Finally, several control objectives in DC-MGs can be formulated as a consensus problem of multi-agent systems.
In the next chapter, we consider the challenges of current sharing, average voltage regulation and state-of-charge balancing for a DC-MG where the control laws will be designed in a distributed fashion.

Chapter 2

Current Sharing, Average Voltage Regulation and State-of-charge Balancing

Contents

In this chapter, we study the problem of Current Sharing (CS), Average Voltage Regulation (AVR) and State-of-charge Balancing (SB) for DC-MGs composed of DGUs, SUs, resistive-inductive power lines and loads. The chapter is divided into four parts. In Section 2.1, we present the considered DC-MG model. Then in Section 2.2, we consider the problem of CS and AVR for a DC-MG composed of only DGUs, resistive power lines and loads. To achieve the control objectives, the model is augmented with two distributed consensus-like integral actions. A change of variable will be proposed to transform the system into several decoupled subsystems (DGU augmented with local integral actions). We show that if there exists a unique feedback gain that stabilizes the subsystems under a passivity condition, the global exponential convergence of the nominal model is ensured. At the end of the section, we give an LMI formulation for the design of the controller gain. In Section 2.3, a DC-MG composed of only SUs with resistive power lines and loads is considered where the problem of SB is studied. To achieve the control objectives, a leader-follower consensus algorithm is proposed. The design steps of the controllers are similar to those in Section 2.2.
In Section 2.4, we show that the designed controllers in the previous sections can be used to reach Objectives 2.1-2.3 at the same time for a DC-MG comprises both DGUs and SUs and even resistive-inductive power lines. Finally, Section 2.5 concludes the chapter.

2.1 DC Microgrid Model

In this work, we consider a DC-MG comprising m Distributed Generation Units (DGUs) and p Storage Units (SUs) interconnected through q resistive-inductive (RL) power lines; $N = m + p$ is the number of agents (DGUs and SUs) in the MG.
The DC-MG is represented by a graph $\mathcal{G}^{pow} = (\mathcal{V}^{pow}, \mathcal{E}^{pow})$ where $\mathcal{V}^{pow}$ is the set of all the agents and $\mathcal{E}^{pow} = \mathcal{V}^{pow} \times \mathcal{V}^{pow}$ represents the set of power lines. Moreover, $\mathcal{V}^{pow} = \mathcal{V}^{d} \cup \mathcal{V}^{s}$ where $\mathcal{V}^{d} = \{1, \cdots, m\}$ and $\mathcal{V}^{s} = \{1, \cdots, p\}$ define the sets of DGUs and SUs, respectively. A simple electrical scheme of the considered model is shown in Fig. 2.1. We refer the reader to Fig. 2.2 for a representative diagram of an example of DC-MG topology.

The generic energy source of each DGU and SU is modeled as a DC voltage source V_{dc_i} that supplies a local load through a DC-DC converter. The local load is connected to the Point of Common Coupling (PCC) through an RLC (low-pass) filter. Furthermore, two types of local load are considered, resistive load r_{L_i} and unknown constant current source I_{Li} (see Fig. 2.1).

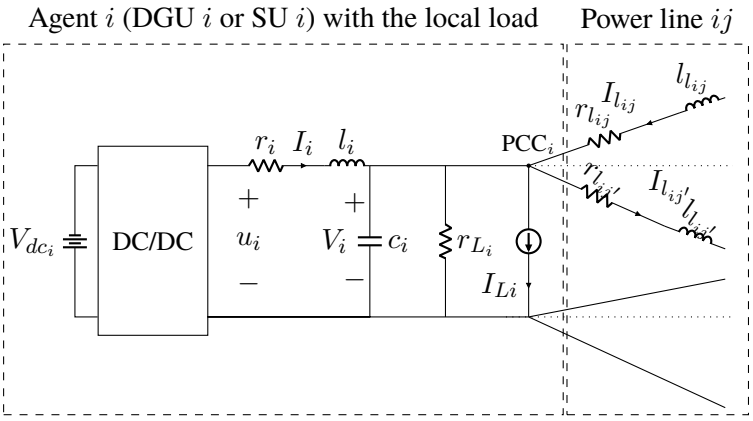

Figure 2.1: The considered electrical scheme of agent i and power lines.

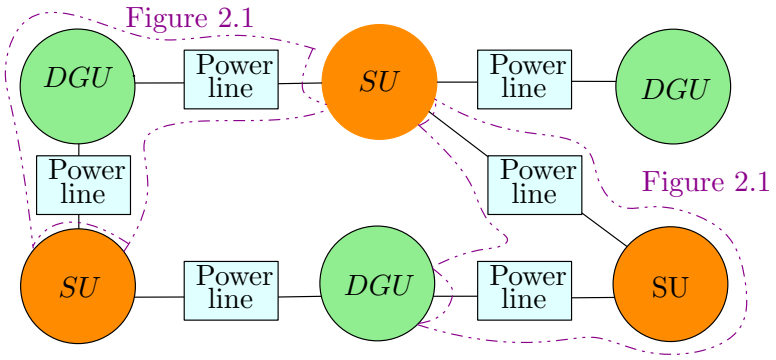

Figure 2.2: An overall view of a DC-MG topology example.

For simplicity, we will first assume that the dynamics of power lines are very fast comparing to the DGUs and SUs dynamics. Thus, by considering the QSL-approximation[1] (i.e., $l_{l_{ij}} = 0,\ \forall (i,j) \in \mathcal{E}^{pow}$) and applying the Kirchhoff's current and voltage laws, the dynamics of the agent i (i.e., DGU i or SU i) can be described by the following generic equation:

$$\begin{aligned} l_i \dot{I}_i &= -r_i I_i - V_i + u_i, \\ c_i \dot{V}_i &= I_i - I_{Li} - \frac{V_i}{r_{Li}} - \sum_{j \in \mathcal{N}_i^{pow}} \frac{1}{r_{l_{ij}}} (V_i - V_j), \end{aligned} \tag{2.1}$$

where $r_{l_{ij}} = r_{l_{ji}}$ and $\mathcal{N}_i^{pow}$ denotes the set of agents neighbors of the agent i.

The state-of-charge (Soc) dynamics at each SU is given as follows:

$$\dot{Soc}_i = -k_i^{soc} I_i \quad \forall i \in \mathcal{V}^s, \tag{2.2}$$

[1] Quasi Stationary Line

with $k_i^{soc} \in \mathbb{R}_{>0}$. Although it is out of the scope of this work, some details about the model used for the state-of-charge estimation can be found in Appendix B.

The notations used in Fig. 2.1 and (2.1) are described in Table 2.1. The use of QSL-approximation in (2.1) means that the power lines are considered mainly resistive. This assumption will be relaxed in Section 2.4 and resistive-inductive power lines will be reconsidered.

Table 2.1: Description of the used notations.

State variables	
I_i	Generated current of Agent i.
V_i	Voltage at the PCC near Agent i.
$I_{l_{ij}}$	Current of power line ij.
Parameters	
r_i	Output filter resistance of Agent i.
l_i	Output filter inductance of Agent i.
v_i	Output filter capacitor of Agent i.
r_{Li}	Local resistive load near Agent i.
$r_{l_{ij}}$	Power line resistance.
$l_{l_{ij}}$	Power line inductance.
Inputs	
u_i	Output voltage of the converter (Control input of Agent$_i$).
I_{Li}	Load current near Agent i.

Remark 2.1. (Very fast converter) The DC/DC dynamics is considered very fast regarding the other dynamics of the power network. In fact, this is a mild assumptions since modern converters can switch at very high frequency [78].

Remark 2.2. (Kron reduction) The topology of the considered DC-MG model is such that the loads are connected to the PCC of each agent (Fig. 2.2). If the loads are connected elsewhere, the Kron reduction method can be used to map it to the PCC [79], [80].

The overall diagram of the proposed controller is illustrated in Fig. 2.3. The control scheme consists of two modules. The first module includes two distributed integral actions to guarantee the CS and AVR. Each local controller receives the voltage reference V_i^{ref} and, from its neighbors, the weighted (per-unit[2]) current $\omega_j I_j$ and the control variables $\omega_j \gamma_j$. Then it generates two control variables ϕ_i and γ_i. These two variables, with

[2]We will see later that the weight ω_i can be defined as the inverse of the rated current of DGU i

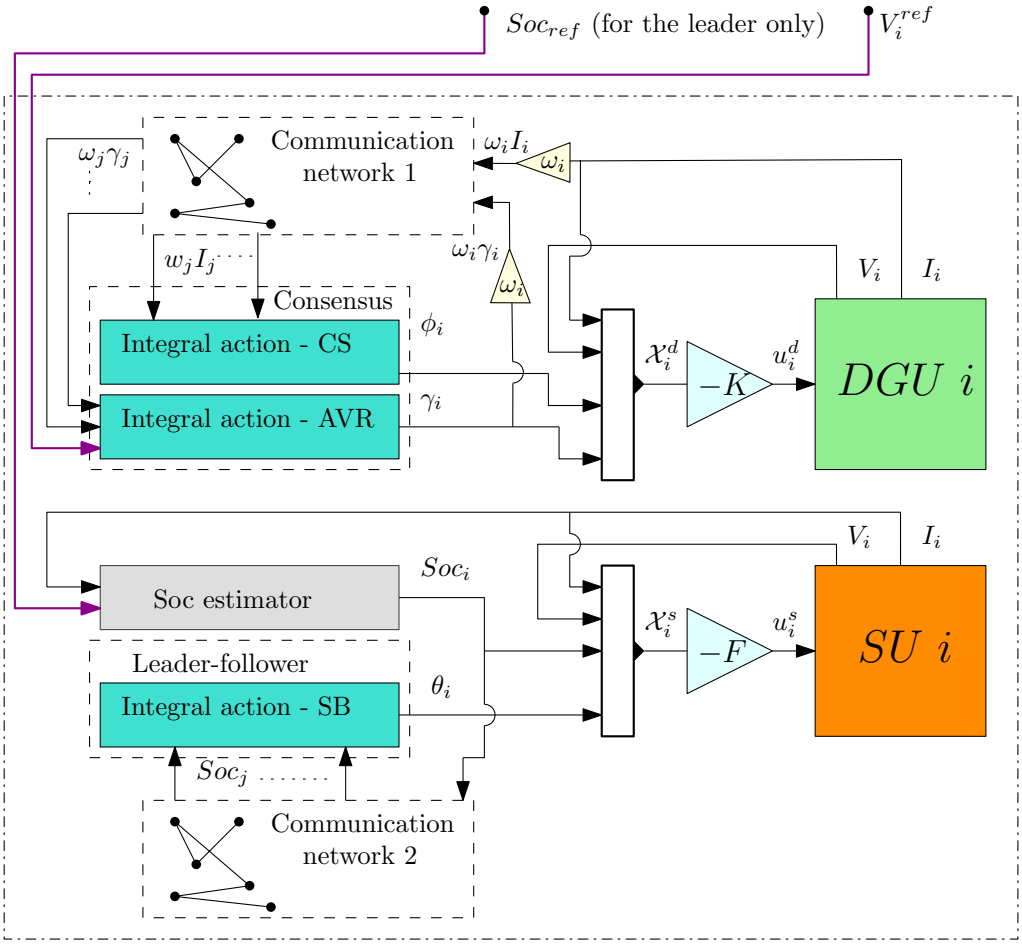

Figure 2.3: Structure of the proposed distributed cooperative controller.

the local current I_i and voltage V_i, will define the augmented state of the DGU i ($\mathcal{X}_i^d$). Then, the augmented state is multiplied by a feedback gain K to generate the local controller u_i^d.

The second module includes a distributed integral action to ensure the SB. The state-of-charge is estimated locally. Each local controller receives from its neighbors the state-of-charge Soc_j and generates a control variable θ_i. Note that if the SU i is the leader, its local controller will also receive the Soc_{ref} from a high-level monitor (e.g., a tertiary controller). The control variable θ_i with the local current I_i, the voltage V_i and the state-of-charge Soc_i will define the augmented state of SU i ($\mathcal{X}_i^s$). Then, the augmented state is multiplied by a feedback gain F to generate the local controller u_i^s.

In what follows, we aim to design the distributed controller gains (K and F) with the corresponding integral actions. However, the existence of physical coupling between the Agents (the term $\sum_{j\in\mathcal{N}_i^{pow}} \frac{1}{r_{l_{ij}}}(V_i - V_j)$ in (2.1)) makes the design difficult. To relax this difficulty, the controller gains of the DGUs and SUs will be

designed separately. First, a DC-MG composed of only DGUs is considered where the model is augmented with m integral actions, and the gain K is synthesized. Then, we consider a model of the MG that includes only SUs where the state is augmented with p integral actions, and the gain F is designed.

2.2 Current Sharing and Average Voltage Regulation

In this section, we consider a DC-MG consists only of DGUs, i.e., $\mathcal{V}^{pow} = \mathcal{V}^{d}$ where the overall MG system can be written from (2.1), compactly, as:

$$\begin{aligned} L\dot{I} &= -RI - V + u, \\ C\dot{V} &= I - (R_L^{-1} + \mathcal{L}^{pow})V - I_L, \end{aligned} \tag{2.3}$$

with I, V, I_L, $u \in \mathbb{R}^m$. As well, L, C, R, $R_L \in \mathbb{R}^{m\times m}$ are positive definite diagonal matrices, e.g, $L = diag(l_1, \cdots, l_m)$. The Laplacian matrix $\mathcal{L}^{pow} \in \mathbb{R}^{m\times m}$ represents the topology of the power network.

2.2.1 Problem Formulation

In this section, we present the considered control objectives. At steady state (2.3) becomes:

$$0 = -RI^e - V^e + u^e, \tag{2.4a}$$

$$0 = I^e - (R_L^{-1} + \mathcal{L}^{pow})V^e - I_L. \tag{2.4b}$$

By left-multiplying (2.4b) by $\mathbb{1}^\top$ we get

$$\mathbb{1}^\top I^e = \mathbb{1}^\top R_L^{-1} V^e + \mathbb{1}^\top I_L, \tag{2.5}$$

that is, the sum of the generated current is equal to the total current demand[3]. The latter should be shared proportionally and not necessarily equally. If this requirement is not taken into account, the module with low power may be driven to deliver its maximum rated current and sometimes beyond. This situation can lead to overloading and temperature stresses which can spoil the module.

[3]The total current demand is the sum of all the currents of the resistance loads ($R_L^{-1}V^e$) and all the load currents (I_L)

Objective 2.1. (**Current sharing**) At steady state, currents have to reach an equilibrium I^e (depending on the total current demand) s.t.:

$$\omega_i I_i^e = \omega_j I_j^e \quad \forall i, j \in \mathcal{V}^d,$$

where the weights ω_i, $\forall i \in \mathcal{V}^d$, are given parameters.

In fact, ω_i^{-1} can be chosen as the corresponding DGU i rated current. Hence, a relatively small value of ω_i corresponds to a relatively large generation capacity of DGU i and Objective 2.1 can be read as follows: At steady state all the DGUs generate the same percentage of their rated currents.

Example 2.1. Consider a DC-MG composed of four DGUs with a total current demand equal to 96 A. Table 2.2 shows the rated current I_i^r, the generated current I_i and the associated weight of each DGU when Objective 2.1 is achieved. As we can see in Table 2.1 all the DGUs converge to 80% of their rated current.

	DGU 1	DGU 2	DGU 3	DGU 4
$I_i^r\ (A)$	10	20	40	50
ω_i	0.1	0.05	0.025	0.02
$I_i\ (A)$	8	16	32	40
$\omega_i I_i$	0.8	0.8	0.8	0.8

Table 2.2: Generated currents of a DC-MG with current sharing objective.

Table 2.3 illustrates a case when Objective 2.1 is not considered. We can see clearly that the DGU with the lower power generates beyond of its nominal capacity whereas the one with the higher power provides less than its nominal capacity (DGU 1 with 180% of its rated current, and DGU 2 with 60% of its rated current). This can causes several problems as mentioned in Section 1.2.

	DGU_1	DGU_2	DGU_3	DGU_4
$I_i^r\ (A)$	10	20	40	50
ω_i	0.1	0.05	0.025	0.02
$I_i\ (A)$	18	26	22	30
$\omega_i I_i$	1.8	1.3	0.55	0.6

Table 2.3: Generated current of a DC-MG without current sharing objective.

Note that Objective 2.1 can be re-written as:

$$I^e = W^{-1}\mathbb{1}i^*, \tag{2.6}$$

where $W = \text{diag}(\omega_1, \cdots, \omega_m)$ and $i^* = \dfrac{\mathbb{1}^\top (R_L^{-1} V^e + I_L)}{\mathbb{1}^\top W^{-1} \mathbb{1}} \in \mathbb{R}$.

Another requirement for a good operation of the MG is that the voltages stay near to its nominal values under any perturbation. Generally, achieving Objective 2.1 does not permit to attend an equilibrium voltage $V_i^e = V_i^{ref}, \forall i \in \mathcal{V}^d$, at the same time. Indeed, from (2.4b) we have[4]:

$$V^e = (R_L^{-1} + \mathcal{L}^{pow})^{-1} (I^e - I_L). \tag{2.7}$$

Note that, if Objective 2.1 is achieved, I^e is fixed (see (2.6)), and V^e will be also fixed (see (2.7)). Thus, we can not ensure $V_i^e = V_i^{ref}, \forall i \in \mathcal{V}^d$ simultaneously with CS. However, we still have the freedom to shift the voltages with the same constant without influencing Objective 2.1. Indeed, if we shift the voltages with the same value ($V^e + \mathbb{1} v^*$, where $v^* \in \mathbb{R}$), using (2.6) the currents at steady state becomes:

$$\begin{aligned} I^e &= \frac{W^{-1}\mathbb{1}}{\mathbb{1}^T W^{-1} \mathbb{1}} \mathbb{1}^\top (R_L^{-1}(V^e + \mathbb{1} v^*) + I_L), && (2.8)\\ &= W^{-1}\mathbb{1} \frac{(\mathbb{1}^\top R_L^{-1} V^e + \mathbb{1}^\top I_L)}{\mathbb{1}^T W^{-1} \mathbb{1}} + W^{-1}\mathbb{1} \frac{\mathbb{1}^\top R_L^{-1} \mathbb{1} v^*}{\mathbb{1}^T W^{-1} \mathbb{1}}, && (2.9)\\ &= W^{-1}\mathbb{1} i^* + W^{-1}\mathbb{1} \frac{\mathbb{1}^\top R_L^{-1} \mathbb{1} v^*}{\mathbb{1}^T W^{-1} \mathbb{1}}, && (2.10)\\ &= W^{-1}\mathbb{1} (i^* + \frac{\mathbb{1}^\top R_L^{-1} \mathbb{1} v^*}{\mathbb{1}^T W^{-1} \mathbb{1}}). && (2.11) \end{aligned}$$

Since $\dfrac{\mathbb{1}^\top R_L^{-1} \mathbb{1} v^*}{\mathbb{1}^T W^{-1} \mathbb{1}}$ is a scalar, it is obvious that Objective 2.1 is still reached.
Consequently, we will consider an average voltage regulation, where the controller aims to shift the voltages with the same suitable value such that the weighted average value of V_i^e, $i \in \mathcal{V}^d$, equal to the weighted average value of the desired reference voltages V_i^{ref}, $i \in \mathcal{V}^d$ and the second control objective can be stated as

Objective 2.2. (**Average voltage regulation**) At steady state, voltages have to reach an equilibrium V^e s.t.:

$$\mathbb{1}_m^T W^{-1} V^e = \mathbb{1}_m^T W^{-1} V^{ref},$$

where $W = \text{diag}(\omega_1, \cdots, \omega_m)$, $\omega_i > 0, \forall i \in \mathcal{V}^d$.

[4]The matrix $(R_L^{-1} + \mathcal{L}^{pow})$ is invertible because R_L^{-1} is symmetric positive definite and $\mathcal{L}^{pow}$ is symmetric positive semidefinite.

The choice of the weights for voltages as ω_i^{-1} is a standard practice motivated by the fact that the DGU_i with the highest capacity should impose the voltage of the MG.

Example 2.2. Consider a DC-MG as in Example 2.1. The following table shows the voltages at PCC with their references when Objective 2.2 is achieved.

It is noteworthy that the voltages stay near to their references while achieving Objective 2.2.

	DGU_1	DGU_2	DGU_3	DGU_4
V_i^{ref}	380	380	380	380
ω_i	0.1	0.05	0.025	0.02
V_i	378.1	379.3	380.2	380.5

Table 2.4: Voltages at the PCC of a DC-MG with AVR controller.

Remark 2.3. Note that CS is always obtained when the voltages are shifted with the same constant, because the variation in current demand ($R_L^{-1}\mathbb{1}v^*$ in (2.11)) caused by the voltage shift is also shared proportionally between the DGUs.

Now, we can state the first control problem as :

Control Problem 1. For a given reference voltage V^{ref} and an unknown load current I_L, design a distributed-based control law u s.t. the state of system (2.3) in closed-loop converges globally and exponentially to a set of equilibrium points whose elements satisfy Objectives 2.1-2.2.

2.2.2 Distributed Controller Design

In this section, a solution to Control Problem 1 is provided. Going back to equations (2.4a) and (2.4b), for a given constant load current I_L, these equations define $2m$ linear independent equations with $3m$ unknown variables (I^e, V^e, u^e). Thus, the equilibrium exists with m degrees of freedom to fix it. Our purpose is then to determine a controller including m integral actions in order to solve Control Problem 1. The proposed control approach exploits a communication network linking the DGUs and fulfilling the following Assumption.

Assumption 2.1. (**Communication network**) The controllers exchange information through a communication network modeled as an undirected graph $\mathcal{G}_d^{com} = (\mathcal{V}^d, \varepsilon^{com}, \mathcal{L}^{com})$ where $\mathcal{L}^{com} \in \mathbb{R}^{m\times m}$ is symmetric positive semidefinite Laplacian matrix which allows to exchange information between the DGUs.

Let us introduce an augmented state $\mathcal{X} = (I, V, \phi, \gamma)$ whose dynamics are given by the following equations:

$$\Sigma^d \begin{cases} L\dot{I} = -RI - V + u, & \text{(2.12a)} \\ C\dot{V} = I - (R_L^{-1} + \mathcal{L}^{pow})V - I_L, & \text{(2.12b)} \\ \dot{\phi} = W^T \mathcal{L}^{com} W I, & \text{(2.12c)} \\ \dot{\gamma} = -W^T \mathcal{L}^{com} W \gamma + \tau(V - V^{ref}), & \text{(2.12d)} \end{cases}$$

where $\mathcal{L}^{com}$ is defined in Assumption 2.1, $\tau \in \mathbb{R}_{>0}$ and the ith line of (2.12c)-(2.12d) is given by:

$$\begin{aligned} \dot{\phi}_i &= \omega_i \sum_{j \in \mathcal{N}_i^{com}} \alpha_{ij}(\omega_i I_i - \omega_j I_j), \\ \dot{\gamma}_i &= -\omega_i \sum_{j \in \mathcal{N}_i^{com}} \alpha_{ij}(\omega_i \gamma_i - \omega_j \gamma_j) + \tau(V_i - V_i^{ref}), \end{aligned} \tag{2.13}$$

where $\mathcal{N}_i^{com}$ is the set of DGUs connected to the DGU i via the communication network with the edge weights $\alpha_{ij} = \alpha_{ji} \in \mathbb{R}_{>0}$. The consensus dynamics in (2.12c)-(2.12d) are used to attend Objectives 2.1-2.2, respectively, this will be detailed in the proof of Proposition 2.2.

Definition 2.1. (Set of equilibrium points) For a given reference voltage V^{ref} and an unknown load current I_L, the set of all the equilibrium points is defined by $S^d(I_L, V^{ref}) = \{\mathcal{X}^e = (I^e,\ V^e,\ \phi^e,\ \gamma^e) \in \mathbb{R}^{4m}$ and $u^e \in \mathbb{R}^m$ s.t.:

$$0 = -RI^e - V^e + u^e, \tag{2.14a}$$
$$0 = I^e - (R_L^{-1} + \mathcal{L}^{pow})V^e - I_L, \tag{2.14b}$$
$$0 = W^T \mathcal{L}^{com} W I^e, \tag{2.14c}$$
$$0 = -W^T \mathcal{L}^{com} W \gamma^e + \tau(V^e - V^{ref}).\} \tag{2.14d}$$

In what follows the following assumption will be considered:

Assumption 2.2. (**Nominal model**) All the DGUs have the same nominal values of parameters, i.e., $l_i = l$, $c_i = c, r_i = r, r_{Li} = r_L, \forall i \in \mathcal{V}^d$, with $l,\ c,\ r, r_L \in \mathbb{R}_{>0}$ represent the nominal values.

Proposition 2.1. (Existence of equilibrium points) For a given reference voltage V^{ref} and an unknown load current I_L, the set $S^d(I_L, V^{ref})$ is not empty.

Proof. Let us introduce the following change of coordinates[a]:

$$(\tilde{I}, \tilde{V}, \tilde{\phi}, \tilde{\gamma}) = (\mathbf{I}_4 \otimes T^T)(I, V, \phi, \gamma), \tag{2.15}$$

where $T \in \mathbb{R}^{m \times m}$ is a unitary matrix s.t. $\tilde{\mathcal{L}}^{com} = T^T W^T \mathcal{L}^{com} W T = \text{diag}(0, \lambda_2, \dots, \lambda_m)$ where $\lambda_i, \forall i \in \mathcal{V}^d$, represent the eigenvalues of $W^T \mathcal{L}^{com} W$ s.t. $\lambda_i < \lambda_j, \forall\, i < j$. The matrix T exists because $W^T \mathcal{L}^{com} W$ is symmetric. Moreover, $\lambda_1 = 0$, since the graph $\mathcal{G}_d^{com}$ is undirected and connected, and because the vector $W^{-1}\mathbb{1}_m$ satisfies $W^T \mathcal{L}^{com} W (W^{-1}\mathbb{1}_m) = 0$.
In this new basis, Σ^d (2.12) can be rewritten as follows:

$$\tilde{\Sigma}^d \begin{cases} L\dot{\tilde{I}} = -R\tilde{I} - \tilde{V} + \tilde{u}, & \text{(2.16a)} \\ C\dot{\tilde{V}} = \tilde{I} - (R_L^{-1} + \tilde{\mathcal{L}}^{pow})\tilde{V} - \tilde{I}_L, & \text{(2.16b)} \\ \dot{\tilde{\phi}} = \underbrace{\begin{bmatrix} 0 & 0 & \cdots & 0 \\ 0 & \lambda_2 & \cdots & 0 \\ \vdots & \vdots & \ddots & \vdots \\ 0 & 0 & \cdots & \lambda_m \end{bmatrix}}_{\tilde{\mathcal{L}}^{com}} \tilde{I}, & \text{(2.16c)} \\ \dot{\tilde{\gamma}} = -\tilde{\mathcal{L}}^{com}\tilde{\gamma} + \tau(\tilde{V} - \tilde{V}^{ref}), & \text{(2.16d)} \end{cases}$$

where $\tilde{\mathcal{L}}^{pow} = T^T \mathcal{L}^{pow} T$ and:

$$(\tilde{u}, \tilde{I}_L, \tilde{V}^{ref}) = (\mathbf{I}_3 \otimes T^T)(u, I_L, V^{ref}). \tag{2.17}$$

Note that the matrices L, C, R and R_L remain unchanged by Assumption 2.2. Let us define the set $\tilde{S}^d(\tilde{I}_L, \tilde{V}^{ref})$ of all the equilibrium points of $\tilde{\Sigma}^d$ as
$\tilde{S}^d(\tilde{I}_L, \tilde{V}^{ref}) = \{\tilde{\mathcal{X}}^e = (\tilde{I}^e, \tilde{V}^e, \tilde{\phi}^e, \tilde{\gamma}^e) \in \mathbb{R}^{4m}, \tilde{u}^e \in \mathbb{R}^m$ s.t.:

$$0 = -R\tilde{I}^e - \tilde{V}^e + \tilde{u}^e, \tag{2.18a}$$
$$0 = \tilde{I}^e - (R_L^{-1} + \tilde{\mathcal{L}}^{pow})\tilde{V}^e - \tilde{I}_L, \tag{2.18b}$$
$$0 = \tilde{\mathcal{L}}^{com}\tilde{I}^e, \tag{2.18c}$$
$$0 = -\tilde{\mathcal{L}}^{com}\tilde{\gamma}^e + \tau(\tilde{V}^e - \tilde{V}^{ref}).\} \tag{2.18d}$$

Obviously, if $(\tilde{\mathcal{X}}^e, \tilde{u}^e) \in \tilde{S}^d(\tilde{I}_L, \tilde{V}^{ref})$, then $(\mathcal{X}^e, u^e) \in S^d(I_L, V^{ref})$ since

$$(\tilde{\mathcal{X}}^e, \tilde{u}^e) = (\mathbf{I}_5 \otimes T^T)(\mathcal{X}^e, u^e). \tag{2.19}$$

Thus, it is sufficient to prove that $\tilde{S}^d(\tilde{I}_L, \tilde{V}^{ref}) \neq \emptyset$, i.e., system (2.18) has at least one solution. From (2.18c) and using the diagonal form of $\tilde{\mathcal{L}}^{com}$, one gets:

$$\tilde{I}_{e_i} = 0 \text{ for } i = 2, \cdots, m. \tag{2.20}$$

Moreover, the first line of (2.18d) gives:

$$\tilde{V}_1^e = \tilde{V}_1^{ref}. \tag{2.21}$$

Thus, for a given $\tilde{I}_L$, reporting (2.20)-(2.21) in (2.18b) yields:

$$\tilde{V}^e_{[2,m]} = -H((\tilde{\mathcal{L}}^{pow})_{[2,m]\times[1]}\tilde{V}_1^{ref} + \tilde{I}_{L[2,m]}), \tag{2.22}$$

where $H = (R_L^{-1} + \tilde{\mathcal{L}}^{pow})^{-1}_{[2,m]\times[2,m]}$. Note that one can easily show that the matrix H is well defined since $(R_L^{-1})_{[2,m]\times[2,m]}$ is diagonal positive definite and $(\tilde{\mathcal{L}}^{pow})_{[2,m]\times[2,m]}$ is positive semidefinite. Furthermore, reporting (2.20)-(2.22) in (2.18b) leads to:

$$\tilde{I}_1^e = r_L^{-1}\tilde{V}_1^{ref} + (\tilde{\mathcal{L}}^{pow})_{[1]\times[1,m]}\tilde{V}^e + \tilde{I}_{L1}. \tag{2.23}$$

Since $\tilde{I}^e$ and $\tilde{V}^e$ are now fixed, it follows from (2.18a) that $\tilde{u}^e$ is also defined by

$$\tilde{u}_1^e = R\tilde{I}_1^e + \tilde{V}_1^{ref}, \tag{2.24}$$

$$\tilde{u}_i^e = \tilde{V}_i^e \text{ for } i = 2, \cdots, m. \tag{2.25}$$

Since $\tilde{\phi}_1(t) = \tilde{\phi}_1(0),\ \forall t \geq 0$, it is obvious from (2.18c)-(2.18d) that:

$$\tilde{\phi}_1^e = \tilde{\phi}_1(0),$$
$$\tilde{\gamma}_i^e = \lambda_i^{-1}\tau(\tilde{V}_i^e - \tilde{V}_i^{ref}), \text{ for } i = 2, \cdots, m.$$

Finally, any value for $\tilde{\gamma}_1^e$ and $\tilde{\phi}_i^e$ for $i = 2, \cdots, m$ is allowed. Thus, system (2.18) has an infinite number

of equilibrium points parameterized by (I_L, V^{ref}). ■

[a] See Appendix A for the definition of the Kronecker product denoted by $\otimes$.

Remark 2.4. It is worthy to note that only relative information are exchanged between the DGUs augmented with the additional states (2.13) (notice that $\alpha_{ij} = 0$ if DGU j is not neighbor of DGU i). Hence, if a state feedback controller that uses only the local state at each DGU, i.e., $(I_i, V_i, \phi_i, \gamma_i)$, $\forall i \in \mathcal{V}^d$, is considered, u will be distributed.

Proposition 2.2. (Augmented system with state feedback) If there exists a state feedback u of the form:

$$u = -K\mathcal{X}, \tag{2.26}$$

where $\mathcal{X} = (I, V, \phi, \gamma)$ and $K \in \mathbb{R}^{m \times 4m}$ s.t., in closed-loop, the couple $(\mathcal{X}, u)$ of system (2.12) converges asymptotically to the set $S^d(I_L, V^{ref})$ then Objectives 2.1-2.2 are always achieved in this set S^d.

Proof. If there exists a state feedback control (2.26) s.t. the couple $(\mathcal{X}, u)$ converges, in closed-loop, asymptotically to the set $S^d(I_L, V^{ref})$, then (2.14c) implies that $I^e \in \mathcal{K}er(W^T \mathcal{L}^{com} W)$. As $\mathcal{L}^{com}$ is a symmetric positive semidefinite Laplacian matrix for which the kernel is provided by the set $\mathcal{K}er(\mathcal{L}^{com}) = \{z \in \mathbb{R}^m : \exists \alpha \in \mathbb{R},\ z = \alpha \mathbb{1}_m\}$ (see Remark 1.3) and as the weighting matrix W is diagonal strictly positive definite, it follows that there exists a scalar α s.t.:

$$WI^e = \alpha \mathbb{1}_m,$$

or equivalently $\omega_i I_i^e = \omega_j I_j^e,\ \forall i, j \in \mathcal{V}^d$. Consequently, Objective 2.1 is achieved. Since

$$rank(W^T \mathcal{L}^{com} W) = m - 1,$$

(2.12c) is equivalent to introduce $m - 1$ integrators. Accordingly, only $(m - 1)$ degrees of freedom are required to attend the first objective and the mth one will be used to achieve Objective 2.2 with an additional distributed integral action. Indeed, left-multiplying (2.14d) with $\mathbb{1}_m^T W^{-1}$ leads to:

$$0 = \mathbb{1}_m^T W^{-1} (V^e - V^{ref}), \tag{2.27}$$

since $\mathbb{1}_m^T \mathcal{L}^{com} = 0$. Thus, it follows that, inside the set S^d, Objective 2.2 is achieved. ■

To summarize, system (2.3) was augmented with the additional state (ϕ, γ) so as to introduce m distributed integral actions to the controller. Then, we showed that the augmented system defined by (2.12) has at least one equilibrium point since $S^d \neq \emptyset$. Finally, it was proved that if the couple $(\mathcal{X}, u)$ of the augmented system converges to one of its equilibrium points, Objectives 2.1-2.2 are achieved thanks to (ϕ, γ).

Now, our goal is to design local controllers u_i that depend only on local variables $x_i = (I_i, V_i, \phi_i, \gamma_i)$, $\forall i \in \mathcal{V}^d$. Hence, the gain matrix K (see (2.26)) should be restricted to the form:

$$K = (K_I, K_V, K_\phi, K_\gamma), \tag{2.28}$$

where $K_I,\ K_V,\ K_\phi, K_\gamma$ are diagonal matrices of dimension $m \times m$.
The main difficulty to find a gain matrix of this form for the augmented system (2.12) is the existence of physical $(\mathcal{L}^{pow})$ and communication $(\mathcal{L}^{com})$ coupling terms.

Proposition 2.3. (Unique gain) If there exists a controller:

$$\tilde{u} = -\tilde{K}\tilde{\mathcal{X}}, \tag{2.29}$$

where $\tilde{\mathcal{X}} = (\tilde{I}, \tilde{V}, \tilde{\phi}, \tilde{\gamma})$, $\tilde{K} = (\mathcal{K} \otimes \mathbf{I}_m)$ and $\mathcal{K} = \begin{bmatrix} k_I & k_V & k_\phi & k_\gamma \end{bmatrix} \in \mathbb{R}^{1\times 4}$ s.t., in closed-loop, the couple $(\tilde{\mathcal{X}}, \tilde{u})$ of system $\tilde{\Sigma}^d$ converges asymptotically to the set $\tilde{S}^d(\tilde{V}^{ref}, \tilde{I}_L)$ (see (2.18)-(2.19)) then the couple $(\mathcal{X}, u)$ of system Σ^d with:

$$u = -(\mathcal{K} \otimes \mathbf{I}_m)\mathcal{X} \tag{2.30}$$

converges asymptotically to the set $S^d(V^{ref}, I_L)$. Moreover, $K = (\mathcal{K} \otimes \mathbf{I}_m)$ satisfies (2.28).

Proof. As $u = T\tilde{u}$, $\tilde{\mathcal{X}} = (\mathbf{I}_4 \otimes T^T)\mathcal{X}$ (see (2.15)),

$$\tilde{K} = (\mathcal{K} \otimes \mathbf{I}_m) = (k_I\mathbf{I}_m, k_V\mathbf{I}_m, k_\phi\mathbf{I}_m, k_\gamma\mathbf{I}_m),$$

and since T is a unitary matrix, it follows:

$$u = -T \begin{bmatrix} k_I T^T & k_V T^T & k_\phi T^T & k_\gamma T^T \end{bmatrix} \mathcal{X}, \tag{2.31}$$

$$= -(\mathcal{K} \otimes \mathbf{I}_m)\mathcal{X}. \tag{2.32}$$

Since the change of coordinates (2.15) and (2.17) is bijective, the asymptotic convergence of $(\tilde{\mathcal{X}}, \tilde{u})$ to $\tilde{S}^d$ implies that $(\mathcal{X}, u)$ converges asymptotically to the set $S^d(V^{ref}, I_L)$.
Finally, $K = (\mathcal{K} \otimes \mathbf{I}_m)$ is of the required form (2.28) since it can be rewritten as

$$K = (k_I \mathbf{I}_m, k_V \mathbf{I}_m, k_\phi \mathbf{I}_m, k_\gamma \mathbf{I}_m).$$

■

Proposition 2.4. (Unicity of the equilibrium point) For a given reference voltage V^{ref} and an unknown load current I_L, the equilibrium point of system (2.12) is uniquely determined by the feedback :

$$u = -(\mathcal{K} \otimes \mathbf{I}_m)\mathcal{X}.$$

Proof. As it has been shown in the proof of Proposition 2.1 after a change of coordinates, only some components of $\tilde{\phi}$ and $\tilde{\gamma}$ have remained undetermined. Using the expressions $\tilde{u}^e = -(\mathcal{K} \otimes \mathbf{I}_m)\tilde{\mathcal{X}}^e$ and $\tilde{\mathcal{X}}^e = (\tilde{I}^e, \tilde{V}^e, \tilde{\phi}, \tilde{\gamma})$, a simple calculation leads to:

$$\begin{aligned}
\tilde{\gamma}_1^e &= \frac{-1}{k_\gamma}(\tilde{u}_1^e + k_I \tilde{I}_1^e + k_V \tilde{V}_1^e + k_\phi \tilde{\phi}_1^e), \\
\tilde{\phi}_i^e &= \frac{-1}{k_\phi}(\tilde{u}_i^e + k_I \tilde{I}_i^e + k_V \tilde{V}_i^e + k_\gamma \tilde{\gamma}_i^e),\ i = 2, \cdots, m.
\end{aligned}$$

Recalling that $\tilde{\phi}_1^e = \tilde{\phi}_1(0)$ and from the proof of Proposition 2.1, it can be concluded that the equilibrium is uniquely determined in the set S^d. ■

Remark 2.5. By Propositions 2.1 and 2.4, for a given V^{ref} and I_L the set $\tilde{S}^d$ is equivalent to a straight line parametrized by the initial values of the variable $\tilde{\phi}_1$.

By considering a second change of coordinates of the form

$$\tilde{x} = \mathcal{M}^{d\top} \tilde{\mathcal{X}}, \tag{2.33}$$

where

$$\mathcal{M}^d = \begin{bmatrix} \mathbf{I}_m \otimes [1\ 0\ 0\ 0] \\ \mathbf{I}_m \otimes [0\ 1\ 0\ 0] \\ \mathbf{I}_m \otimes [0\ 0\ 1\ 0] \\ \mathbf{I}_m \otimes [0\ 0\ 0\ 1] \end{bmatrix}. \tag{2.34}$$

Using (2.34) system $\tilde{\Sigma}^d$ with the control law $\tilde{u}$ given by (2.29) can be written as m interconnected subsystems of the form: $\forall i \in \mathcal{V}^d$,

$$\tilde{\Sigma}_i^d \ : \dot{\tilde{x}}_i = A_{cli}\tilde{x}_i + d_i - B_p \sum_{j=i,\ j\in\mathcal{N}_i^{pow}} l_{i,j}^{pow} C_p \tilde{x}_i, \tag{2.35}$$

where

- $\tilde{x} = (\tilde{x}_1, \cdots, \tilde{x}_m)$, $\tilde{x}_i = (\tilde{I}_i, \tilde{V}_i, \tilde{\phi}_i, \tilde{\gamma}_i)$,
- $d_i = -(0, \frac{1}{c}\tilde{I}_{Li}, 0, \tau\tilde{V}_i^{ref})$,
- $B_p = \begin{bmatrix} 0 & c^{-1} & 0 & 0 \end{bmatrix}^T$, $C_p = \begin{bmatrix} 0 & 1 & 0 & 0 \end{bmatrix}$,
- $l_{i,j}^{pow}$ for $1 \leq\ i, j \leq m$ denotes the elements of $\tilde{\mathcal{L}}^{pow}$,
- $A_{cl_i} = A_{o_i} - B_u\mathcal{K}$ where

$$A_{o_i} = \begin{bmatrix} A & \mathbb{0}_{2\times 2} \\ \lambda_i \ 0 & 0 \ 0 \\ 0 \ \tau & 0 \ -\lambda_i \end{bmatrix},\ B_u = \begin{bmatrix} \frac{1}{l} \\ \mathbb{0}_{3\times 1} \end{bmatrix} \text{ and}$$
$$A = \begin{bmatrix} -\frac{r}{l} & -\frac{1}{l} \\ \frac{1}{c} & -\frac{1}{cr_L} \end{bmatrix}. \tag{2.36}$$

In this basis, it can be noticed that the local variables $\tilde{x}_i = (\tilde{I}_i, \tilde{V}_i, \tilde{\phi}_i, \tilde{\gamma}_i)$, $\forall i \in \mathcal{V}^d$, are only coupled by the term $B_p \sum_{j=i,\ j\in\mathcal{N}_i} l_{i,j}^{pow} C_p \tilde{x}_i$ (related to the matrix $\tilde{\mathcal{L}}^{pow}$). The next theorem shows how it is possible to determine the gain matrix $\mathcal{K}$ in (2.30) using some passivity arguments.

Theorem 2.1. *If there exists a static state feedback* $\mathcal{K} = \begin{bmatrix} k_I & k_V & k_\phi & k_\gamma \end{bmatrix}$ *s.t. the triple* (A_{cl_i}, B_p, C_p) *for* $i = 2, \cdots, m$ *and* $(\breve{A}cl_1, \breve{B}_1, \breve{C}_1)$ *are strictly passive where:*

$$\breve{A}_{cl_1} = \begin{bmatrix} A & \mathbb{0}_{2\times 1} \\ 0\ \tau & 0 \end{bmatrix} - \begin{bmatrix} \frac{1}{l} \\ \mathbb{0}_{2\times 1} \end{bmatrix} \begin{bmatrix} k_I & k_V & k_\gamma \end{bmatrix},$$
$$\breve{B}_1 = \begin{bmatrix} 0 & c^{-1} & 0 \end{bmatrix}^T,\ \breve{C}_1 = \begin{bmatrix} 0 & 1 & 0 \end{bmatrix}, \tag{2.37}$$

and where A_{cl_i}, B_p, C_p *and* A *are given with subsystems* (2.35)*, then the couple* $(\mathcal{X}, u = -(\mathcal{K} \otimes \boldsymbol{I}_m)\mathcal{X})$ *of*

the augmented system (2.12) converges exponentially to an equilibrium $(\mathcal{X}^e, u^e) \in S^d(V^{ref}, I_L)$ *for which the control objectives 2.1-2.2 are satisfied.*

Proof. Using Proposition 2.3, it is sufficient to prove the convergence of the couple $(\tilde{\mathcal{X}}, \tilde{u} = -(\mathbf{I}_m \otimes \mathcal{K})\tilde{\mathcal{X}})$ to the set $\tilde{S}^d(\tilde{V}^{ref}, \tilde{I}_L)$.
A state space representation of system $\tilde{\Sigma}^d$ with the controller $\tilde{u}$ in Proposition 2.3 can be written from subsystems defined by (2.35) as:

$$\dot{\tilde{x}} = (\mathcal{A} - \mathcal{B}\tilde{\mathcal{L}}^{pow}\mathcal{C})\tilde{x} + d, \tag{2.38}$$

where

- $\mathcal{A} = \text{diag}(A_{cl_1}, \cdots, A_{cl_m})$,
- $\mathcal{B} = \mathbf{I}_m \otimes B_p$,
- $\mathcal{C} = (\mathbf{I}_m \otimes C_p)$ and
- $d = (d_1, \cdots, d_m)$.

From the expression of $\tilde{\mathcal{L}}^{com}$ in (2.16c), it is clear that $\dot{\tilde{\phi}}_1 = 0$. Thus, this variable is not controllable and acts as a constant disturbance like the terms d. Thus, for the purpose of stability analysis, $\tilde{\phi}_1$ can be removed from systems $\tilde{\Sigma}^d_1$. Accordingly, it is sufficient to design the gain $\mathcal{K}$ such that the matrices A_{cl_i}, $i = 2, \cdots, m$ and $\breve{A}cl_1$ are Hurwitz (see (2.36) and (2.37)).
In other words, if $\breve{x}$ denotes the vector $\tilde{x}$ whose mentioned constant component ($\tilde{\phi}_1$) have been removed, then it is sufficient to prove the asymptotic stability of the following reduced system:

$$\dot{\breve{x}} = (\breve{\mathcal{A}} - \breve{\mathcal{B}}\tilde{\mathcal{L}}^{pow}\breve{\mathcal{C}})\breve{x} + \breve{d}, \tag{2.39}$$

where

- $\breve{\mathcal{A}} = \text{diag}(\breve{A}_{cl_1}, A_{cl_2}, \cdots, A_{cl_m})$,
- $\breve{\mathcal{B}} = \text{diag}(\breve{B}_1, (\mathbf{I}_{m-1} \otimes B_p))$,

- $\breve{\mathcal{C}} = \text{diag}(\breve{C}_1, (\mathbf{I}_{m-1} \otimes C_p))$,
- $\breve{d} = (\breve{d}_1, d_2, \cdots, d_m)$, $\breve{d}_1 = -(0, \frac{1}{c}\tilde{I}_{L1}, \tau\tilde{V}_1^{ref})$.

By assumption, the triple (A_{cl_i}, B_p, C_p) for $i = 2, \cdots, m$ and $(\breve{A}cl_1, \breve{B}_1, \breve{C}_1)$ are strictly passive, i.e, there exist matrices $P_i = P_i^T > 0$ and $\epsilon_i > 0$ such that for $i = 2, \cdots, m$

$$A_{cl_i}^T P_i + P_i A_{cl_i} \leq -\epsilon_i P_i, \tag{2.40a}$$

$$P_i B_p = C_p^T, \tag{2.40b}$$

and for $i = 1$

$$\breve{A}_{cl_1}^T P_1 + P_1 \breve{A}_{cl_1} \leq -\epsilon_1 P_1, \tag{2.41a}$$

$$P_1 \breve{B}_1 = \breve{C}_1^T. \tag{2.41b}$$

The stability of system (2.39) can then be guaranteed by considering the Lyapunov function $V^d(\breve{x}) = \breve{x}^T P \breve{x}$, with

$$P = \text{diag}(P_1, \cdots, P_m). \tag{2.42}$$

Indeed, by derivation of V^d along the trajectories, we get:

$$\dot{V}^d(\breve{x}) = \breve{x}^T((\breve{\mathcal{A}} - \breve{\mathcal{B}}\tilde{\mathcal{L}}^{pow}\breve{\mathcal{C}})^T P + P(\breve{\mathcal{A}} - \breve{\mathcal{B}}\tilde{\mathcal{L}}^{pow}\breve{\mathcal{C}}))\breve{x}, \tag{2.43}$$

it follows:

$$\dot{V}^d(\breve{x}) = 2\breve{x}^T P(\breve{\mathcal{A}} - \breve{\mathcal{B}}\tilde{\mathcal{L}}^{pow}\breve{\mathcal{C}})\breve{x}, \tag{2.44}$$

using (2.40)-(2.41), (2.44) can be written as:

$$\dot{V}^d(\breve{x}) = \sum_{i=1}^{m} 2\breve{x}_i^T P_i \breve{A}_{cl_i}\breve{x}_i - 2\breve{x}^T\breve{\mathcal{C}}^T\tilde{\mathcal{L}}^{pow}\breve{\mathcal{C}}\breve{x}, \tag{2.45a}$$

$$\leq -\sum_{i=1}^{m} 2\epsilon_i \breve{x}_i^T P_i \breve{x}_i - 2\breve{x}^T\breve{\mathcal{C}}^T\tilde{\mathcal{L}}^{pow}\breve{\mathcal{C}}\breve{x}, \tag{2.45b}$$

since $\breve{\mathcal{C}}^T \tilde{\mathcal{L}}^{pow} \breve{\mathcal{C}} \geq 0$, we can conclude that:

$$\dot{V}^d(\breve{x}) < 0, \ \breve{x} \neq 0. \tag{2.46}$$

Consequently, system (2.39) is asymptotically stable and the state $\breve{x}$ converges asymptotically to the equilibrium point $\breve{x}^e = -(\breve{\mathcal{A}} - \breve{\mathcal{B}}\tilde{\mathcal{L}}^{pow}\breve{\mathcal{C}})^{-1}\breve{d}$. Hence, the state $\tilde{x}$ converges asymptotically to the equilibrium point $\tilde{x}^e$ given by:

$$\tilde{x}_i^e = \breve{x}_i^e, \text{ for } i = 2, \cdots, m,$$

$$\tilde{x}_1^e = \begin{bmatrix} \breve{x}_{1_1}^e & \breve{x}_{1_2}^e & \tilde{\phi}_1(0) & \breve{x}_{1_3}^e \end{bmatrix}.$$

Since $\tilde{\mathcal{X}} = \mathcal{M}\tilde{x}$, where $\mathcal{M}$ is given by (2.34), the state $\tilde{\mathcal{X}}$ converges asymptotically to the equilibrium point $\tilde{\mathcal{X}}^e = \mathcal{M}\tilde{x}^e$. Moreover, it is obvious that the couple $(\tilde{\mathcal{X}}^e, \tilde{u}^e = -(\mathbf{I}_m \otimes \mathcal{K})\tilde{\mathcal{X}}^e)$ verifies (2.18). Thus, the couple $(\tilde{\mathcal{X}}, \tilde{u} = -(\mathbf{I}_m \otimes \mathcal{K})\tilde{\mathcal{X}})$ converges asymptotically to the set $\tilde{S}^d(\tilde{V}^{ref}, \tilde{I}_L)$.
By Propositions 2.3-2.4, the couple $(\mathcal{X}, u = -(\mathbf{I}_m \otimes \mathcal{K})\mathcal{X})$ converges asymptotically to the set $S^d(V^{ref}, I_L)$. Furthermore, by Proposition 2.2, Objectives 2.1-2.2 are reached. Finally, since the system is linear the convergence is exponential and Theorem 2.1 is proved. ■

2.2.3 LMI Computational Algorithm

Now, we show how to compute the controller gain matrices $\mathcal{K}$ so as to comply with the conditions of Theorems 2.1. By considering Assumptions 2.2, one can remark that the only parameter values that change between matrices $A_{o_i}, \ \forall i \in \mathcal{V}^d$, (see (2.36)) are the values of the eigenvalues $\lambda_i, \ \forall i \in \mathcal{V}^d$. Thus, the design of the controllers can be addressed by considering, a problem of robust stability for polytopic systems. A polytope with two vertices is considered, where the first and second vertices correspond to the highest and smallest eigenvalues of $W^T \mathcal{L}^{com} W$, respectively. Therefore, at each vertex we have:

$$\overline{A}_o = \begin{bmatrix} A & & \mathbb{0}_{2\times 2} \\ \lambda_{max} \ \ 0 & & 0 \ \ 0 \\ 0 \ \ \tau & & 0 \ \ -\lambda_{max} \end{bmatrix},$$

$$\underline{A}_o = \begin{bmatrix} A & & \mathbb{0}_{2\times 2} \\ \lambda_{min} & 0 & 0 & 0 \\ 0 & \tau & 0 & -\lambda_{min} \end{bmatrix},$$

where $\lambda_{min} = min(\lambda_i)$, $\lambda_{max} = max(\lambda_i)$; $\quad i = 2, \cdots, m$. Thus, all matrices A_{o_i} lie in the straight segment between this two vertices, i.e., the change zone is a convex combination of vertices $\overline{A}_o$ and $\underline{A}_o$: $\forall i = 2, \cdots, m, \exists \alpha \in [0, 1]$ s.t. $A_{o_i} = \alpha \overline{A}_o + (1-\alpha)\underline{A}_o$. Hence, the gain $\mathcal{K}$ can be computed by solving the following LMI: there exist a constant $\epsilon > 0$ and matrices $M_1 = M_1^T > 0$ and M_2 of appropriate dimensions s.t.

$$\overline{A}_o M_1 + M_1 \overline{A}_o^T - B_u M_2 - M_2^T B_u^T \leq -\epsilon M_1, \tag{2.47a}$$

$$\underline{A}_o M_1 + M_1 \underline{A}_o^T - B_u M_2 - M_2^T B_u^T \leq -\epsilon M_1, \tag{2.47b}$$

$$B_p = M_1 C_p^T, \tag{2.47c}$$

where B_u, B_p and C_p are given in (2.35)-(2.36). Then, $\mathcal{K} = [k_I \; k_V \; k_\phi \; k_\gamma] = M_2 M_1^{-1}$.
Using, $[k_I \; k_V \; k_\gamma]$ computed from (2.47) verify the following LMI: there exist a constant $\epsilon_1 > 0$ and a matrix $\breve{P} = \breve{P}^T > 0$ of appropriate dimension s.t.:

$$\breve{A}_{cl_1}^T \breve{P} + \breve{P} \breve{A}_{cl_1} \leq -\epsilon_1 \breve{P}, \tag{2.48a}$$

$$\breve{P} \breve{B}_1 = \breve{C}_1^T, \tag{2.48b}$$

where $\breve{A}_{cl_1}$, $\breve{B}_1$ and $\breve{C}_1$ are given in (2.37).

To resume this part of the chapter, a DC-MG composed of only DGUs has been considered with the problems of CS and AVR. The objectives have been achieved by means of two distributed integral actions. The proof of the convergence of the augmented system in closed-loop with the proposed static state feedback controller was based on two ideas, a change of coordinates to overcome the communication coupling between the agents, and a passivity condition during the design of the feedback gain to ensure the convergence despite the physical coupling. Finally, an LMI algorithm has been given to simplify the design of the controller gain. The next step will be the design of controllers for SB objective.

2.3 State-of-charge Balancing

In this part, we study the problem of SB, for a DC-MG that includes only SUs. We start first by presenting the considered model and formulating the control problem. Next, we augment the model with distributed leader-follower consensus-like integral actions. By considering similar assumptions as in the previous section, we show that all the states-of-charge converge to the state-of-charge reference. Finally, we give an LMI formulation for the design of the controller gain.

2.3.1 Grid Network

Consider a DC-MG composed of only SUs, i.e., $\mathcal{V}^{pow} = \mathcal{V}^{s}$. Using the generic equation (2.1) and the state-of-charge dynamics (2.2), the overall MG system for all SUs can be written as follows:

$$\begin{aligned} L\dot{I} &= -RI - V + u, \\ C\dot{V} &= I - (R_L^{-1} + \mathcal{L}^{pow})V - I_L, \\ \dot{Soc} &= -K^{soc} I, \end{aligned} \tag{2.49}$$

with I, V, I_L, u, $Soc \in \mathbb{R}^p$. As well, L, C, R, R_L, $K^{soc} \in \mathbb{R}^{p\times p}$ are positive definite diagonal matrices, e.g, $L = diag(l_1, \cdots, l_p)$. The Laplacian matrix $\mathcal{L}^{pow} \in \mathbb{R}^{p\times p}$ represents the topology of the power network.

2.3.2 Problem Formulation

Unbalanced state-of-charge between the SUs can affect the life of the batteries by causing over-charge or over-discharge phenomenon. Thus, balancing the states-of-charge between the SUs is very important to prolong its life and avoid its deterioration.

Objective 2.3. (**State-of-charge balancing**)
At steady state, the state-of-charge have to reach an equilibrium Soc^e s.t.:

$$Soc_i^e = Soc_{ref} \quad \forall i \in \mathcal{V}^s,$$

where the scalar Soc_{ref} represents the state-of-charge reference given by a high-level controller. The latter can use an energy management strategy to define the Soc_{ref} value, e.g. it can send a high Soc_{ref} in case of

low-load operation mode, and small Soc_{ref} in case of high-load operation mode.

Assumption 2.3. (States-of-charge leader) We assume that Soc_{ref} is available only for one SU i_l (called hereafter *leader*), where i_l denotes the index of the leader.

Now, we are able to state the second control problem as :

Control Problem 2. For a given state-of-charge reference Soc_{ref} and an unknown load current I_L, design a distributed-based control law u s.t. the state of system (2.49), in closed-loop, converges globally and asymptotically to an equilibrium for which Objective 3 is satisfied.

2.3.3 Distributed Controller Design

In this section, a solution to Control Problem 2 is provided. Before proceeding to the design of the distributed controllers, similarly to Section 2.2, the following assumptions are considered

Assumption 2.4. (**Nominal model**) All the SUs have the same nominal values of parameters, i.e., $l_i = l$, $c_i = c, r_i = r, r_{Li} = r_L, k_i^{soc} = k^{soc}, \forall i \in \mathcal{V}^s$, with $l,\ c,\ r,\ r_L,\ k^{soc} \in \mathbb{R}_{>0}$ represent the nominal values.

Assumption 2.5. (**Communication network**) The controllers exchange information through a communication network modeled as an undirected graph $\mathcal{G}_s^{com} = (\mathcal{V}^s, \varepsilon^{com}, \mathcal{L}^{com})$ where $\mathcal{L}^{com} \in \mathbb{R}^{p\times p}$ is symmetric positive semidefinite Laplacian matrix which allows to exchange the states-of-charge $Soc_i, \forall i \in \mathcal{V}^s$, between the SUs.

Let us introduce an augmented state $\mathcal{X} = (I, V, Soc, \theta)$ whose dynamics are given as follows:

$$\Sigma^s \begin{cases} L\dot{I} = -RI - V + u, & \text{(2.50a)} \\ C\dot{V} = I - (R_L^{-1} + \mathcal{L}^{pow})V - I_L, & \text{(2.50b)} \\ \dot{Soc} = -K^{soc} I, & \text{(2.50c)} \\ \dot{\theta} = (\mathcal{L}^{com} + \mathcal{J})Soc - Soc_r, & \text{(2.50d)} \end{cases}$$

where the ith line of (2.50d) is given by:

$$\dot{\theta}_i = \sum_{j\in\mathcal{N}_i^{com}} \alpha_{ij}(Soc_i - Soc_j) + \beta_i(Soc_i - Soc_{ref}), \tag{2.51}$$

where $\mathcal{N}_i^{com}$ is the set of SUs connected to the SU i via the communication network with the edge weights $\alpha_{ij} = \alpha_{ji} \in \mathbb{R}_{>0}$, $\beta_i = 0$, $\forall\, i \neq i_l$, and $\beta_{i_l} > 0$ (i_l is the index of leader). Equation (2.50d) represents a leader-follower dynamics where the state-of-charge reference Soc_{ref} is only available for SU_{i_l}. Moreover, $\mathcal{L}^{com}$ is defined in Assumption 2.5 and $\mathcal{J} \in \mathbb{R}^{p\times p}$ is a diagonal matrix of the form

$$\mathcal{J}_{i,i} = \begin{cases} \beta_{i_l} > 0, & i = i_l, \\ 0, & \text{otherwise}, \end{cases} \tag{2.52}$$

and $Soc_r \in \mathbb{R}^p$ is s.t.

$$Soc_{ri} \begin{cases} \beta_{i_l} Soc_{ref}, & i = i_l, \\ 0, & \text{otherwise}. \end{cases} \tag{2.53}$$

Lemma 2.1. The matrix $(\mathcal{L}^{com} + \mathcal{J})$ is invertible and its inverse is symmetric and verifies:

$$[(\mathcal{L}^{com} + \mathcal{J})^{-1}]_{i,i_l} = \frac{1}{\beta_{i_l}}, \quad 1 \leq i \leq p. \tag{2.54}$$

Proof. First, we prove that $(\mathcal{L}^{com} + \mathcal{J})$ is invertible by proving that it is positive definite. Consider a variable $Z = (z_1, ..., z_p) \in \mathbb{R}^p$, we have

$$Z^T(\mathcal{L}^{com} + \mathcal{J})Z = \sum_{(i,j)\in\mathcal{E}^{com}} \alpha_{ij}(z_i - z_j)^2 + \beta_{i_l} z_{i_l}^2,$$

where $\alpha_{ij} \in \mathbb{R}_{>0}$ are defined in (2.51). Since the graph $\mathcal{G}_s^{com}$ is connected and undirected, $(\mathcal{L}^{com} + \mathcal{J})$ is symmetric and $\sum_{(i,j)\in\mathcal{E}^{com}} \alpha_{ij}(z_i - z_j)^2 = 0$ implies $z_i = z_j, \forall i, j \in \mathcal{V}^s$, (consensus).
Hence, one can easily prove that $Z^T(\mathcal{L}^{com} + \mathcal{J})Z$ is positive definite function i.e.:

$$Z^T(\mathcal{L}^{com} + \mathcal{J})Z > 0 \quad \forall Z \neq \mathbb{0}_p. \tag{2.55}$$

Thus, $(\mathcal{L}^{com} + \mathcal{J})$ is invertible.
Now, to prove (2.54), consider the following linear system of equation:

$$(\mathcal{L}^{com} + \mathcal{J})Z = [\mathbf{I}_p]_{*,i_l}, \tag{2.56}$$

with $Z \in \mathbb{R}^p$ and where $[\mathbf{I}_p]_{*,i_l}$ is the i_lth column of the identity matrix $\mathbf{I}_p$.

Since $(\mathcal{L}^{com} + \mathcal{J})$ is invertible, a vector Z solution of (2.56) exists and its unique.

Now, since $\mathcal{L}^{com}$ is a Laplacian matrix we have:

$$(\mathcal{L}^{com} + \mathcal{J})\frac{1}{\beta_{i_l}}\mathbb{1}_p = \mathcal{J}\frac{1}{\beta_{i_l}}\mathbb{1}_p, \tag{2.57}$$

substituting (2.52) in (2.57) yields:

$$(\mathcal{L}^{com} + \mathcal{J})\frac{1}{\beta_{i_l}}\mathbb{1}_p = [\mathbf{I}_p]_{*,i_l}. \tag{2.58}$$

Thus, $Z = \dfrac{1}{\beta_{i_l}}\mathbb{1}_p$ is the unique solution of (2.56). Moreover, we have:

$$(\mathcal{L}^{com} + \mathcal{J})(\mathcal{L}^{com} + \mathcal{J})^{-1} = \mathbf{I}_p, \tag{2.59}$$

it follows:

$$(\mathcal{L}^{com} + \mathcal{J})[(\mathcal{L}^{com} + \mathcal{J})^{-1}]_{*,i_l} = [\mathbf{I}_p]_{*,i_l}, \tag{2.60}$$

where $[(\mathcal{L}^{com} + \mathcal{J})^{-1}]_{*,i_l}$ is the i_lth column of the matrix $(\mathcal{L}^{com} + \mathcal{J})^{-1}$.

Since $(\mathcal{L}^{com} + \mathcal{J})$ is symmetric, (2.58) and (2.60) yields

$$[(\mathcal{L}^{com} + \mathcal{J})^{-1}]_{*,i_l} = \frac{1}{\beta_{i_l}}\mathbb{1}_p. \tag{2.61}$$

Finally, (2.54) is proved. ■

Yet again, it is noteworthy that in (2.51), $\alpha_{ij} = 0$ if SU j is not neighbor of SU i. Hence, only local information are exchanged between the SUs augmented with the additional states (2.51). Thus, if a state feedback controller depending only on the local state at each SU, i.e, $(I_i, V_i, Soc_i, \theta_i), \forall i \in \mathcal{V}^s$, is considered, u will be distributed. Therefore, our goal is to design a distributed controller of the form:

$$u = -F\mathcal{X}, \tag{2.62}$$

where the gain matrix F should be restricted to the form:

$$F = (F_I, F_V, F_{soc}, F_\theta), \tag{2.63}$$

where $F_I,\ F_V,\ F_{soc}, F_\theta$ are diagonal matrices of dimension $p \times p$.

Proposition 2.5. (Equilibrium point) For a given state-of-charge reference Soc_{ref} and an unknown load current I_L, system (2.50) with a stabilizing control input of the form (2.62) has a unique equilibrium point. Moreover, Objective 3 is achieved at that equilibrium.

Proof. At the equilibrium, (2.50) yields to the following conditions:

$$0 = -RI^e - V^e + u^e, \tag{2.64a}$$
$$0 = I^e - (R_L^{-1} + \mathcal{L}^{pow})V^e - I_L, \tag{2.64b}$$
$$0 = -K^{soc} I^e, \tag{2.64c}$$
$$0 = (\mathcal{L}^{com} + \mathcal{J})Soc^e - Soc_r. \tag{2.64d}$$

From (2.64c) we have:

$$I^e = 0. \tag{2.65}$$

Replacing (2.65) in (2.64b) yields:

$$V^e = (R_L^{-1} + \mathcal{L}^{pow})^{-1} I_L, \tag{2.66}$$

note that $(R_L^{-1} + \mathcal{L}^{pow})^{-1}$ is well defined because R_L^{-1} is positive definite matrix and $\mathcal{L}^{pow}$ positive semidefinite matrix.

By Lemma 2.1, (2.64d) gives:

$$Soc^e = (\mathcal{L}^{com} + \mathcal{J})^{-1} Soc_r. \tag{2.67}$$

Substituting (2.65) in (2.64a) gives:

$$u^e = V^e. \tag{2.68}$$

Since in closed-loop $u^e = -F_I I^e - F_V V^e - F_{soc} Soc^e - F_\theta \theta^e$ (see (2.62)-(2.63)), (2.68) yields:

$$\theta^e = -F_\theta^{-1}((F_V + \mathbf{I}_p)V^e + F_{soc} Soc^e). \tag{2.69}$$

Thus, the equilibrium exists and is unique. Moreover, using Lemma 2.1, (2.67) gives:

$$Soc^e = \mathbb{1}_p Soc_{ref}, \tag{2.70}$$

it follows that, at the equilibrium, Objective 3 is achieved. ■

Similarly to Theorem 2.1, the next theorem shows how it is possible to determine the gain matrix F in (2.62).

Theorem 2.2. *If there exists a state feedback gain* $\mathcal{F} = \begin{bmatrix} f_I & f_V & f_{soc} & f_\theta \end{bmatrix}$ *s.t. the triple* (A_{cl_i}, B_p, C_p) *for* $i = 1, \cdots, p$ *are strictly passive, where* $B_p = \begin{bmatrix} 0 & c^{-1} & 0 & 0 \end{bmatrix}^T$, $C_p = \begin{bmatrix} 0 & 1 & 0 & 0 \end{bmatrix}$, $A_{cl_i} = A_{o_i} - B_u \mathcal{F}$, $B_u = \begin{bmatrix} l^{-1} & \mathbb{0}_{3\times 1} \end{bmatrix}^T$

$$A_{o_i} = \begin{bmatrix} A & & \mathbb{0}_{2\times 2} \\ -k^{soc} & 0 & 0 & 0 \\ 0 & 0 & \lambda_i & 0 \end{bmatrix}, A = \begin{bmatrix} -\frac{r}{l} & -\frac{1}{l} \\ \frac{1}{c} & -\frac{1}{cr_L} \end{bmatrix} \text{ and}$$

where λ_i, $i \in \mathcal{V}^s$, *are the eigenvalues of the matrix* $(\mathcal{L}^{com} + \mathcal{J})$ *then the equilibrium point of the augmented system* (2.50) *in closed loop with the state feedback control law*

$$u = -(\mathcal{F} \otimes \boldsymbol{I}_p)(I, V, Soc, \theta) \tag{2.71}$$

is globally exponentially stable and Objective 2.3 is satisfied.

Proof. Let $\tilde{\Sigma}^s$ be the system (2.50) after applying the following change of coordinates:

$$(\tilde{I}, \tilde{V}, \tilde{Soc}, \tilde{\theta}) = (\mathbf{I}_4 \otimes T^T)(I, V, Soc, \theta), \tag{2.72}$$

$$(\tilde{u}, \tilde{I}_L, \tilde{Soc}_r) = (\mathbf{I}_3 \otimes T^T)(u, I_L, Soc_r), \tag{2.73}$$

where $T \in \mathbb{R}^{p\times p}$ is a unitary matrix s.t.

$$(\tilde{\mathcal{L}}^{com} + \tilde{\mathcal{J}}) = T^T(\mathcal{L}^{com} + \mathcal{J})T = \text{diag}(\lambda_1, \dots, \lambda_p),$$

where $\lambda_i, \forall i \in \mathcal{V}^s$, represent the eigenvalues of $(\mathcal{L}^{com} + \mathcal{J})$ s.t. $\lambda_i < \lambda_j, \forall\, i < j$.

Remark 2.6. Note that, differently from (2.16), in $\tilde{\Sigma}^s$ $\lambda_1 \neq 0$; hence, the design of the controller will be easier since system $\tilde{\Sigma}^s$ does not include any uncontrollable constant state as $\tilde{\phi}_1$ in system (2.16).

We denote by $\tilde{\mathcal{X}}^e$ the equilibrium point of system $\tilde{\Sigma}^s$. Similar to the proof of Theorem 2.1, it is sufficient to prove the asymptotic stability of the equilibrium point $\tilde{\mathcal{X}}^e$.
By applying a second change of coordinates of the form

$$\tilde{x} = \mathcal{M}^{s\top}\tilde{\mathcal{X}}, \tag{2.74}$$

where

$$\mathcal{M}^s = \begin{bmatrix} \mathbf{I}_p \otimes [1\ 0\ 0\ 0] \\ \mathbf{I}_p \otimes [0\ 1\ 0\ 0] \\ \mathbf{I}_p \otimes [0\ 0\ 1\ 0] \\ \mathbf{I}_p \otimes [0\ 0\ 0\ 1] \end{bmatrix}, \tag{2.75}$$

another state space representation of system $\tilde{\Sigma}^s$ with the controller (2.71) can be written as:

$$\dot{\tilde{x}} = (\mathcal{A} - \mathcal{B}\tilde{\mathcal{L}}^{pow}\mathcal{C})\tilde{x} + v, \tag{2.76}$$

where

- $\tilde{x} = (\tilde{x}_1, \cdots, \tilde{x}_p)$, $\tilde{x}_i = (\tilde{I}_i, \tilde{V}_i, \tilde{Soc}_i, \tilde{\theta}_i)$,
- $v = (v_1, \cdots, v_p)$, $v_i = (0, -\frac{1}{c}\tilde{I}_{Li}, 0, \tilde{Soc}_{ri})$,
- $\mathcal{A} = \text{diag}(A_{cl_1}, \cdots, A_{cl_p})$,
- $\mathcal{B} = (\mathbf{I}_p \otimes B_p)$,

- $\mathcal{C} = (\mathbf{I}_p \otimes C_p)$.

By assumption, the triple (A_{cl_i}, B_p, C_p) for $i = 1, \cdots, p$ are strictly passive, i.e, there exist matrices $Q_i = Q_i^T > 0$ and $\mu_i > 0$ such that for $i = 1, \cdots, p$

$$A_{cl_i}^T Q_i + Q_i A_{cl_i} \leq -\mu_i Q_i, \tag{2.77a}$$

$$Q_i B_p = C_p^T. \tag{2.77b}$$

Similarly to Theorem 2.1, the proof of Theorem 2.2 can be done by considering the Lyapunov function $V^s(x) = x^T Q x$, with

$$Q = \text{diag}(Q_1, \cdots, Q_p). \tag{2.78}$$

■

2.3.4 LMI Computational Algorithm

The computation of the gain $\mathcal{F}$ can be done similarly to $\mathcal{K}$ by solving the following LMI: there exist a constant $\mu > 0$ and matrices $M_3 = M_3^T > 0$ and M_4 of appropriate dimensions s.t.

$$\overline{A}_o M_3 + M_3 \overline{A}_o^T - B_u M_4 - M_4^T B_u^T \leq -\mu M_3, \tag{2.79a}$$

$$\underline{A}_o M_3 + M_3 \underline{A}_o^T - B_u M_4 - M_4^T B_u^T \leq -\mu M_3, \tag{2.79b}$$

$$B_p = M_3 C_p^T, \tag{2.79c}$$

where B_u, B_p and C_p are given in Theorem 2 and

$$\overline{A}_o = \begin{bmatrix} A & & \mathbb{0}_{2\times 2} \\ -k^{soc} & 0 & 0 \quad 0 \\ 0 \quad 0 & & \lambda_{max} \quad 0 \end{bmatrix},$$

$$\underline{A}_o = \begin{bmatrix} A & & \mathbb{0}_{2\times 2} \\ -k^{soc} & 0 & 0 \quad 0 \\ 0 \quad 0 & & \lambda_{min} \quad 0 \end{bmatrix},$$

where $\lambda_{min} = min(\lambda_i)$, $\lambda_{max} = max(\lambda_i)$, $\ i = 1, \cdots, p$. Then, $\mathcal{F} = M_4 M_3^{-1}$.

2.4 DC-MG with DGUs and SUs

In this part, we show that using the designed controllers in the previous parts, Objectives 2.1-2.3 are achieved simultaneously for a DC-MG that comprises both DGUs and SUs and resistive-inductive power lines (Figs. 2.1 and 2.2).

2.4.1 DC-MG with Resistive Power Lines

In this section, we consider a DC-MG composed of m DGUs, p SUs and resistive power lines, the overall compact DC-MG model is as follows:

$$\begin{aligned} L \begin{bmatrix} \dot{I}^d \\ \dot{I}^s \end{bmatrix} &= -R \begin{bmatrix} I^d \\ I^s \end{bmatrix} - \begin{bmatrix} V^d \\ V^s \end{bmatrix} + \begin{bmatrix} u^d \\ u^s \end{bmatrix}, \\ C \begin{bmatrix} \dot{V}^d \\ \dot{V}^s \end{bmatrix} &= \begin{bmatrix} I^d \\ I^s \end{bmatrix} - (R_L^{-1} + \mathcal{L}^{pow}) \begin{bmatrix} V^d \\ V^s \end{bmatrix} - \begin{bmatrix} I_L^d \\ I_L^s \end{bmatrix}, \\ \dot{Soc} &= -K^{soc} I^s, \end{aligned} \tag{2.80}$$

where I^d, V^d, u^d, $I_L^d \in \mathbb{R}^m$ are related to the DGUs and I^s, V^s, Soc, u^s, $I_L^s \in \mathbb{R}^p$ are related to the SUs with L, C, R, $R_L \in \mathbb{R}^{N \times N}$, $K^{soc} \in \mathbb{R}^{p \times p}$ are diagonal matrices.

Note that the physical coupling is not only between DGU-DGU and SU-SU but also between DGU-SU, since the matrix $\mathcal{L}^{pow}$ is of the following form:

$$\mathcal{L}^{pow} = \begin{bmatrix} \mathcal{L}_{dd}^{pow} & \mathcal{L}_{ds}^{pow} \\ \mathcal{L}_{sd}^{pow} & \mathcal{L}_{ss}^{pow} \end{bmatrix}, \tag{2.81}$$

where $\mathcal{L}_{dd}^{pow} \in \mathbb{R}^{m \times m}$, $\mathcal{L}_{ss}^{pow} \in \mathbb{R}^{p \times p}$, $\mathcal{L}_{ds}^{pow} \in \mathbb{R}^{m \times p}$ and $\mathcal{L}_{sd}^{pow} \in \mathbb{R}^{p \times m}$.

Remark 2.7. (Notation) In Sections 2.2 and 2.3, for the sake of simplicity, generic equation and, mostly, the same notations were used to present the design of the controllers for the DGUs and SUs. However, in what

follows, for more clarity, when it is necessary the indices 'd' and 's' are used for the parameters and variables related to the DGUs and SUs, respectively, as in (2.80).

At this stage, we consider the following problem:

Control Problem 3. Consider Assumptions 2.1-2.5, for a given reference voltage V^{ref}, an unknown load current $I_L = (I_L^d, I_L^s)$ and a state-of-charge reference Soc_{ref}, design a distributed-based control law

$$u = (u^d, u^s)$$

s.t. the state of system (2.80) in closed-loop converges globally and exponentially to a set of equilibrium points whose elements satisfy Objectives 2.1-2.2 for the DGUs and Objective 2.3 for the SUs.

Similarly to Sections 2.2 and 2.3, we denote by Σ system (2.80) augmented with the following additional state:

$$\begin{aligned} \dot{\phi} &= W^T \mathcal{L}_d^{com} W I^d, \\ \dot{\gamma} &= -W^T \mathcal{L}_d^{com} W \gamma + (V^d - V^{ref}), \\ \dot{\theta} &= (\mathcal{L}_s^{com} + \mathcal{J}) Soc - Soc_r. \end{aligned} \tag{2.82}$$

Let $\mathcal{X}$ be the state of system Σ defined as

$$\mathcal{X} = (\mathcal{X}^d, \mathcal{X}^s), \tag{2.83}$$

where $\mathcal{X}^d = (I^d, V^d, \phi, \gamma)$ and $\mathcal{X}^s = (I^s, V^s, Soc, \theta)$.

Definition 2.2. (Set of equilibrium points) For a given reference voltage V^{ref}, an unknown load current $I_L = (I_L^d, I_L^s)$ and a state-of-charge reference Soc_{ref} the set of all the equilibrium points is defined by $S^r = \{\mathcal{X}^e \in \mathbb{R}^{4N} \text{ and } u^e \in \mathbb{R}^N \text{ s.t.: } \dot{\mathcal{X}} = 0\}$.

The following theorem gives a solution to Control Problem 3.

Theorem 2.3. *Consider system Σ, let Assumptions 2.1-2.5, if there exists a state feedback controller*

$$u = -[\mathcal{K} \otimes \boldsymbol{I}_m \;\; \mathcal{F} \otimes \boldsymbol{I}_p]\mathcal{X}, \tag{2.84}$$

where $\mathcal{K}$, $\mathcal{F}$ respect the conditions of Theorems 2.1 and 2.2, respectively. Then, the couple $(\mathcal{X},u)$ of system Σ, in closed-loop, converges globally exponentially to the set of all equilibrium points S^{τ} where Objectives 2.1-2.3 are satisfied.

Proof. Let $\tilde{\Sigma}$ represents system Σ after applying the same changes of coordinates given by (2.15), (2.17), (2.72) and (2.73) for DGUs and SUs, respectively.

As in Sections 2.2 and 2.3 (e.g., (2.35)) one can easily write system $\tilde{\Sigma}$ as N interconnected subsystems whose states are $\tilde{x}_i^d = (\tilde{I}_i^d, \tilde{V}_i^d, \tilde{\phi}_i, \tilde{\gamma}_i), \forall i \in \mathcal{V}^d$, and $\tilde{x}_i^s = (\tilde{I}_i^s, \tilde{V}_i^s, \tilde{Soc}_i, \tilde{\theta}_i), \forall i \in \mathcal{V}^s$.

Now, by pursuing the same reasoning as in the poofs of Theorems 2.1 and 2.2, one can easily prove Theorem 2.3, i.e., first, by considering $\breve{x}^d$ as the vector $\tilde{x}^d$ for which the uncontrollable variable[a] ($\tilde{\phi}_1$) has been removed and by considering the following Lyapunov function:

$$V(\breve{x}^d, \tilde{x}^s) = \breve{x}^{d\top} P \breve{x}^d + \tilde{x}^{s\top} Q \tilde{x}^s, \tag{2.85}$$

where $\breve{x}^d = (\breve{x}_1^d, \cdots, \tilde{x}_m^d)$, $\breve{x}_1^d = (\tilde{I}_1^d, \tilde{V}_1^d, \tilde{\gamma}_1)$, $\tilde{x}^s = (\tilde{x}_1^s, \cdots, \tilde{x}_p^s)$ and where $P = diag(P_1, \cdots, P_m)$ and $Q = diag(Q_1, \cdots, Q_p)$ are symmetric positive definite matrices defined by (2.42) and (2.78), respectively, and respect (2.40)-(2.41) and (2.77), respectively. ■

[a] $\tilde{\phi}_1$ is uncontrollable because it is a constant since $\dot{\tilde{\phi}}_1 = 0$.

2.4.2 DC-MG with Resistive-Inductive Power Lines

In this section, we consider that the power lines are resistive-inductive. Hence, the dynamics of the agents (2.1) becomes:

$$\begin{aligned} l_i \dot{I}_i &= -r_i I_i - V_i + u_i, \\ c_i \dot{V}_i &= I_i - I_{Li} - \frac{V_i}{r_{Li}} - \sum_{k \in \xi_i^{pow}} I_{l_k}. \end{aligned} \tag{2.86}$$

The dynamics of the power line k, $k \in \xi_i^{pow}$ is given by:

$$l_{l_k} \dot{I}_{l_k} = -r_{l_k} I_{l_k} + V_i - V_j, \tag{2.87}$$

where ξ_i^{pow} is the set of power lines connected to agent i .

Remark 2.8. Note that for simplicity and without loss of generality, we have changed the power line index to k rather than ij. Furthermore, by considering a non-zero inductance for power lines, they are no longer static, i.e., we have more dynamics in the system.

Similarly to (2.80), the overall model of the DC-MG with resistive-inductive power lines can be written from (2.86), (2.87) and (2.2) as

$$\begin{aligned} L\begin{bmatrix}\dot{I}^d\\ \dot{I}^s\end{bmatrix} &= -R\begin{bmatrix}I^d\\ I^s\end{bmatrix} - \begin{bmatrix}V^d\\ V^s\end{bmatrix} + \begin{bmatrix}u^d\\ u^s\end{bmatrix}, \\ C\begin{bmatrix}\dot{V}^d\\ \dot{V}^s\end{bmatrix} &= \begin{bmatrix}I^d\\ I^s\end{bmatrix} - R_L^{-1}\begin{bmatrix}V^d\\ V^s\end{bmatrix} + \mathcal{H}I_l - \begin{bmatrix}I_L^d\\ I_L^s\end{bmatrix}, \end{aligned} \tag{2.88}$$

$$\dot{Soc} = -K^{soc}I^s,$$

$$L_l\dot{I}_l = -R_lI_l - \mathcal{H}^TV, \tag{2.89}$$

where $I_l = [I_{l_1}, \cdots, I_{l_q}] \in \mathbb{R}^q$ and $R_l = diag(r_{l_1}, \cdots, r_{l_q})$, $L_l = diag(l_{l_1}, \cdots, l_{l_q}) \in \mathbb{R}^{q\times q}$. The topology of the network is now described by the incidence matrix $\mathcal{H} \in \mathbb{R}^{N\times q}$. The ends of the power line k are arbitrarily labeled with a $+$ and a $-$, and the entries of $\mathcal{H}$ are given by

$$\mathcal{H}_{ik}\begin{cases} +1 & \text{if } i \text{ is the positive end of power line } k \\ -1 & \text{if } i \text{ is the negative end of power line } k \\ 0 & \text{otherwise.} \end{cases} \tag{2.90}$$

Note that the physical coupling between the agents is no more static and the term $-\mathcal{L}^{pow}V$ in (2.80) is replaced by the term $\mathcal{H}I_l$. The next theorem shows that the distributed controllers proposed in Theorem 2.3 can solve Control Problem 3 even if the power lines are resistive-inductive.

Theorem 2.4. ***(main result)*** *The triple $(\mathcal{X}, I_l, u)$ of system (2.88)-(2.89) augmented with (2.82), and in closed-loop with the state feedback controller (2.84) that respects the conditions of Theorem 2.3, converges globally exponentially to the set of all equilibrium points*

$$S^{rl} = \{\mathcal{X}^e \in \mathbb{R}^{4N},\ I_l \in \mathbb{R}^q \text{ and } u^e \in \mathbb{R}^N \text{ s.t.: } \dot{\mathcal{X}} = 0 \text{ and } \dot{I}_l = 0\},$$

where Objectives 2.1-2.3 are satisfied.

Proof. The proof of Theorem 2.4 is based on the passivity of System (2.88) augmented with (2.82) and the inherent passivity of the power lines (2.89). Hence, the proposed Lyapunov function will be composed of the Lyapunov functions used in the proofs of Theorems 2.1 and 2.2 and the storage function of the power lines.

By applying the change of variables (2.17), (2.15), (2.33), and (2.72)-(2.74) on System (2.88)-(2.89) augmented with (2.82) in closed-loop with the control input (2.84) we get:

$$\dot{\tilde{x}} = \mathcal{A}\tilde{x} + \mathcal{B}\mathcal{H}I_l + \mathcal{D}, \tag{2.91}$$

$$L_l\dot{I}_l = -R_lI_l - \mathcal{H}^\top\mathcal{C}\tilde{x}. \tag{2.92}$$

where

- $\tilde{x} = \left[\tilde{x}^d, \tilde{x}^s\right]^\top$,
- $\mathcal{A} = diag(\mathcal{A}^d, \mathcal{A}^s)$,
- $\mathcal{C} = diag(\mathcal{C}^d, \mathcal{C}^s)$,
- $\mathcal{B} = diag(\mathcal{B}^d, \mathcal{B}^s)$,
- $\mathcal{D} = \begin{bmatrix} d & v \end{bmatrix}^\top$,
- $\tilde{x}^d$, $\mathcal{A}^d$, $\mathcal{C}^d$, $\mathcal{B}^d$ and d are defined in (2.38),
- $\tilde{x}^s$, $\mathcal{A}^s$, $\mathcal{C}^s$, $\mathcal{B}^s$ and v are defined in (2.76).

Now, the global exponential convergence of the triple $(\mathcal{X}, I_l, u)$ to the set $\mathcal{S}^{rl}$ can be concluded by the same reasoning in the proof of Theorems 2.1 and 2.2, i.e., first considering $\breve{x}$ as the vector $\tilde{x}$ for which the uncontrollable variable ($\tilde{\phi}_1$) has been removed and by considering the following Lyapunov function:

$$V(\breve{x}, I_l) = \frac{1}{2}\breve{x}^\top \Lambda \breve{x} + \frac{1}{2} I_l^\top L_l I_l, \tag{2.93}$$

where

$$\Lambda = \begin{bmatrix} P & 0 \\ 0 & Q \end{bmatrix},$$

and where P and Q are positive definite matrices defined by (2.42) and (2.78). By differentiating $V(.,.)$ along the trajectories we get:

$$\dot{V}(\breve{x}, I_l) = \breve{x}^{d\top} P \mathcal{A}^d \breve{x}^d + \breve{x}^{s\top} Q \mathcal{A}^s \breve{x}^s + \breve{x}^\top \Lambda \mathcal{B} \mathcal{H} I_l - I_l^\top R_l I_l - I_l^\top \mathcal{H}^\top \mathcal{C} \breve{x}, \tag{2.94}$$

by considering the passivity conditions defined by (2.40) and (2.77), (2.94) becomes

$$\begin{aligned} \dot{V}(\breve{x}, I_l) &= \breve{x}^{d\top} P \mathcal{A}^d \breve{x}^d + \breve{x}^{s\top} Q \mathcal{A}^s \breve{x}^s + \breve{x}^\top \mathcal{C}^\top \mathcal{H} I_l - I_l^\top R_l I_l - I_l^\top \mathcal{H}^\top \mathcal{C} \breve{x}, \\ &= \breve{x}^{d\top} P \mathcal{A}^d \breve{x}^d + \breve{x}^{s\top} Q \mathcal{A}^s \breve{x}^s - I_l^\top R_l I_l, \\ &\leq -\epsilon \breve{x}^{d\top} P \breve{x}^d - \mu \breve{x}^{s\top} Q \breve{x}^s - I_l^\top R_l I_l, \\ &< 0, \end{aligned} \tag{2.95}$$

where $\epsilon = diag(\epsilon_1, \cdots, \epsilon_m)$ and $\mu = diag(\mu_1, \cdots, \mu_p)$. Consequently, the state vector $\begin{bmatrix} \breve{x} & I_l \end{bmatrix}^T$ converges globally exponentially to the equilibrium point $\begin{bmatrix} \breve{x}^e & I_l^e \end{bmatrix}^\top$ whose value depends on the constant vector $\mathcal{D}$ in (2.91).

■

Remark 2.9. (Independent communication networks) The communication networks of the DGUs and SUs are independent, i.e., it can be separated and do not need to have the same topology or the same Laplacian matrix. Furthermore, the topology of the communication network does not necessarily have to be the same as the topology of the physical network.

Remark 2.10. (Power lines infromation) The controller proposed in this thesis does not need to measure the power line current I_{l_k} and the load current I_L or to know the power line parameters L_{l_k}, R_{l_k}.

Remark 2.11. Assumptions 2.2 and 2.4 can be viewed as conservative. In practice, the values of the parameters of the agents are prescribed within a fixed range that notably depends in particular on the power of the DGU and SU. Moreover, we will see in the next chapter that the ability of the proposed controllers to reject the discrepancies between nominal and real parameters is noticeable. Although it is not the scope of the thesis, additional stability results for the MG with the controller can be formulated using a polytopic approach. This approach gives the possibility to check the stability of the proposed controllers when parameters are within a prescribed range of values [81].

2.5 Conclusion

Under the assumption that the agents (DGUs or SUs) have the same physical parameter values (Assumptions 2.2 and 2.4). A distributed-based static-state-feedback control law, including integral actions to achieve, provably and simultaneously, proportional current sharing, average voltage regulation and state-of-charge balancing in DC power networks has been proposed.

First, the problems of CS and AVR were considered for a DC-MG composed of only DGUs with resistive power lines and loads. The system is augmented with two distributed consensus-like integral actions. The existence of equilibrium points for the augmented system was proved (Proposition 2.1) and a distributed-based static state feedback control architecture was proposed (Proposition 2.3). We provided proof of global convergence of the augmented system state to a set of equilibrium for which the two objectives are achieved (Theorem 2.1).

Second, the problem of SB was addressed for a DC-MG composed of only SUs with resistive power lines and loads. The system is augmented with a distributed leader-follower-like integral action where the information about the state-of-charge reference Soc_{ref} is provided to only one SU, that we called *the leader*. Similarly to the previous part, the proofs of the existence of equilibrium points for the augmented system (Proposition 2.5) and the global exponential stability (Theorem 2.2) were provided.

Finally, we combined the previous results to achieve simultaneously CS, AVR, and SB for a DC-MG that includes both DGUs and SUs. First, by considering resistive power lines (Theorem 2.3) and then resistive-inductive power lines (Theorem 2.4). LMI computational algorithms were given to simplify the design of the controllers.

In the next chapter, several tests using both Matlab/Simulink simulation and real-time hardware-in-the-loop experiment will be performed to evaluate the performance of the proposed controllers.

Chapter 3

Case Study: Matlab Simulation and Real-Time HIL Implementation

Contents

In this chapter, the controllers proposed in Chapter 2 are tested. In Section 3.1, we present the considered DC-MG case study with its topology, parameter values, the controller gains values, etc. In section 3.2, a Matlab/Simulink simulation scenario is considered to show the performance of the controller in case of resistive and resistive-inductive power lines. In this scenario, the agents (DGUs or SUs) have the same parameter values. In Section 3.3, more scenarios are considered for HIL experiments e.g., current demand variation, voltage reference variation, state-of-charge reference variation, etc. In each scenario of this section,

the efficiency of the controller is assessed in two cases i.e. when the agents have the same or different physical parameter values.

3.1 Case Study

We consider a MG composed of 3 DGUs and 3 SUs as shown in Fig. 3.1, where also two independent communication networks are depicted. The nominal and real parameters of each DGU and SU, load current and power lines parameters are reported in Tables 3.1-3.4. In this example, we consider that the information about the Soc_{ref} is available only for SU 1 (the leader). The computed controller gains are

$$\begin{aligned} \mathcal{K} &= \begin{bmatrix} 1501.96 & 1.11 & 0.47 & 68.49 \end{bmatrix}, \\ \mathcal{F} &= \begin{bmatrix} 02.98 & 0.168 & -537.18 & -0.09 \end{bmatrix}. \end{aligned} \tag{3.1}$$

The parameter τ in (2.12d) is set to 400 and the gain β_{i_l} in (2.51) is set to 10. The Laplacian matrices of the power and communication networks are, respectively, as follows:

$$\mathcal{L}_d^{com} = 28.10^4 \begin{bmatrix} 1 & -1 & 0 \\ -1 & 2 & -1 \\ 0 & -1 & 1 \end{bmatrix}, \mathcal{L}_s^{com} = \begin{bmatrix} 10 & -10 & 0 \\ -10 & 20 & -10 \\ 0 & -10 & 10 \end{bmatrix}.$$

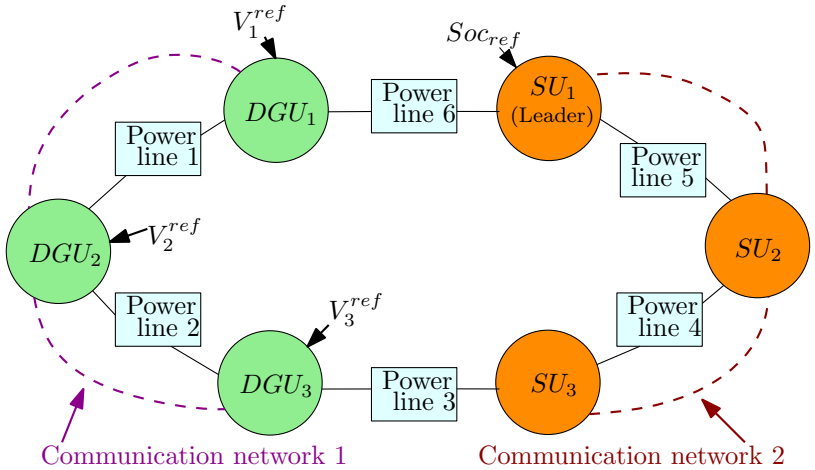

Figure 3.1: MG with 3 DGUs, 3 SUs, power lines and two independent communication networks.

Remark 3.1. Note that, the use of $\bullet \in \{d, s\}$ in Tables 3.1-3.3 is to distinguish the parameters and variables

Table 3.1: MG nominal parameters values with $\bullet \in \{d, s\}$.

Agent	DGU 1	DGU 2	DGU 3	SU 1	SU 2	SU 3
$l^{\bullet}$ (mH)	4	4	4	3	3	3
$c^{\bullet}$ (mF)	6	6	6	1	1	1
$r^{\bullet}$ $(m\Omega)$	1	1	1	2	2	2
$r_L^{\bullet}$ (Ω)	50	50	50	80	80	80
k^{soc}	/	/	/	0.01	0.01	0.01

Table 3.2: MG real parameters values with $\bullet \in \{d, s\}$.

Agent	DGU 1	DGU 2	DGU 3	SU 1	SU 2	SU 3
$l_i^{\bullet}$ (mH)	1.6	4	24	1.2	3	18
$c_i^{\bullet}$ (mF)	2.4	6	36	0.4	1	6
$r_i^{\bullet}$ $(m\Omega)$	0.4	1	6	0.8	2	12
$r_{Li}^{\bullet}$ (Ω)	20	50	300	32	80	480
k_{soc_i}	/	/	/	0.01	0.02	0.03

Table 3.3: Voltage references, state-of-charge references, load current and weights.

Agent	DGU 1	DGU 2	DGU 3	SU 1	SU 2	SU 3
ω_i^{-1}	80	60	30	/	/	/
$V^{ref}(0)$ (V)	380	380	380	/	/	/
$Soc_{ref}(0)$ $(\%)$	/	/	/	60	0	0
$I_{Li}^{\bullet}(0)$ (A)	30	20	25	15	5	10

Table 3.4: Power line parameters values.

Power line	1	2	3	4	5	6
$r_{l_{ij}}$ $(m\Omega)$	80	60	50	40	30	70
$l_{l_{ij}}$ (μH)	2	1.9	1.8	2.3	2.1	2.4

of the DGUs and SUs, e.g. r^d for DGU and r^s for SU.

In what follows, the power line can be considered as resistive or resistive-inductive. In the case of resistive

power lines, the topology of the DC-MG in Fig. 3.1 is represented by a Laplacian matrix given by:

$$\mathcal{L}^{pow} = \begin{bmatrix} 26.8 & -12.5 & 0 & -14.3 & 0 & 0 \\ -12.5 & 29.2 & -16.7 & 0 & 0 & 0 \\ 0 & -16.7 & 36.7 & 0 & 0 & -20 \\ -14.3 & 0 & 0 & 47.6 & -33.3 & 0 \\ 0 & 0 & 0 & -33.3 & 58.3 & -25 \\ 0 & 0 & -20 & 0 & -25 & 45 \end{bmatrix}.$$

In the other case the topology of the MG is represented by the following incidence matrix:

$$\mathcal{H} = \begin{bmatrix} -1 & 0 & 0 & 0 & 0 & 1 \\ 1 & -1 & 0 & 0 & 0 & 0 \\ 0 & 1 & -1 & 0 & 0 & 0 \\ 0 & 0 & 0 & 0 & 1 & -1 \\ 0 & 0 & 0 & 1 & -1 & 0 \\ 0 & 0 & 1 & -1 & 0 & 0 \end{bmatrix}.$$

3.2 Matlab Simulation

In this section, the DC-MG is implemented in Matlab/Simulink environment. To investigate the performance of the proposed control approach, two cases are considered with the same scenario. In the first case, we consider that the power lines are only resistive. However, in the second one, resistive-inductive power lines are considered. Moreover, in both of the cases, the proposed controller is tested with the nominal parameters of DC-MG (see Table 3.1).

The system is initially at the steady state with $I_L(0)$, $V^{ref}(0)$ and $Soc_{ref}(0)$. Then, at the time instant $t = t_1$ the load current I_L is stepped up with

$$\Delta I_L = \begin{bmatrix} 15 & 10 & -5 & 7.5 & 5 & -2.5 \end{bmatrix} A$$

.

As we can see in Fig. 3.2, in the two cases, the weighted currents converge to the same consensus value

achieving Objective 2.1 and the generated currents converge to the desired steady-state, and all the DGUs are at the same percentage of their rated current. Moreover, Objective 2.1 is still maintained during the transient phase. The voltages at the PCC, in the two cases, are illustrated in Fig. 3.3. Note that the weighted average voltage converges to the weighted average value of the reference voltages (see Objective 2.2). Furthermore, the voltages at the PCC converge, without oscillations, to a steady-state near to the reference voltage. The state-of-charge and currents of the SUs are illustrated in Fig. 3.4. One can appreciate that, after the load current variation, the state-of-charge converge to their reference (Objective 2.3) by pursuing their leader Soc_1. However, their convergence is very slow since their time constants are very big regarding the other time constants of the system.

The results illustrate the ability of the controller to practically maintain the same performance in the two considered cases and its robustness under the change of the unknown load current.

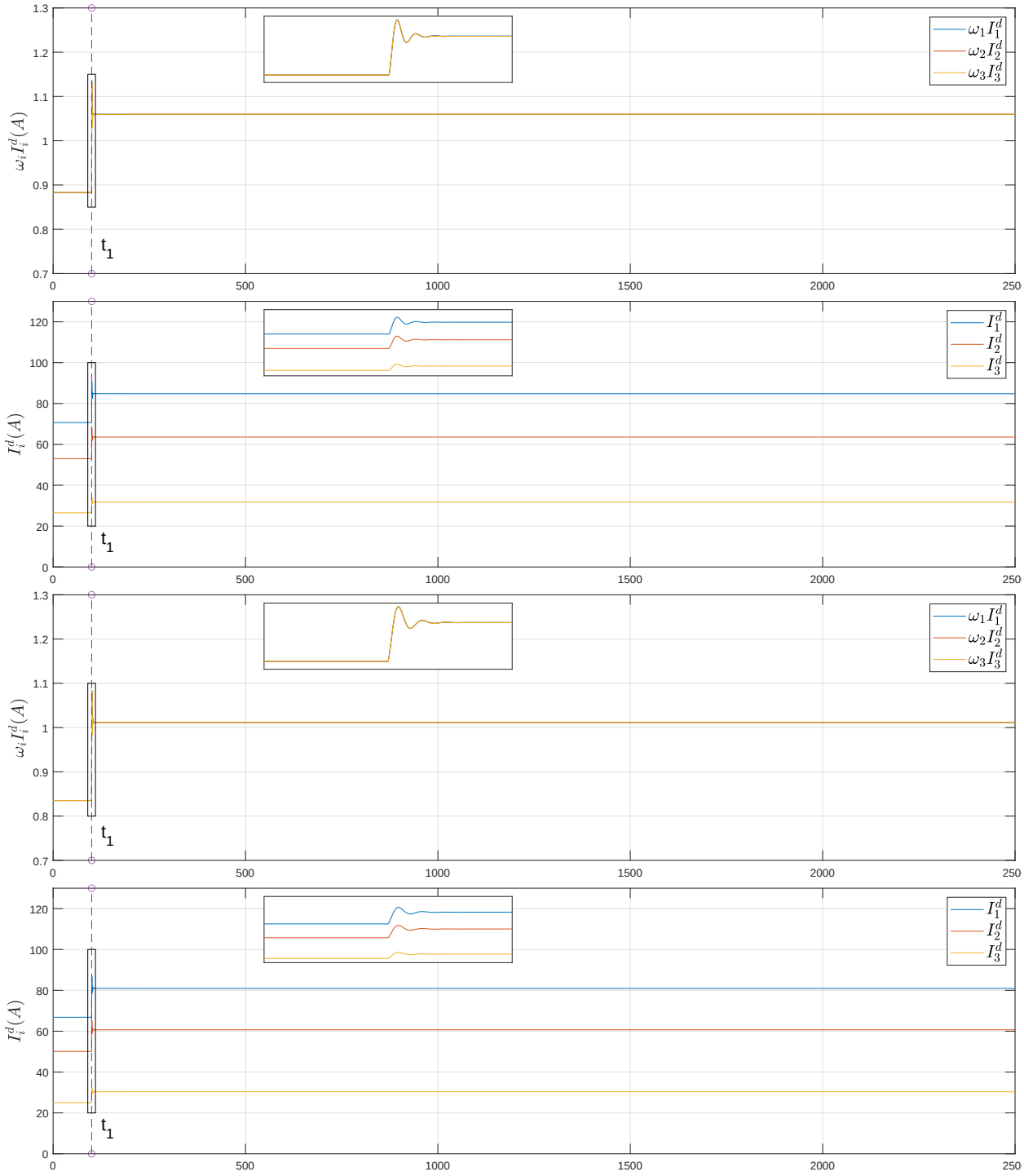

Figure 3.2: Matlab Simulation: from the top, weighted generated currents and generated currents of the DGUs in case of resistive and resistive-inductive power lines, respectively.

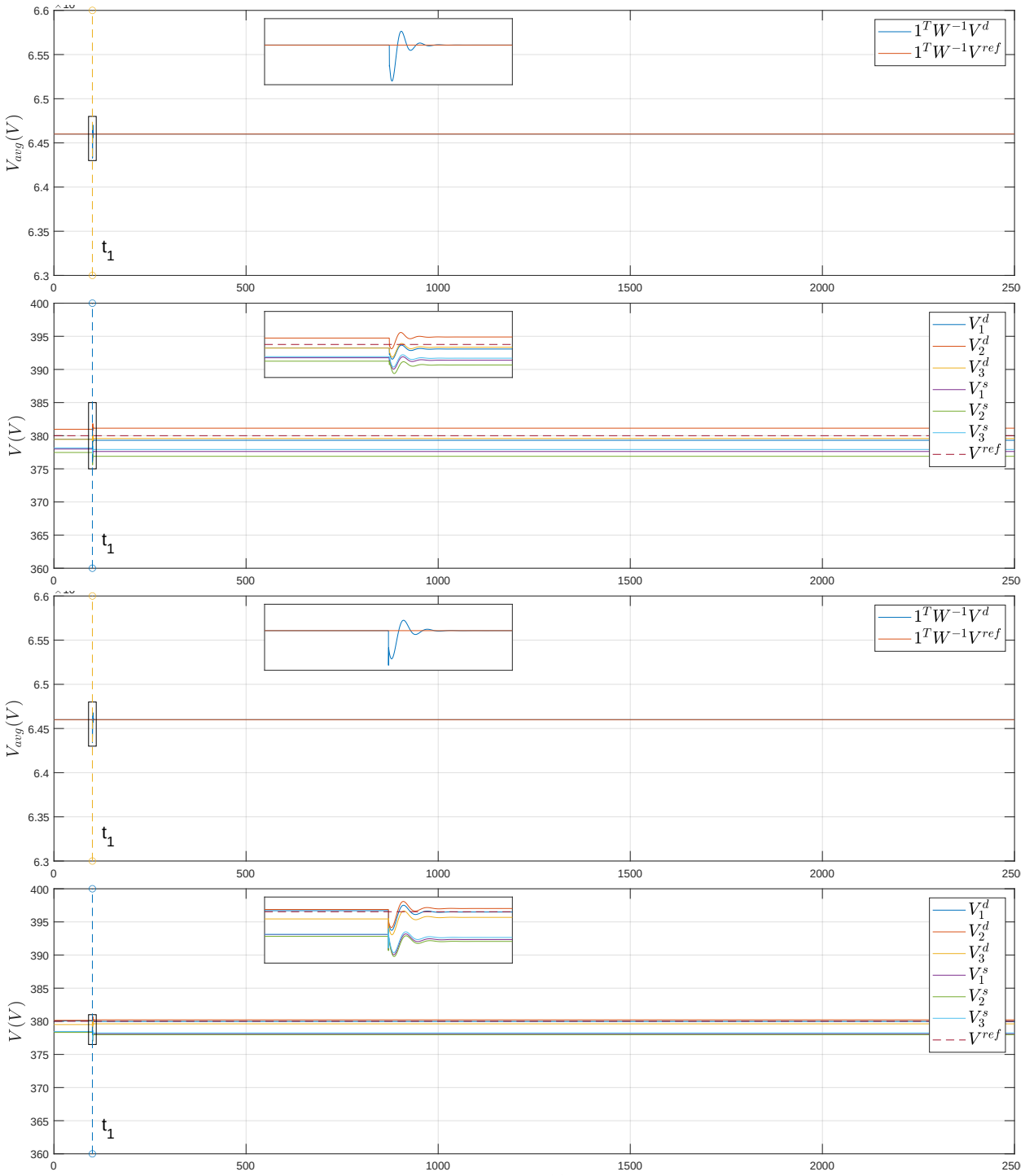

Figure 3.3: Matlab Simulation: from the top, weighted average voltage at the PCC near the DGUs together with the weighted average voltage reference value (dashed line); voltage at the PCC of each DGU and SU together with the reference value (dashed line) in case of resistive and resistve-inductive power lines, respectively.

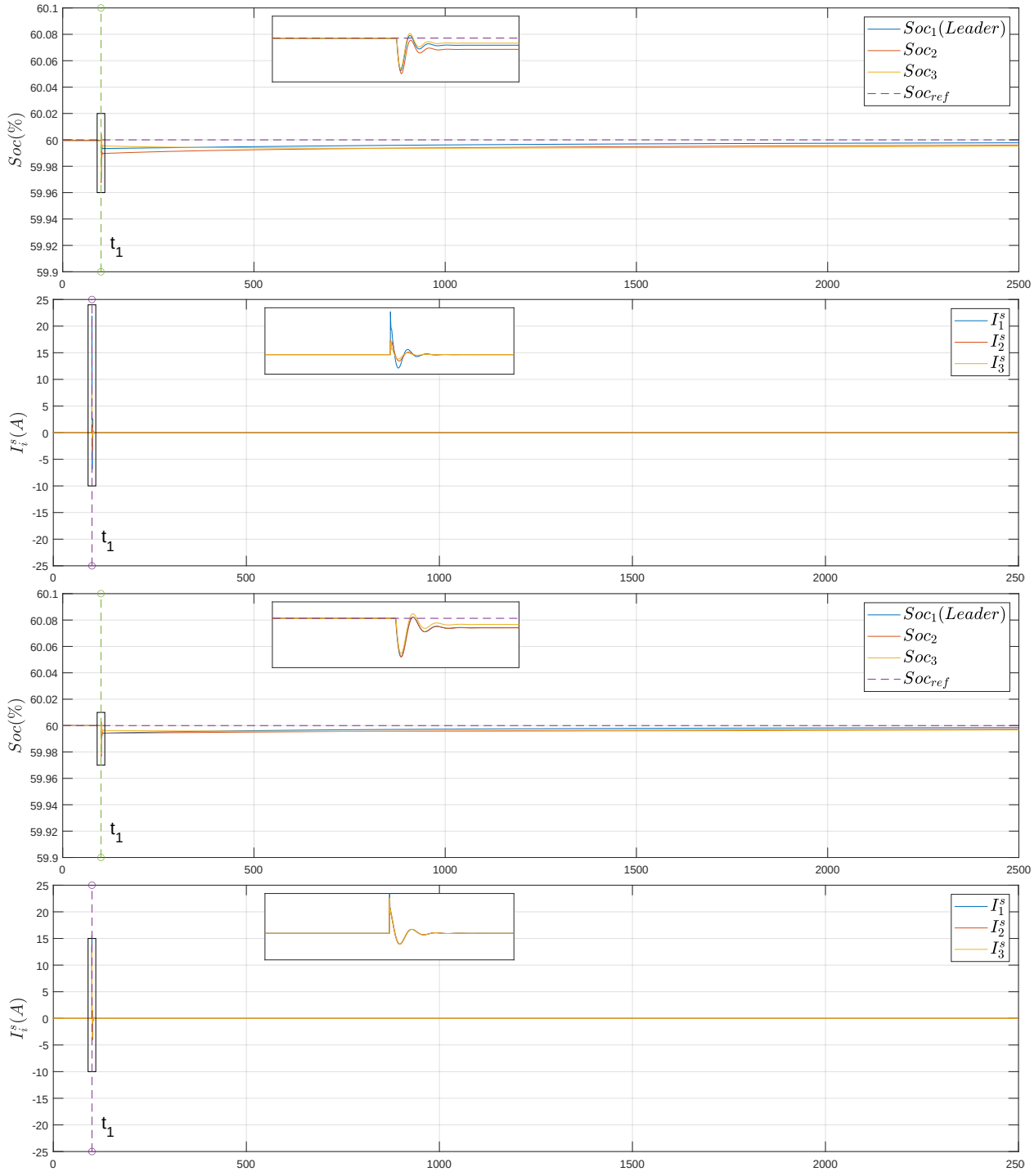

Figure 3.4: Matlab Simulation: from the top, states-of-charge of the SUs; generated current of SUs in case of resistive and resisitive-inductive power lines, respectively.

3.3 Real-Time Hardware-In-the-Loop Tests

In this section, we aim to validate the proposed controller by Real-Time hardware-in-the-loop tests. The MG was emulated using National-Instruments (NI) PXI system (PXIe-1082 chassis with NI PXIe-8135, FPGA and Input/Output modules). A MicroLabBox of dSPACE with DS1202 baseboard is used to receive the information and send the commands.

Differently from Section 3.2, we consider more scenarios to assess the proposed control methodology. In each scenario, two cases are considered. The first one corresponds to a DC-MG with nominal parameters (Table 3.1) while the second one correspond to the DC-MG with real parameters (Table 3.2) both with resistive-inductive power lines.

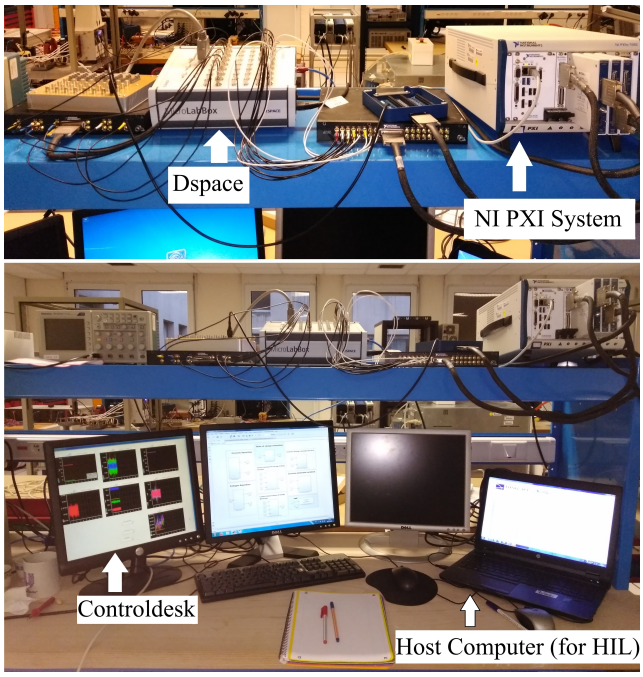

Figure 3.5: Experimental platform of the proposed HIL simulation system.

3.3.1 Scenario 1: load current variation near DGUs

In this scenario, we investigate the effectiveness of the proposed controllers under a load current variation near the DGUs. The system is initially at the steady state with $I_L(0)$, $V^{ref}(0)$ and $Soc_{ref}(0)$. Then:

- At the time instant $t = t_1$ the load current I^d_{L1} near DGU 1 is stepped up with $\Delta I^d_{L_1} = 15$ A.
- At the time instant $t = t_2$ the load current I^d_{L2} near DGU 2 is stepped up with $\Delta I^d_{L_2} = 15$ A.
- At the time instant $t = t_3$ the load current I^d_{L3} near DGU 3 is stepped up with $\Delta I^d_{L_3} = 15$ A.
- At the time instant $t = t_4$ the load current I^d_{L1} near DGU 1 is stepped down with $-\Delta I^d_{L_1}$.
- At the time instant $t = t_5$ the load current I^d_{L2} near DGU 2 is stepped down with $-\Delta I^d_{L_2}$.
- At the time instant $t = t_6$ the load current I^d_{L3} near DGU 3 is stepped down with $-\Delta I^d_{L_3}$.

The currents and the weighted current of the DGUs are illustrated in Fig. 3.6. One can appreciate that the weighted currents converge to the same consensus value achieving Objective 2.1 and the generated currents converge to the desired steady-state, and all the DGUs are at the same percentage of their rated current. Moreover, note that Objective 2.1 is still maintained during the transient phase. Finally, Objectives 2.2 and 2.3 are also still reached (Fig. 3.7 and 3.8).

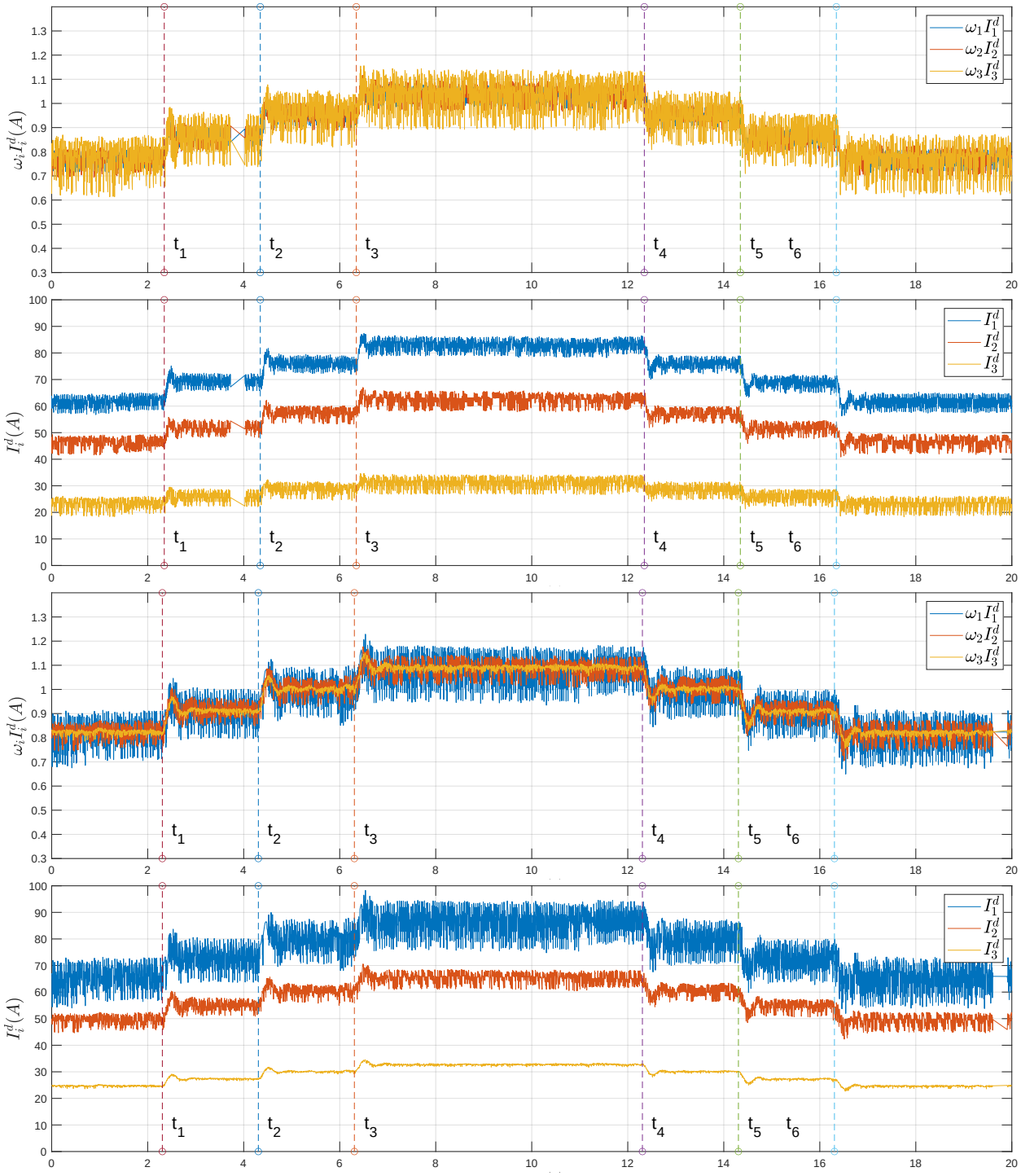

Figure 3.6: Real-Time tests - Scenario 1: from the top, weighted generated currents and generated currents of the DGUs in case of the nominal and real models, respectively.

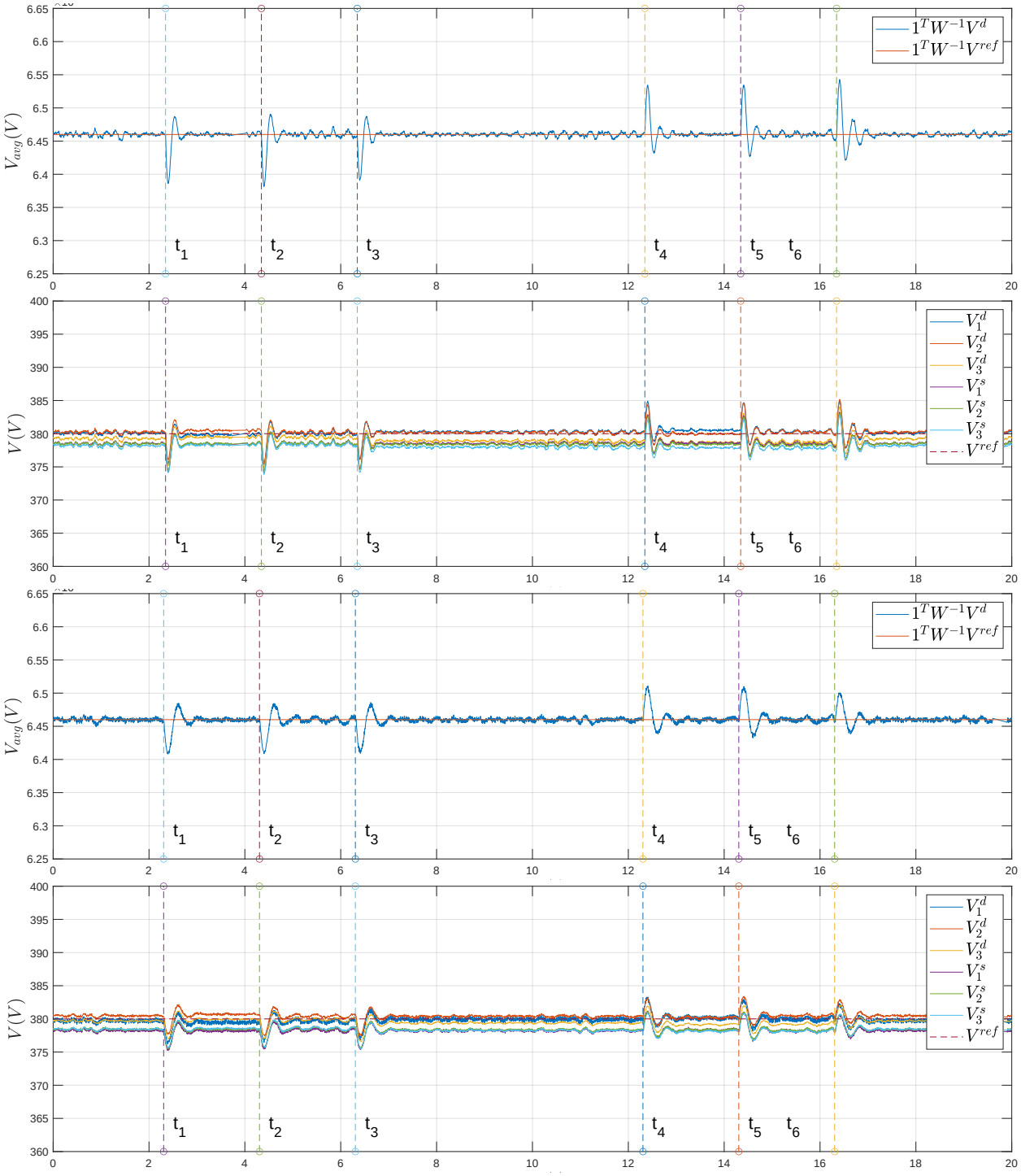

Figure 3.7: Real-Time tests - Scenario 1: from the top, weighted average voltage at the PCC near the DGUs together with the weighted average voltage reference value (dashed line); voltage at the PCC of each DGU and SU together with the reference value (dashed line) in case of the nominal and real models, respectively.

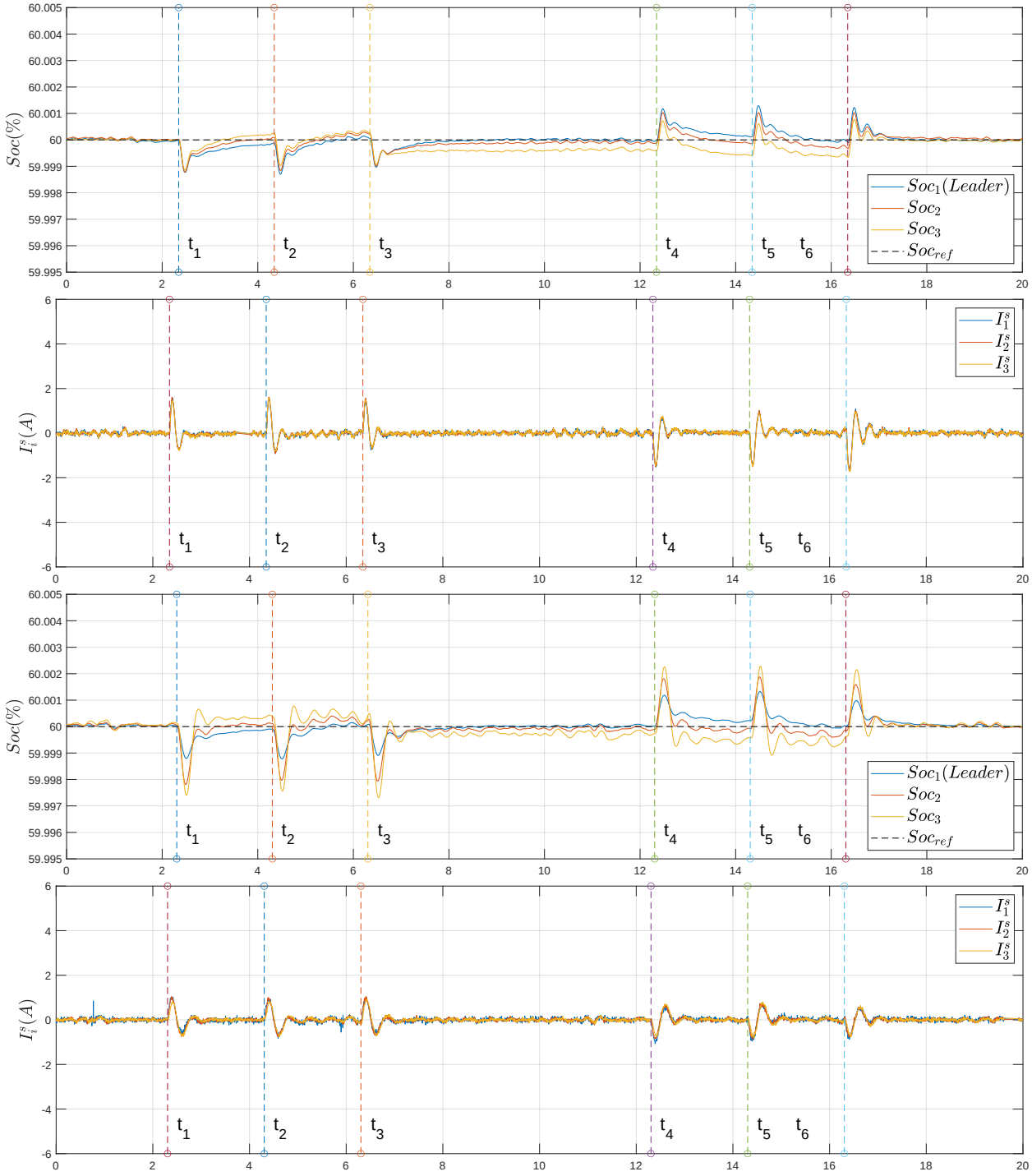

Figure 3.8: Real-Time tests - Scenario 1: from the top, states-of-charge of the SUs; generated current of SUs in case of the nominal and real models, respectively.

3.3.2 Scenario 2: load current variation near SUs

In the second scenario, the performance of the proposed controllers is tested under a load current variation near the SUs. The system is initially at the steady-state with $I_L(0)$, $V^{ref}(0)$ and $Soc_{ref}(0)$. Then:

- At the time instant $t = t_1$ the load current I^s_{L1} near SU 1 is stepped up with $\Delta I^s_{L_1} = 15$ A.
- At the time instant $t = t_2$ the load current I^s_{L2} near SU 2 is stepped up with $\Delta I^s_{L_2} = 15$ A.
- At the time instant $t = t_3$ the load current I^s_{L3} near SU 3 is stepped up with $\Delta I^s_{L_3} = 15$ A.
- At the time instant $t = t_4$ the load current I^s_{L1} near SU 1 is stepped down with $-\Delta I^s_{L_1}$.
- At the time instant $t = t_5$ the load current I^s_{L2} near SU 2 is stepped down with $-\Delta I^s_{L_2}$.
- At the time instant $t = t_6$ the load current I^s_{L3} near SU 3 is stepped down with $-\Delta I^s_{L_3}$.

As we can see in Fig. 3.9 and 3.10, Objectives 2.1 and 2.2 are still respected. The state-of-charge and the currents of the SUs are illustrated in Fig. 3.11. One can note how the state-of-charge react to load current differently than Scenario 1 (see Fig. 3.8). Indeed, in this scenario, the state-of-charge are more reactive to the load current i.e. when the load current increases the state-of-charge decrease more than Scenario 1 and take more time to go back to their reference. This aims to compensate the load current variation because when the state-of-charge decrease the generated currents of the SUs increase.

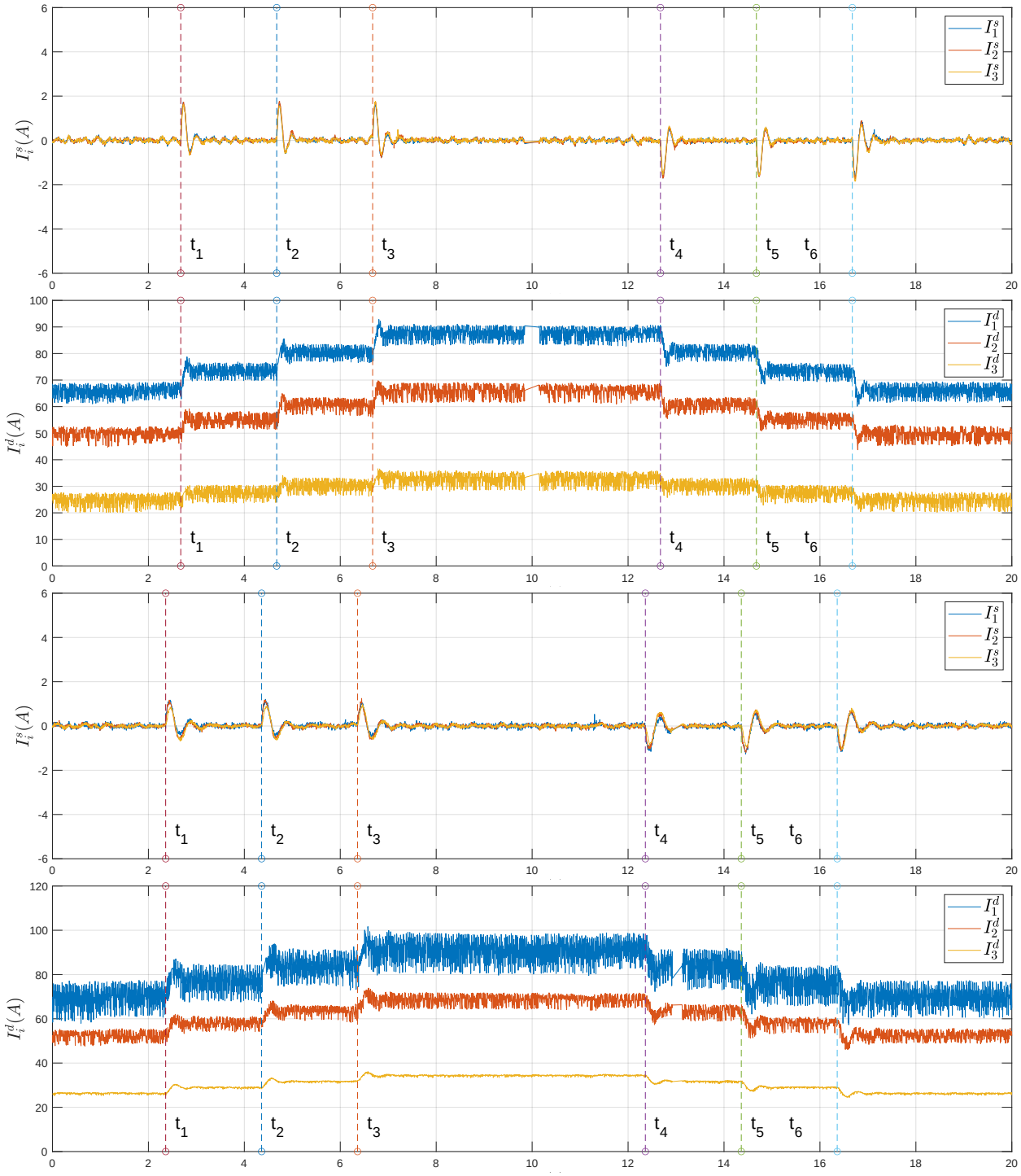

Figure 3.9: Real-Time tests - Scenario 2: from the top, weighted generated currents and generated currents of the DGUs in case of the nominal and real models, respectively.

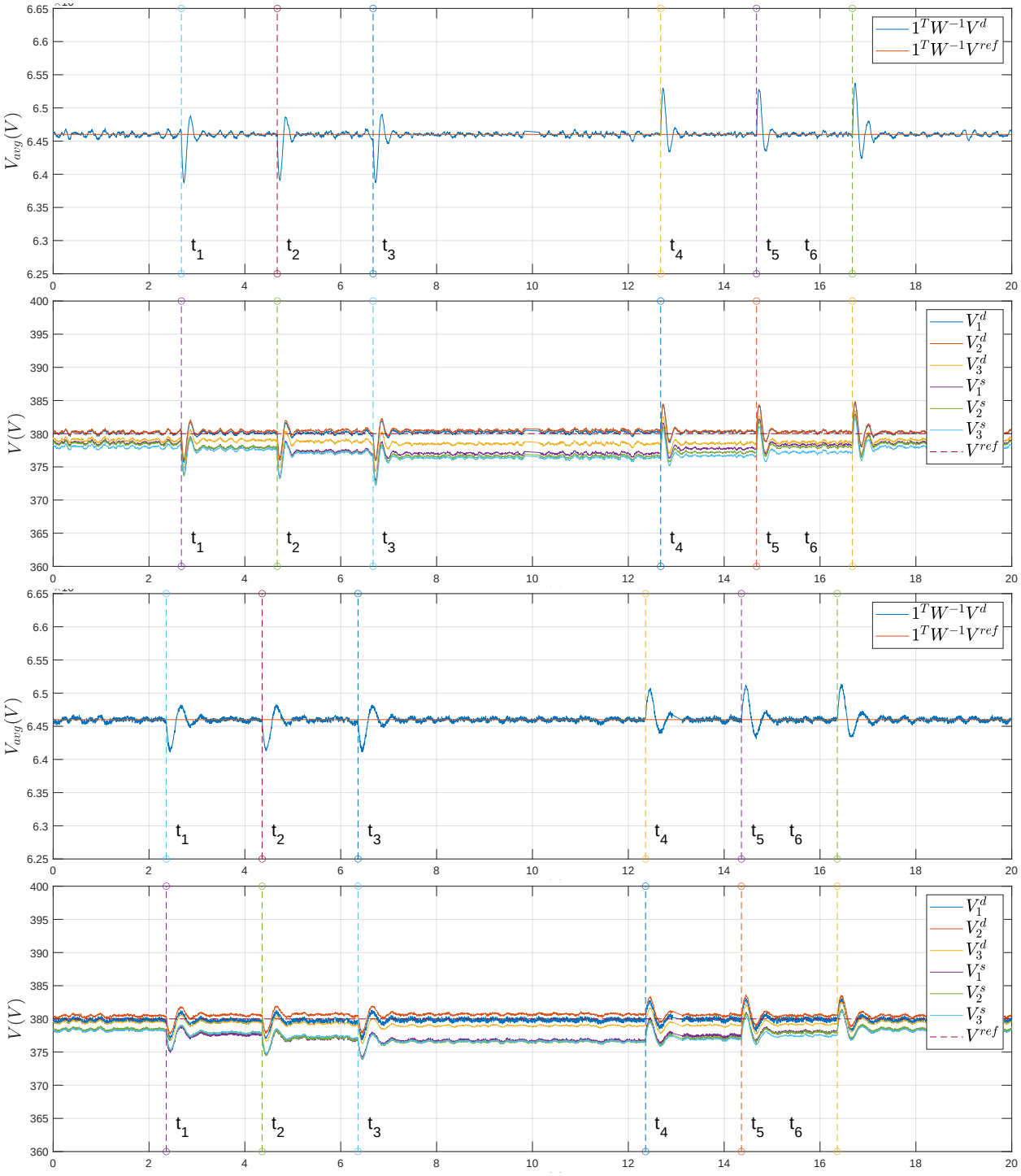

Figure 3.10: Real-Time tests - Scenario 2: from the top, weighted average voltage at the PCC near the DGUs together with the weighted average voltage reference value (dashed line); voltage at the PCC of each DGU and SU together with the reference value (dashed line) in case of the nominal and real models, respectively.

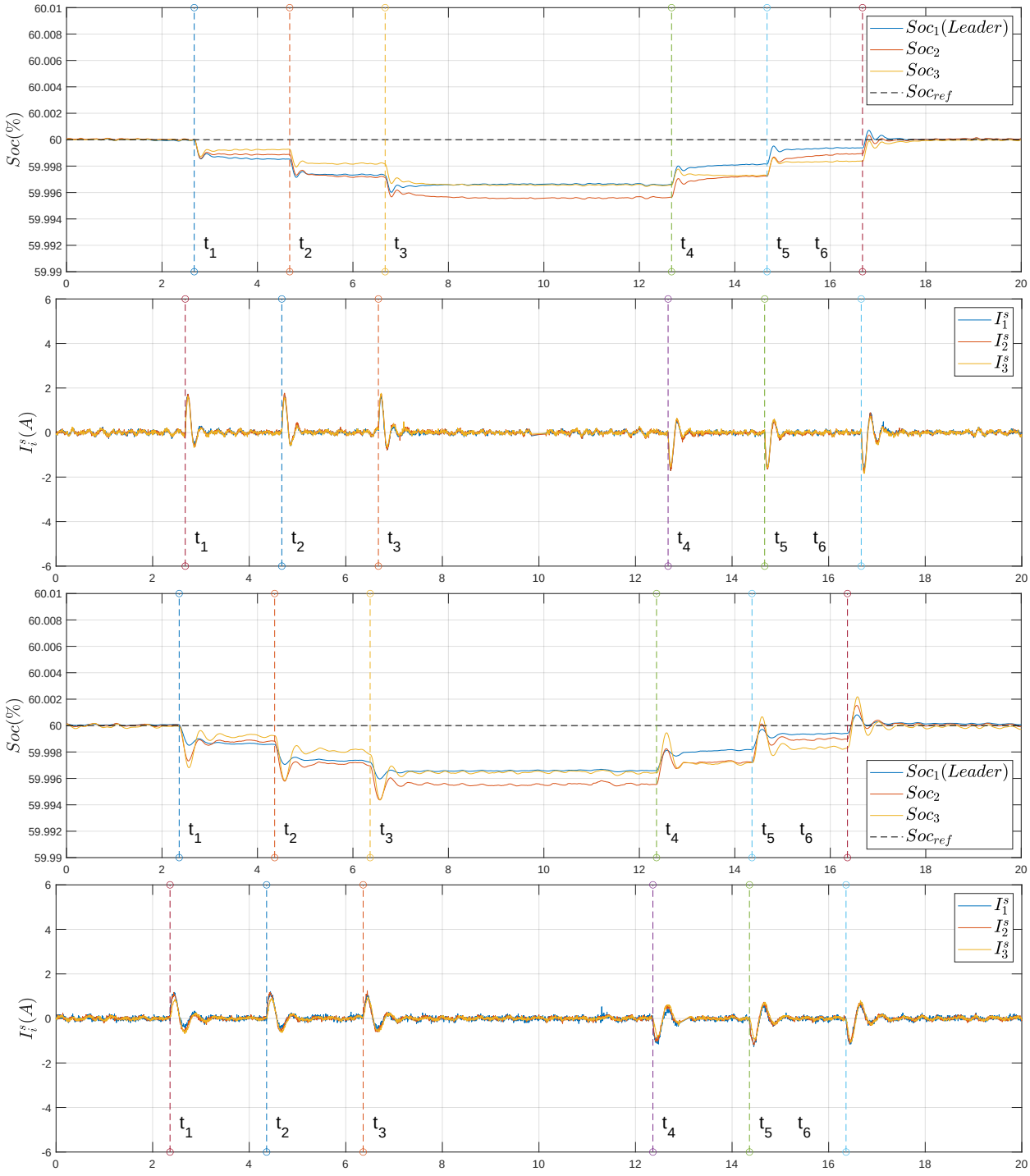

Figure 3.11: Real-Time tests - Scenario 2: from the top, states-of-charge of the SUs; generated current of SUs in case of the nominal and real models, respectively.

3.3.3 Scenario 3: high-load operating mode

In the third scenario, the performance of the proposed controllers is assessed in the case of high-load operation mode. The system is initially at the steady state with $I_L(0)$, $V^{ref}(0)$ and $Soc_{ref}(0)$. Then:

- At the time instant $t = t_1$ the load current I_L^d near the DGUs is stepped up with $\Delta I_L^d = \begin{bmatrix} 40 & 40 & 40 \end{bmatrix}$ A.
- At the time instant $t = t_2$ the load current I_L^d near the DGUs is stepped down with $-\Delta I_L^d$ A.

Fig. 3.12-3.14 illustrate the ability of the MG in closed loop with the proposed controllers, to manage an instantaneous transition between high-load and small-load operating modes ($\pm 120A$).

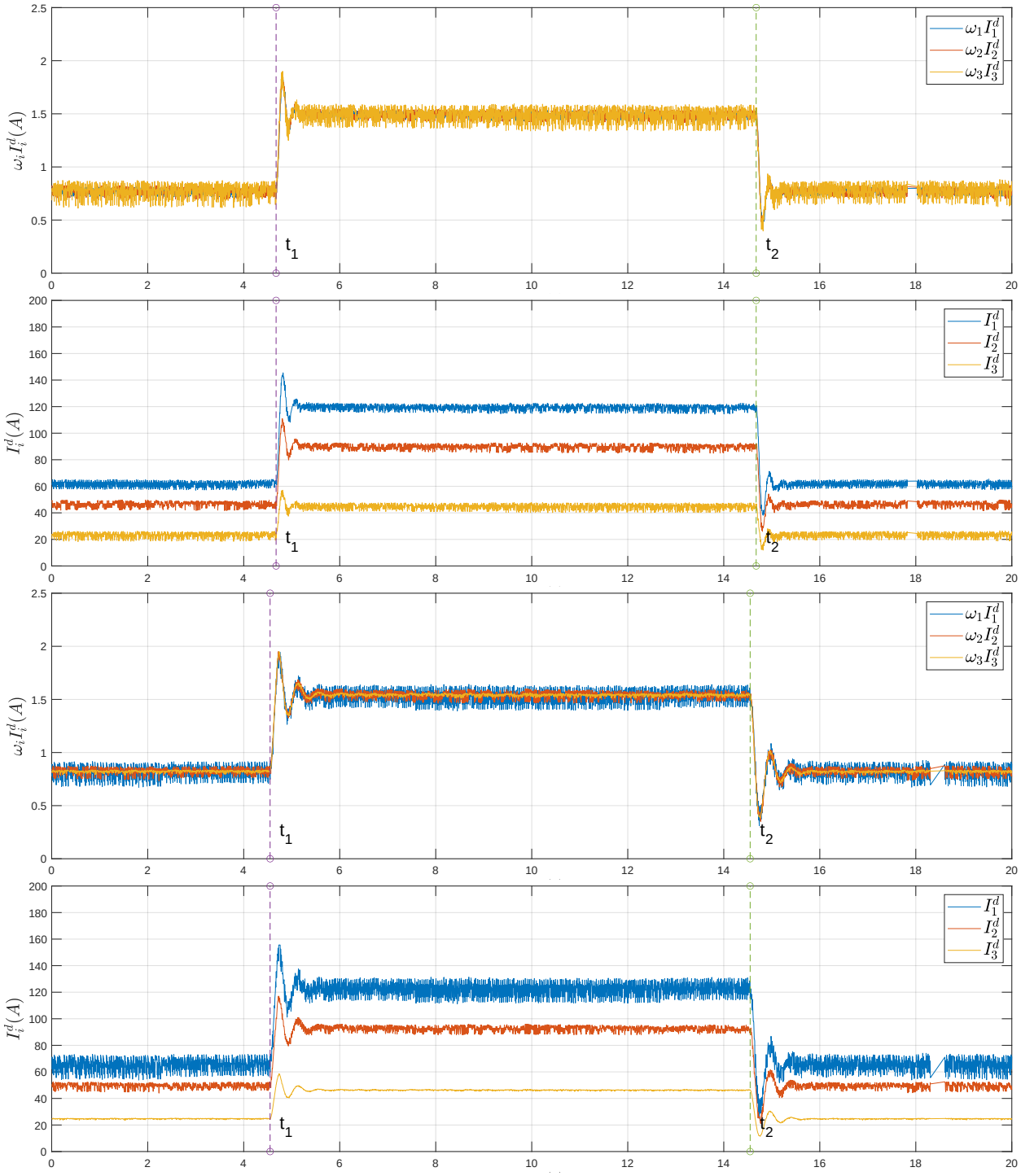

Figure 3.12: Real-Time tests - Scenario 3: from the top, weighted generated currents and generated currents of the DGUs in case of the nominal and real models, respectively.

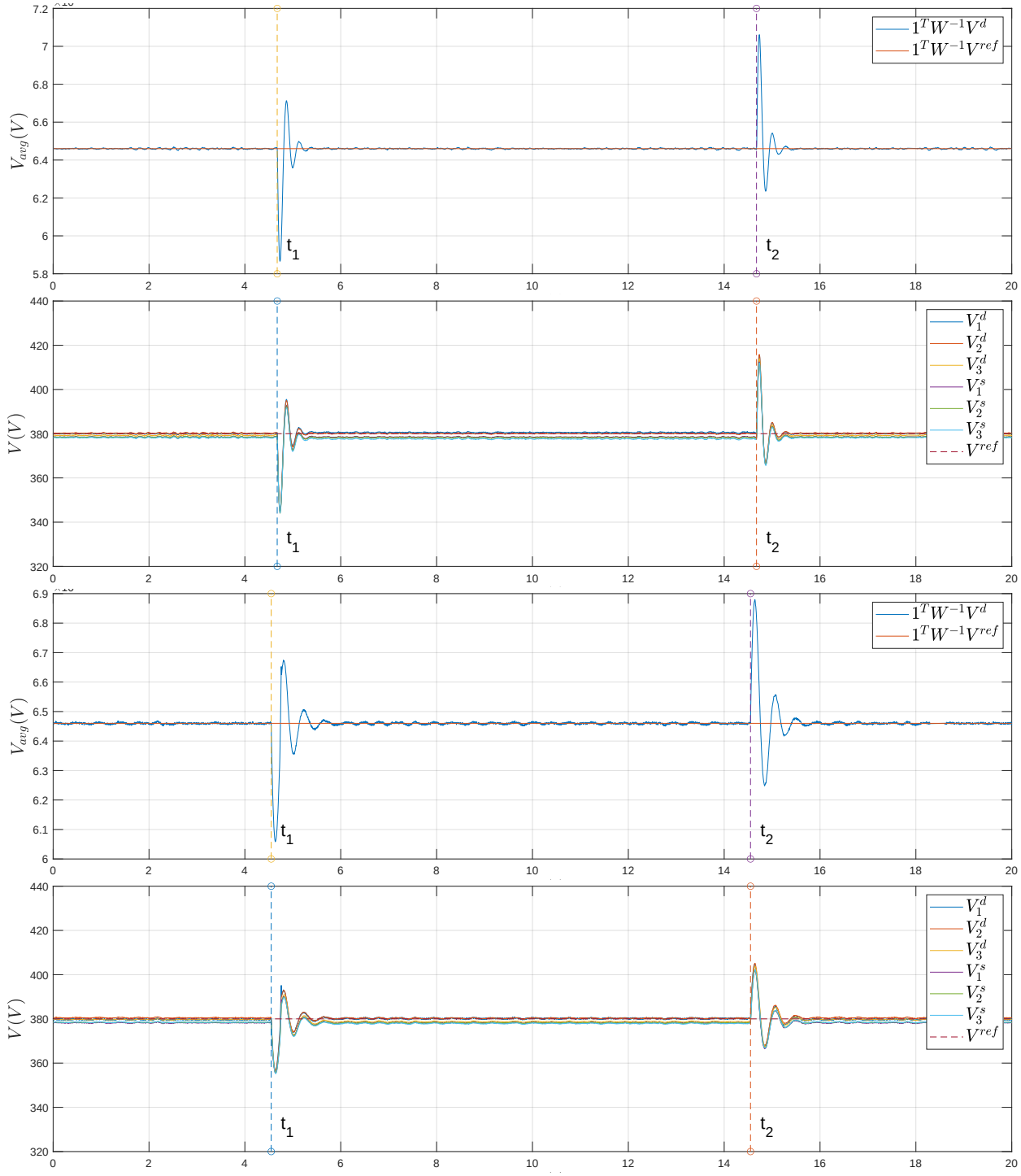

Figure 3.13: Real-Time tests - Scenario 3: from the top, weighted average voltage at the PCC near the DGUs together with the weighted average voltage reference value (dashed line); voltage at the PCC of each DGU and SU together with the reference value (dashed line) in case of the nominal and real models, respectively.

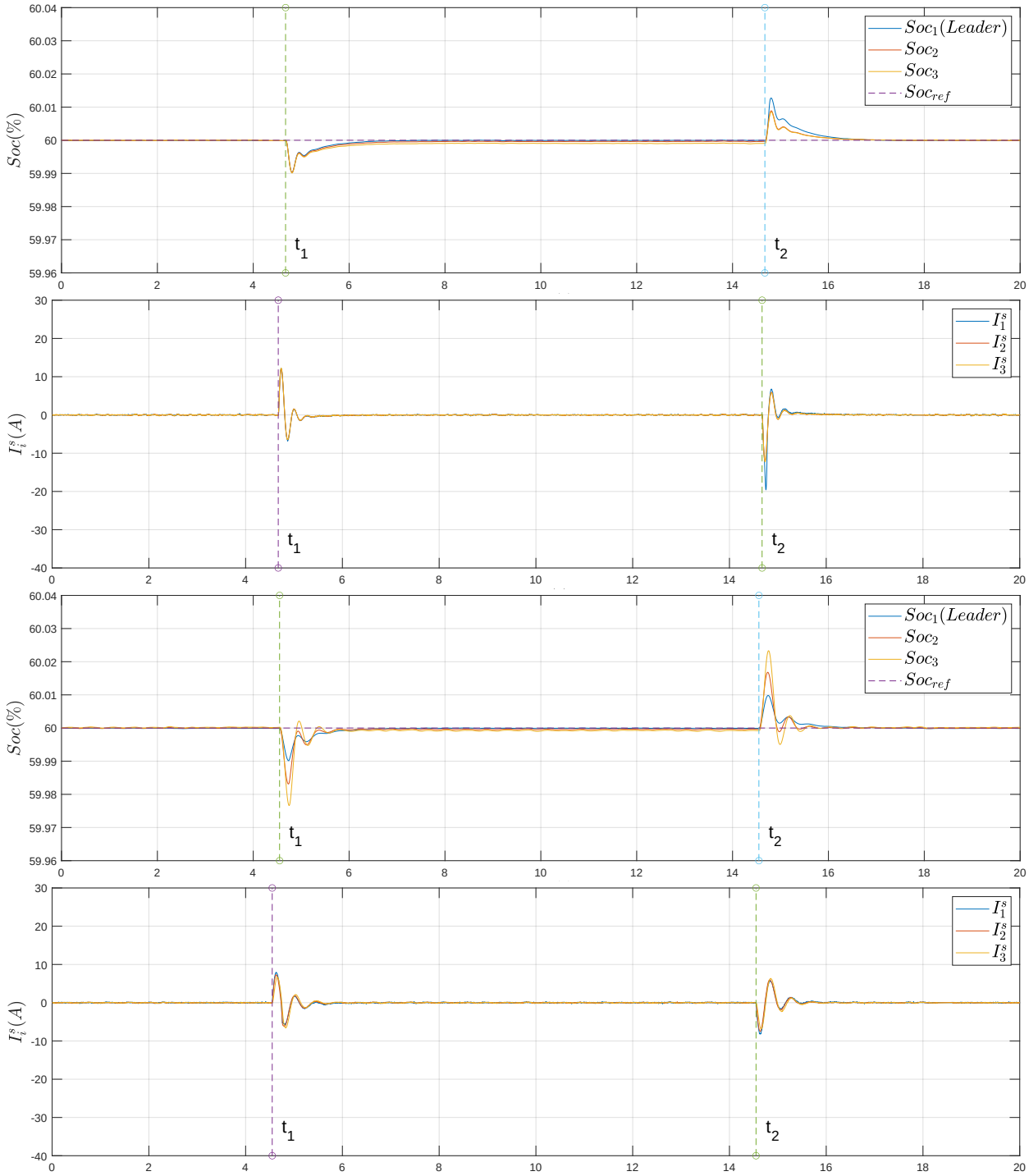

Figure 3.14: Real-Time tests - Scenario 3: from the top, states-of-charge of the SUs; generated current of SUs in case of the nominal and real models, respectively.

3.3.4 Scenario 4: voltage reference variation

In the fourth scenario, we investigate the performance of the proposed controllers under a voltage reference variation of the PCC near the DGUs. The system is initially at the steady state with $I_L(0)$, $V^{ref}(0)$ and $Soc_{ref}(0)$. Then:

- At the time instant $t = t_1$ the voltage reference V^{ref} is stepped up with $\Delta V^{ref} = \begin{bmatrix} 5 & 5 & 5 \end{bmatrix} V$.

One can appreciate that Objectives 2.1 and 2.3 are still achieved (see Figs. 3.15 and 3.17). The voltages at the PCC are illustrated in Fig. 3.16. We can see clearly that the average of the voltages at the PCC near the DGUs converge the average voltage reference (Objective 2.2). Note that even if the voltages of the SUs storage units are not controlled, all the voltage at the PCC is within the range of $385 \pm 2V$ during the steady-state and $385 \pm 4V$ during the transient phase, implying that the voltage deviations are less than 0.5% of the reference value $V^{ref} = 385$ V during the steady state and less than 1% of the reference value $V^{ref} = 385$ V during the transient phase.

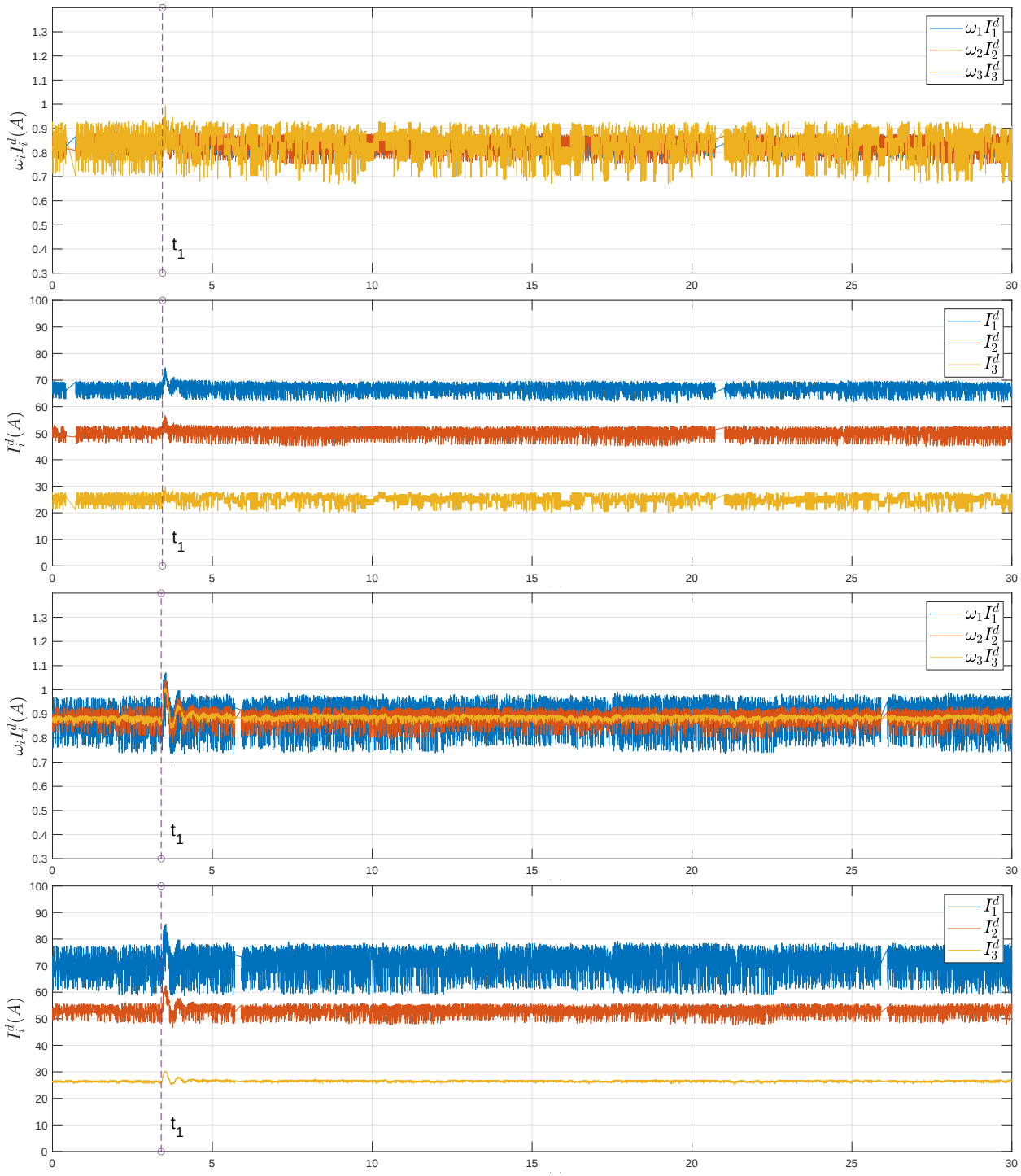

Figure 3.15: Real-Time tests - Scenario 4: from the top, weighted generated currents and generated currents of the DGUs in case of the nominal and real models, respectively.

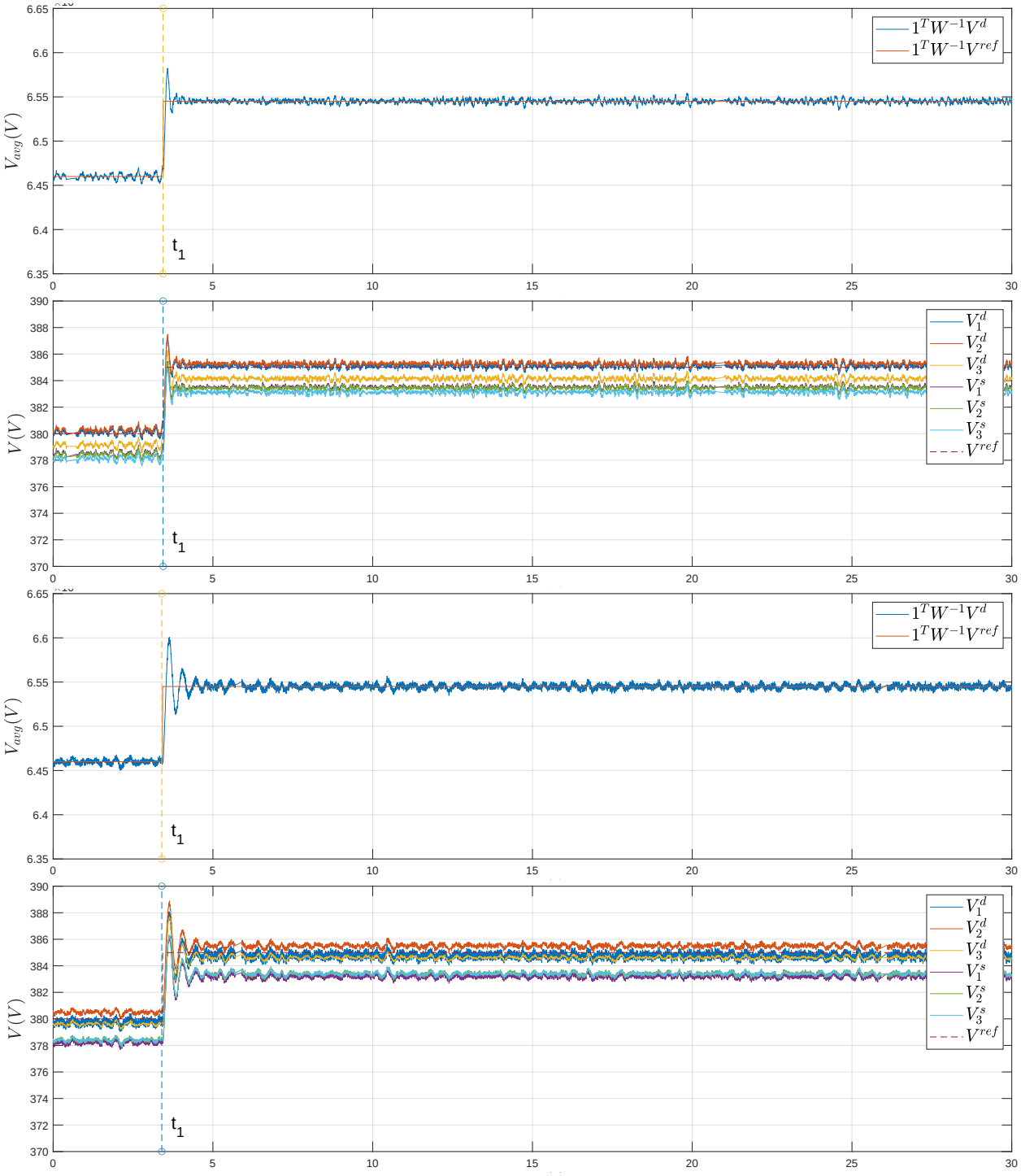

Figure 3.16: Real-Time tests - Scenario 4: from the top, weighted average voltage at the PCC near the DGUs together with the weighted average voltage reference value (dashed line); voltage at the PCC of each DGU and SU together with the reference value (dashed line) in case of the nominal and real models, respectively.

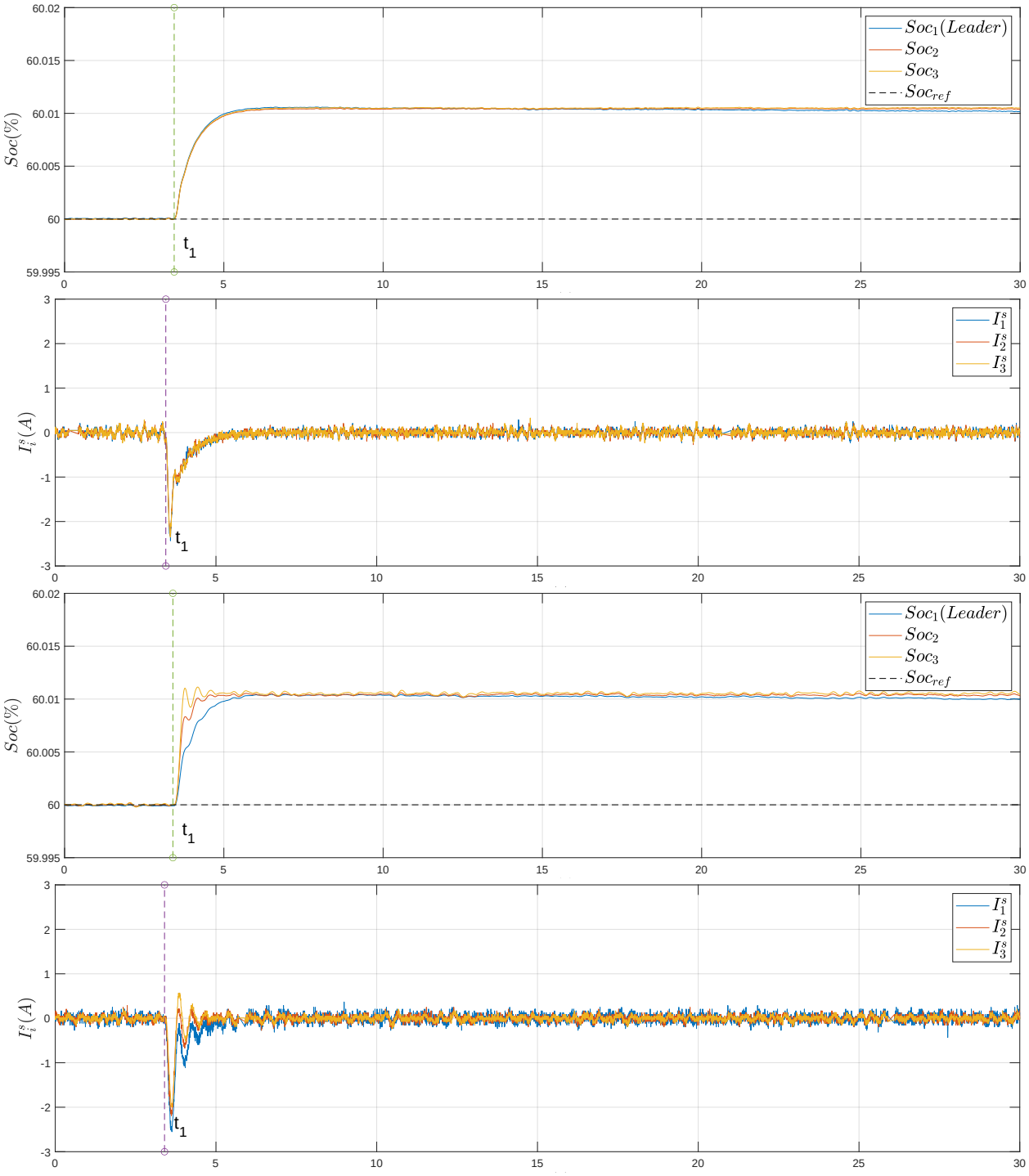

Figure 3.17: Real-Time tests - Scenario 4: from the top, states-of-charge of the SUs; generated current of SUs in case of the nominal and real models, respectively.

3.3.5 Scenario 5: state-of-charge reference variation

In the fifth scenario, we investigate the effectiveness of the proposed controllers under a variation in the state-of-charge reference. The system is initially at the steady state with $I_L(0)$, $V^{ref}(0)$ and $Soc_{ref}(0) = 60\%$. Then, at the time instant $t = t_1$ the Soc_{ref} is stepped up with 10%. As we can see in Fig. 3.20, the states-of-charges of the SUs converges to the new Soc_{ref} asymptotically while Objectives 2.1-2.2 still achieved (Fig. 3.18-3.19). Furthermore, one can appreciate that the current generated by the SUs converges to zero after being negative in order to charge the batteries. The results illustrate the robust performance of the proposed controllers under the change in the state-of-charge reference.

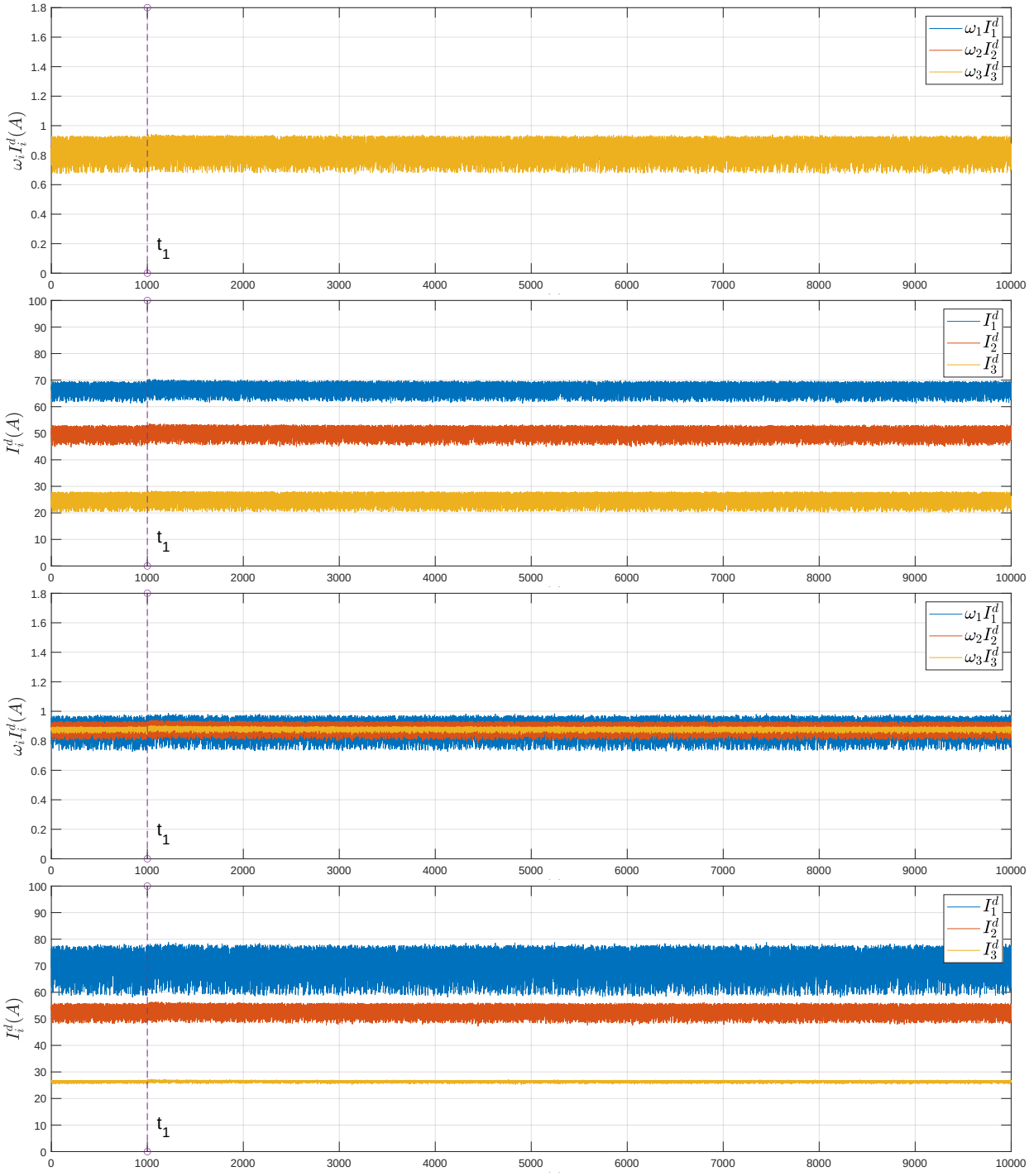

Figure 3.18: Real-Time tests - Scenario 5: from the top, weighted generated currents and generated currents of the DGUs in case of the nominal and real models, respectively.

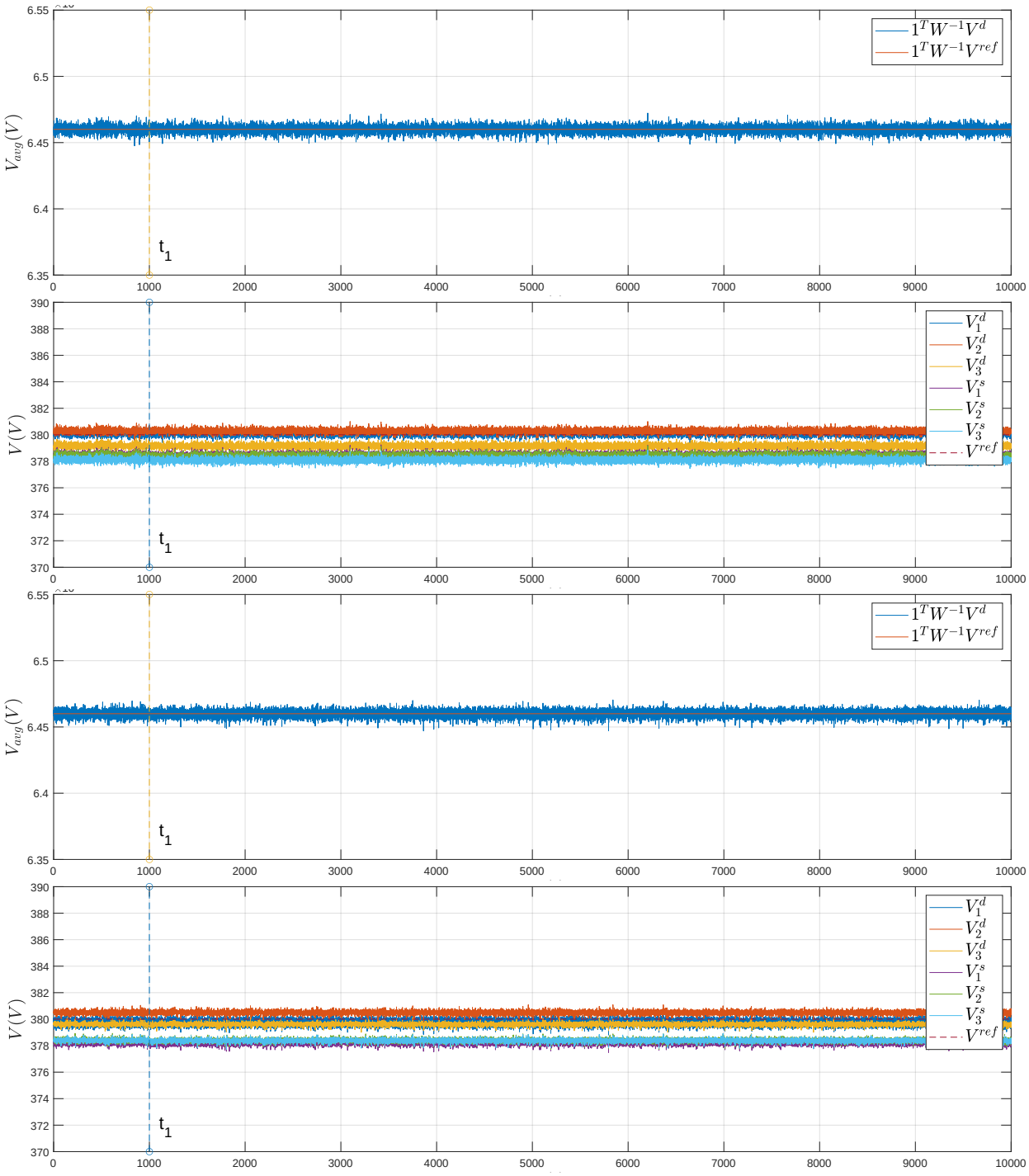

Figure 3.19: Real-Time tests - Scenario 5: from the top, weighted average voltage at the PCC near the DGUs together with the weighted average voltage reference value (dashed line); voltage at the PCC of each DGU and SU together with the reference value (dashed line) in case of the nominal and real models, respectively.

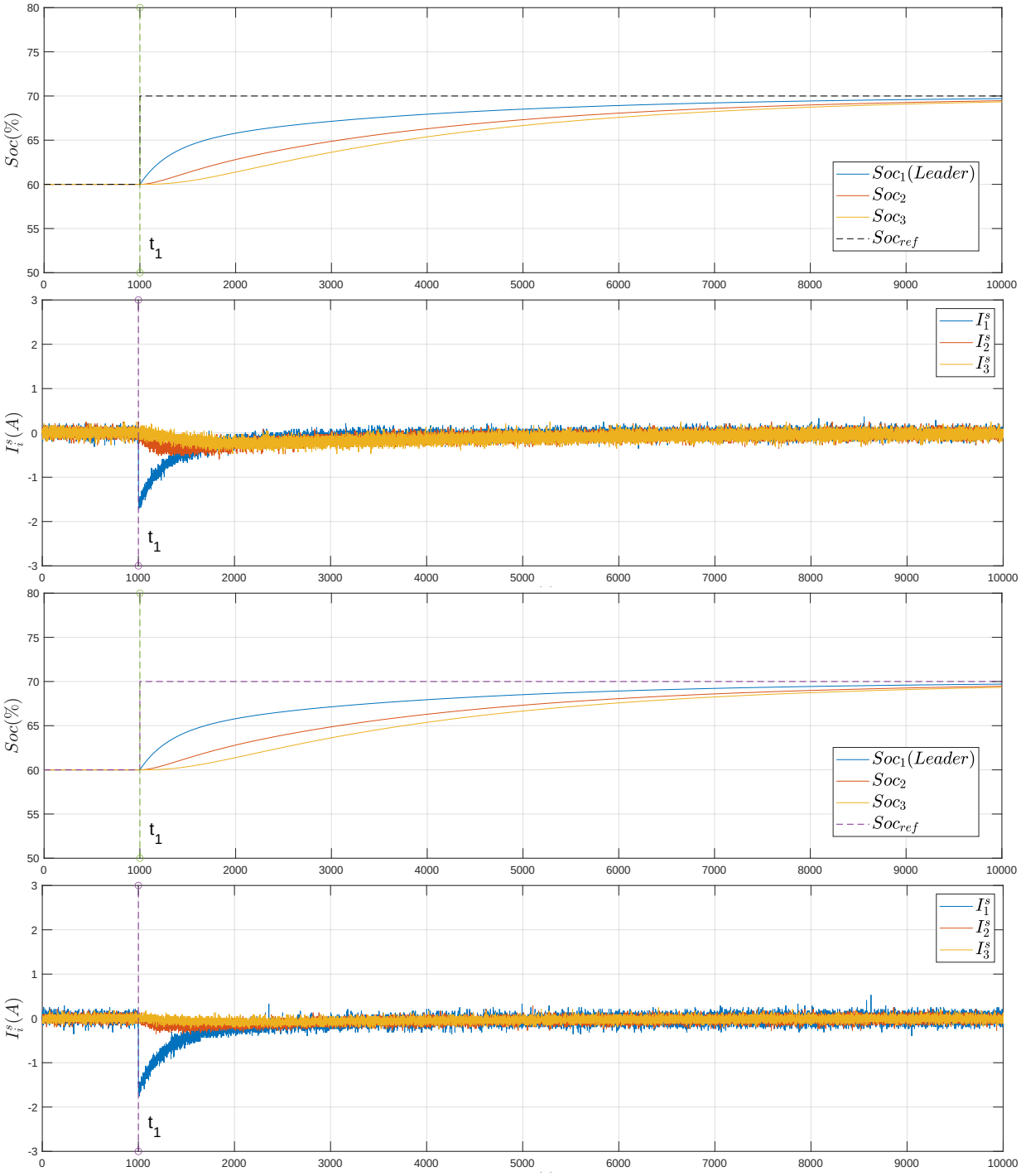

Figure 3.20: Real-Time tests - Scenario 5: from the top, states-of-charge of the SUs; generated current of SUs in case of the nominal and real models, respectively.

3.3.6 Scenario 6: state-of-charge balancing without leader

In the last scenario, we investigate the behavior of the system in closed-loop with the proposed controllers when there is no state-of-charge reference for the SU, i.e., the SUs do not have any leader and the parameter β_{i_l} in (2.51) is set to 0.

The system is initially at the steady state with $I_L(0)$, $V^{ref}(0)$, $Soc_1(0) = 50\%$, $Soc_2(0) = 20\%$ and $Soc_3 = 80\%$. Then at the time instant $t = t_1$ we activate the controllers without any leader. Note that in Fig. 3.23 the states-of-charges of the SUs converge asymptotically to the average of their initial values while Objectives 2.1-2.2 are still achieved (Fig. 3.21-3.22). This gives an additional option if one does not have a high-level strategy to manage the states-of-charge or in case of a communication problem when transmitting the Soc_{ref} to the leader. This can protect Objective 2.3 from the single point of failure. Moreover, one can remark that the currents of the DGUs are not influenced by the variation of the state-of-charge. In fact, the currents demand due to the charging of SU 2 is compensated by the current generated from the discharging of the other SUs (Fig. 3.23).

Finally, one can appreciate that in all the scenarios, even if the system is implemented in a near realistic environment, and with parametric discrepancies from the nominal parameter values i.e. time constants for the interconnection RLC filters that differ significantly from their nominal values: e.g.,

$$
\begin{aligned}
(l_1^d, c_1^d, l_1^s, c_1^s) &= 0.4(l^d, c^d, l^s, c^s),\\
(l_3^d, c_3^d, l_3^s, c_3^s) &= 6(l^d, c^d, l^s, c^s),\\
(r_{L3}^d, r_{L3}^s) &= 6(r_L^d, r_L^s),\\
k_{soc_2} &= 2k_{soc},\\
k_{soc_3} &= 3k_{soc},
\end{aligned}
$$

the performances of the proposed control approach are not practically affected.

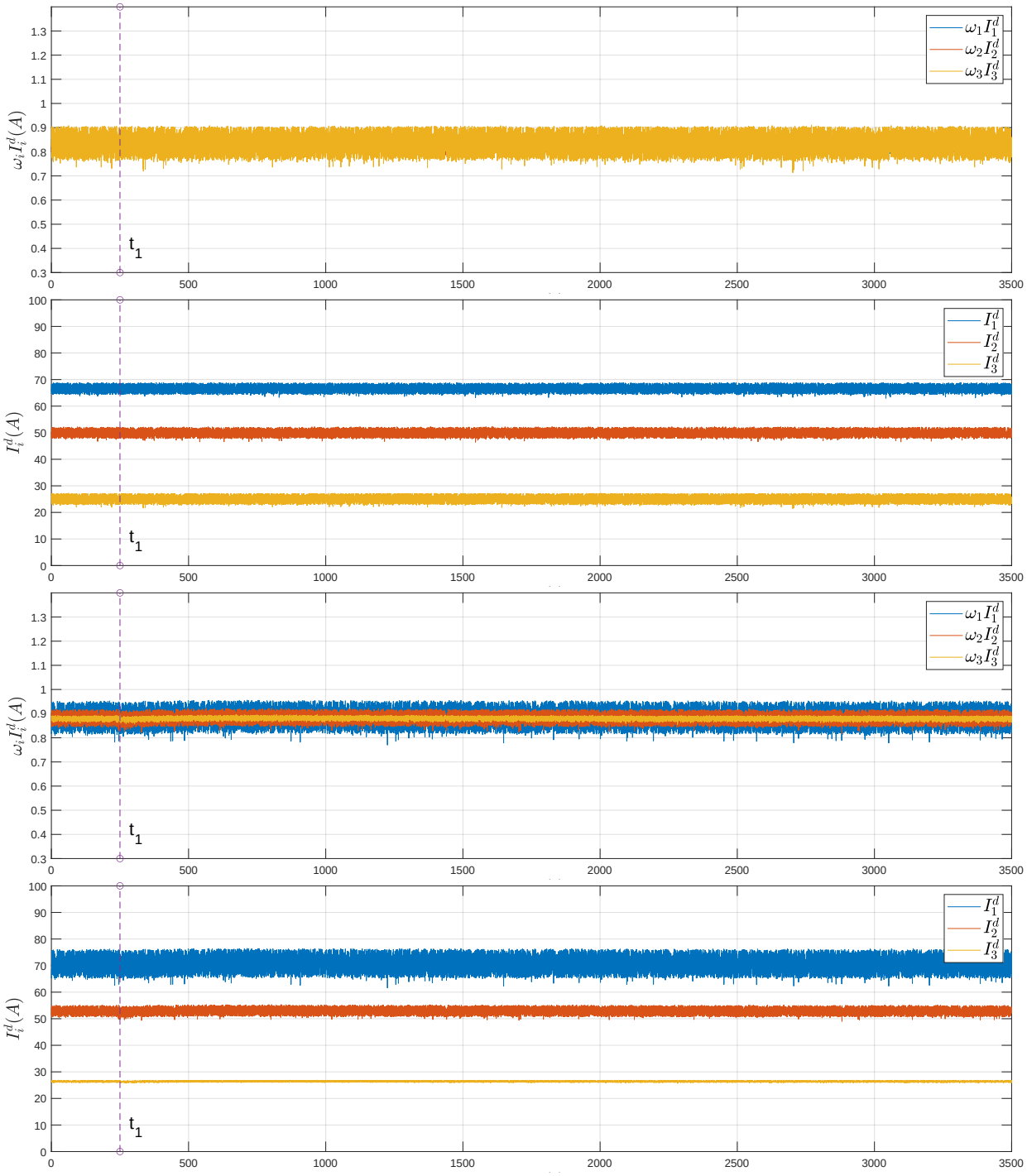

Figure 3.21: Real-Time tests - Scenario 6: from the top, weighted generated currents and generated currents of the DGUs in case of the nominal and real models, respectively.

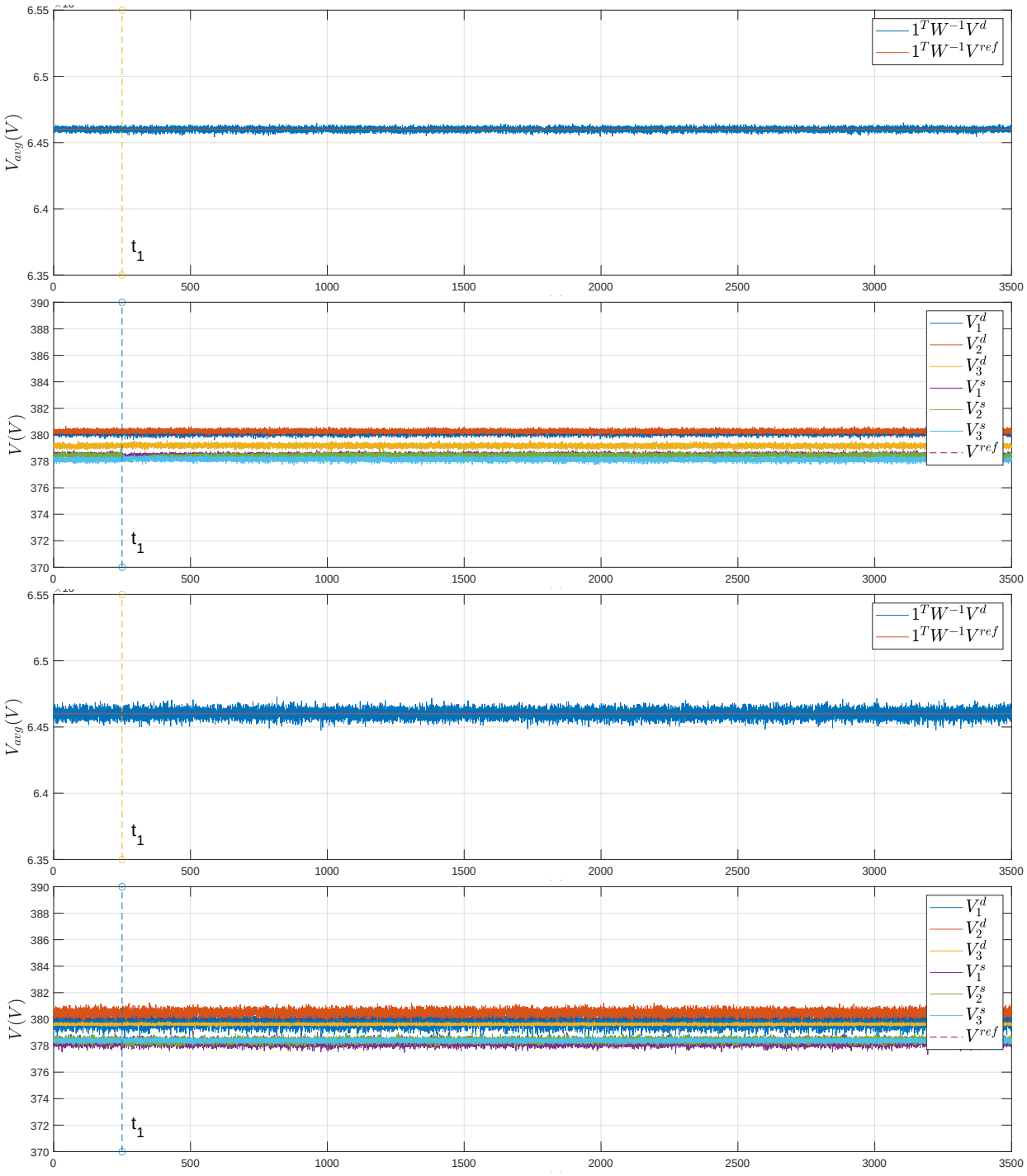

Figure 3.22: Real-Time tests - Scenario 6: from the top, weighted average voltage at the PCC near the DGUs together with the weighted average voltage reference value (dashed line); voltage at the PCC of each DGU and SU together with the reference value (dashed line) in case of the nominal and real models, respectively.

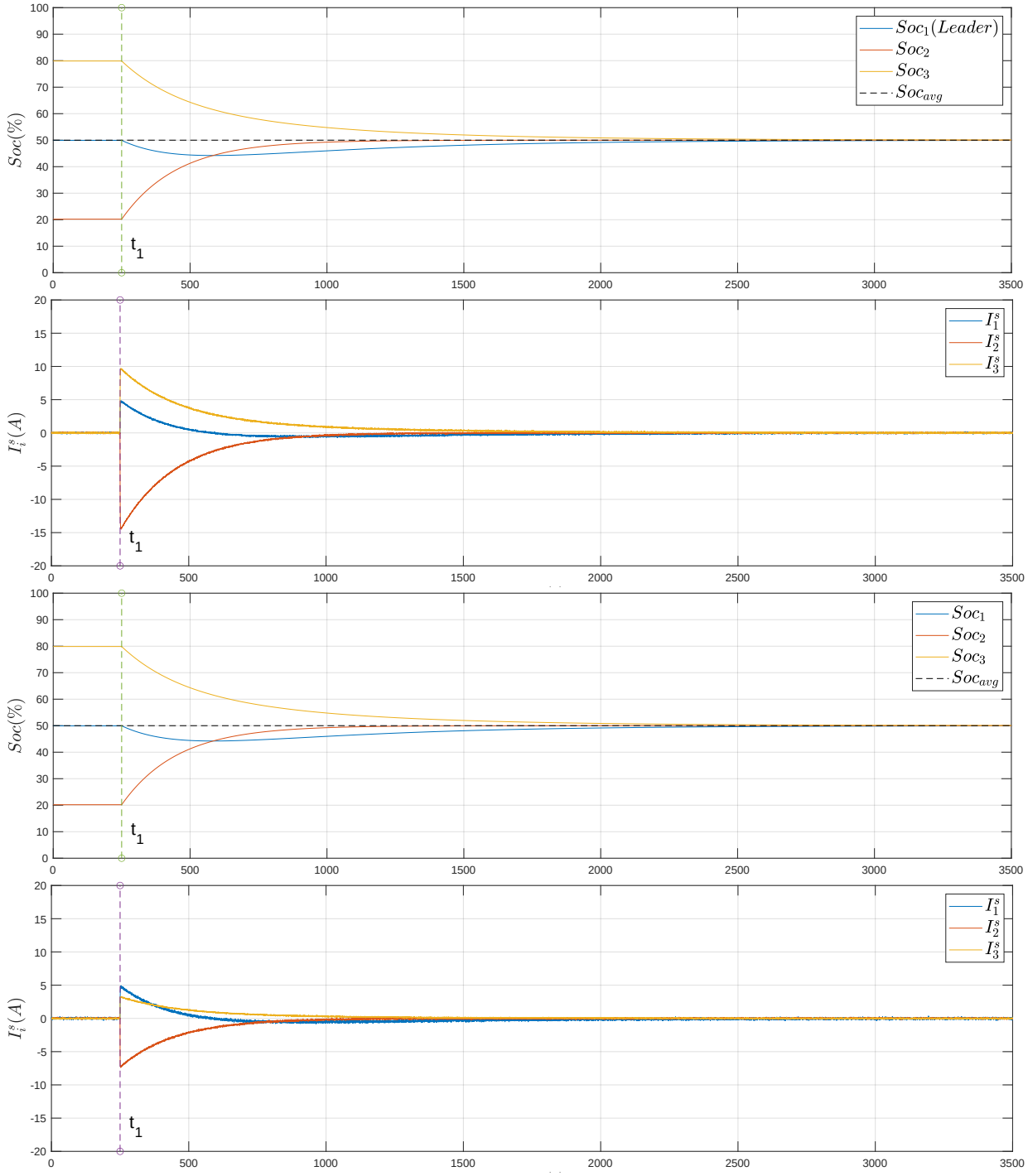

Figure 3.23: Real-Time tests - Scenario 6: from the top, states-of-charge of the SUs; generated current of SUs in case of the nominal and real models, respectively. Soc_{avg} represents the average of the initial values of the state-of-charge

3.4 Conclusion

In this chapter, the distributed control approach proposed in Chapter 2 was assessed. The considered DC-MG was composed of three DGUs, three SUs, resistive inductive power line and loads. Several scenarios were considered and implemented in Matlab/Simulink (Section 3.2) and real-time HIL platform (Section 3.3). The results of each of these scenarios show that the proposed control methodology provides precise current sharing, average voltage regulation and state-of-charge balancing even in case of resistive or resistive-inductive power lines, agents with the same or different parameter values, current demand and references variations, etc. The results of Section 3.3.6 also show that if no state-of-charge reference is defined by the user (or if the SU leader losses the Soc reference due to a communication problem), the state-of-charge will converge to the average of their initial values providing more flexibility for state-of-charge balancing.

Chapter 4

Final Conclusions

The purpose of this work was the design of a new distributed control approach for DC-MGs to achieve three main objectives, Current Sharing (CS), Average Voltage Regulation (AVR) and State-of-charge Balancing (SB). The studied DC-MG was composed of Distributed Generation Units (DGUs), Storage Units (SUs) and loads interconnected through power lines. Moreover, consensus in multi-agent systems, passivity, Lyapunov stability, Linear Matrix Inequalities (LMI) and state-feedback control were the main tools used for the design of the controllers.

We started with a brief introduction to the theoretic concept, a literature review of the existing control strategies for DC-MG and preliminaries related to this work (Chapter 1). Then, we turn our attention to the design of a new distributed-based static-state-feedback control law including distributed consensus-like integral actions to reach the considered objectives (Chapter 2). The controllers exploit two sparse communication networks, one for the DGUs and another for the SUs. Under the assumption that the agents (DGUs or SUs) have the same physical parameter values, we have proved that the state of the closed-loop system converges exponentially and globally to the set of all equilibrium points. The proof was based on the passivity of each agent in closed loop with the local controller, and the inherent passivity of power lines. In the proposed control paradigm, the DGUs exchange relative information with their neighbors about weighted (per-unit) generated currents and control variables, and accordingly adjust the local controllers to reach CS and AVR. Analogously, the SUs share their state-of-charge with their neighbors and update their local controllers to reach SB.

The main contribution of the thesis was the *proof* of global exponential convergence of the studied DC-MG in closed-loop with the proposed controller despite its meshed topology, the communication coupling between its components, the unknown variation of the load, and the fact that the three objectives should be achieved *simultaneously*. In addition, the convergence is independent of the initial conditions of the power network and the controller state. The proposed control strategy includes a leader-follower approach which ensures the convergence of all the state-of-charge to a common reference state Soc_{ref} available only for one SU (called *the leader*). This gives the possibility for high-level monitoring of the states-of-charge through an energy management strategy, which defines the Soc_{ref} value e.g. it can send a high Soc_{ref} in case of low-load operation mode, and small Soc_{ref} in case of high-load operation mode. Moreover, the controllers do not need any information about the topology of the MG or the currents and parameters of the *resistive-inductive* power lines. The topology of the power network does not need to be the same as the topology of the communication network. Furthermore, we applied the proposed controllers to a DC-MG composed of three DGUs, three SUs, resistive-inductive power lines, loads and two communication networks (Chapter 3). The DC-MG was implemented in two environments, Matlab/Simulink software and Real-Time Hardware-In-the-Loop (HIL) platform. Several scenarios were considered where the results showed the efficiency of the proposed control methodology and where the control objectives were successfully achieved. The results shows also that SB can be achieved without defining a state-of-charge reference. In this case, all the state-of-charge converge to the average of their initial values, which illustrates the flexibility of the proposed technique.

The results of the work developed in this thesis lead to various possible extensions and new researches. For instance, this approach can be applied for AC-MGs by considering dq transformation and already synchronized MG [25]. Even though the HIL tests (Section 3.3) showed that the proposed controllers work in the case when the DGUs and SUs have different physical parameter values, it could be of interest to consider relaxing Assumptions 2.2 and 2.4 in the proof of the global convergence. Another possible enhancement of the proposed control approach can be the use of observers to estimate the value of the local voltage or the local current rather than measuring it. Looking at the load side, it may be interesting to consider Constant Power Load (CPL) with proof of global convergence. The plug-and-play functionality of DC-MGs with the proposed approach can also be an interesting extension of this work. Regarding the communication network, other issues can also be considered such as transmission delay, switching topology and optimization of the communication cost [26]. Finally, more tests can be performed by applying the proposed control approach on a real DC-MG prototype.

Appendix A

Tools

Definition A.1. (Hurwitz matrix) Let A be a square matrix. A is Hurwitz if every eigenvalue λ_i of A has strictly negative real part, i.e.,

$$real(\lambda_i) < 0, \text{ for all } \lambda_i. \tag{A.1}$$

Definition A.2. (Positive definite function) A function $V(x) : \mathbb{R}^n \to \mathbb{R}$ is positive definite (positive semidefinite) if:

- $V(0) = 0$,
- $V(x) > 0$ $(V(x) \geq 0)$ $\forall x \in \mathbb{R}\backslash\{0\}$.

Definition A.3. (Positive definite matrix) A symmetric matrix $A \in \mathbb{R}^{n\times n}$ is positive definite (positive semidefinite) if $\forall x \in \mathbb{R}^n$, $x^\top Ax$ is positive (positive semidefinite).

Definition A.4. (Kronecker Product) Let $A \in \mathbb{R}^{n\times m}$ and $B \in \mathbb{R}^{p\times q}$ be two matrices whose entries are $a_{ij} = [A]_{ij}$ and $b_{ij} = [B]_{ij}$, respectively. The Kronecker product $A \otimes B$ of the size $np \times mq$ is the block matrix defined as follows:

$$A \otimes B = \begin{bmatrix} a_{11}B & a_{12}B & \cdots & \cdots & a_{1m}B \\ a_{11}B & a_{12}B & \cdots & \cdots & a_{1m}B \\ \vdots & \vdots & \ddots & & \vdots \\ a_{n1}B & a_{n2}B & \cdots & \cdots & a_{nm}B \end{bmatrix}. \tag{A.2}$$

Appendix B

State-of-charge Dynamics

The state of charge (SOC) of a SU can be defined as the ratio between its available capacity and its maximum available capacity in percentage [82].

$$Soc = \frac{The\ available\ capacity}{The\ maximum\ available\ capacity} \times 100\%. \tag{B.1}$$

The estimation of the state-of-charge can be done by different techniques. This techniques are based on the measurement of the voltage, current or any other convenient parameter that varies with the Soc [83]. In this work we consider that the dynamic of Soc_i, $i \in \mathcal{V}^s$, is given by coulomb counting method [84][1]:

$$\dot{Soc}_i = -\frac{1}{C_i^{dc}} I_i^{dc} \qquad \forall i \in \mathcal{V}^s, \tag{B.2}$$

where C_i^{dc} and I_i^{dc} are the capacity and the output current of the SU.
Let $\mathcal{P}_i^e$ and $\mathcal{P}_i^o$ be the input and output power of the DC/DC converter (Fig. B.1). By neglegting the power losses in the converter, we get:

$$\mathcal{P}_i^e = \mathcal{P}_i^o, \tag{B.3}$$

we can write:

$$V_i^{dc} I_i^{dc} = u_i I_i, \tag{B.4}$$

[1]The details explanations of the SoC estimation techniques is out of the scope of this thesis [83].

where V_i^{dc} is the voltage at the input side of the DC/DC converter, yields:

$$I_i^{dc} = \frac{u_i I_i}{V_i^{dc}}. \tag{B.5}$$

Replacing (B.5) in (B.2) gives:

$$\dot{Soc}_i = -\frac{u_i}{C_i^{dc} V_i^{dc}} I_i \qquad \forall i \in \mathcal{V}^s. \tag{B.6}$$

Generally, the output voltage of a battery (especially Lithium batteries) is almost constant [85]. Moreover, since the resistances of the power lines are very low, the deviation between the voltages at the points of common coupling is very small as well ($\Delta V = r_l I_l$). Hence the output voltage of the interfacing converter can also be considered as constant. Thus, without loss of generality (B.6) becomes:

$$\dot{Soc}_i = -k_{soc_i} I_i \quad \forall i \in \mathcal{V}^s, \tag{B.7}$$

where $k_{soc_i} = \dfrac{u_i}{C_i^{dc} V_i^{dc}}$ is a constant in $\mathbb{R}_{>0}$.

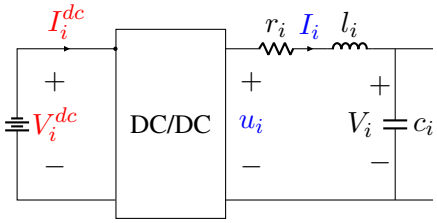

Figure B.1: Power balance between the two sides of a DC/DC converter.

Bibliography

[1] D. E. Olivares, A. Mehrizi-Sani, A. H. Etemadi, C. A. Canizares, R. Iravani, M. Kazerani, A. H. Hajimiragha, O. Gomis-Bellmunt, M. Saeedifard, R. Palma-Behnke, G. A. Jiménez-Estévez, and N. D. Hatziargyriou. Trends in microgrid control. *IEEE Transactions on Smart Grid*, 5(4):1905–1919, July 2014.

[2] Carlos Bordons, Félix Garcia-Torres, and Miguel A. Ridao. *Uncertainties in Microgrids*, pages 169–190. Springer International Publishing, Cham, 2020.

[3] Sudipta Chakraborty, Simões Marcelo G., and William E. Kramer. *Power Electronics for Renewable and Distributed Energy Systems A Sourcebook of Topologies, Control and Integration*. Springer, 2013.

[4] L. Meng, Q. Shafiee, G. F. Trecate, H. Karimi, D. Fulwani, X. Lu, and J. M. Guerrero. Review on control of dc microgrids and multiple microgrid clusters. *IEEE Journal of Emerging and Selected Topics in Power Electronics*, 5(3):928–948, Sep. 2017.

[5] Michele Tucci, Lexuan Meng, Josep M. Guerrero, and Giancarlo Ferrari-Trecate. Stable current sharing and voltage balancing in dc microgrids: A consensus-based secondary control layer. *Automatica*, 95:1 – 13, 2018.

[6] S. Trip, M. Cucuzzella, X. Cheng, and J. Scherpen. Distributed averaging control for voltage regulation and current sharing in dc microgrids. *IEEE Control Systems Letters*, 3(1):174–179, Jan 2019.

[7] M. Tucci, S. Riverso, and G. Ferrari-Trecate. Line-independent plug-and-play controllers for voltage stabilization in dc microgrids. *IEEE Transactions on Control Systems Technology*, 26(3):1115–1123, May 2018.

[8] W. Huang and J. A. Abu Qahouq. Energy sharing control scheme for state-of-charge balancing of distributed battery energy storage system. *IEEE Transactions on Industrial Electronics*, 62(5):2764–2776, May 2015.

[9] Chendan Li, T. Dragicevic, N. L. Diaz, J. C. Vasquez, and J. M. Guerrero. Voltage scheduling droop control for state-of-charge balance of distributed energy storage in dc microgrids. In *2014 IEEE International Energy Conference (ENERGYCON)*, pages 1310–1314, May 2014.

[10] M. Yazdanian and A. Mehrizi-Sani. Distributed control techniques in microgrids. *IEEE Transactions on Smart Grid*, 5(6):2901–2909, Nov 2014.

[11] S. Anand, B. G. Fernandes, and J. Guerrero. Distributed control to ensure proportional load sharing and improve voltage regulation in low-voltage dc microgrids. *IEEE Transactions on Power Electronics*, 28(4):1900–1913, April 2013.

[12] Natarajan Prabaharan, Amalorpavaraj Rini Ann Jerin, Ehsan Najafi, and Kaliannan Palanisamy. 6 - an overview of control techniques and technical challenge for inverters in micro grid. In A. Hina Fathima, N. Prabaharan, K. Palanisamy, Akhtar Kalam, Saad Mekhilef, and Jackson. J. Justo, editors, *Hybrid-Renewable Energy Systems in Microgrids*, Woodhead Publishing Series in Energy, pages 97 – 107. Woodhead Publishing, 2018.

[13] Gaëtan Beneux, Pierre Riedinger, Jamal Daafouz, and Louis Grimaud. Adaptive stabilization of switched affine systems with unknown equilibrium points: Application to power converters. *Automatica*, 99:82 – 91, 2019.

[14] A. Sferlazza, C. Albea-Sanchez, L. Martínez-Salamero, G. García, and C. Alonso. Min-type control strategy of a dc–dc synchronous boost converter. *IEEE Transactions on Industrial Electronics*, 67(4):3167–3179, 2020.

[15] X. Lu, J. M. Guerrero, K. Sun, and J. C. Vasquez. An improved droop control method for dc microgrids based on low bandwidth communication with dc bus voltage restoration and enhanced current sharing accuracy. *IEEE Transactions on Power Electronics*, 29(4):1800–1812, 2014.

[16] S. Adhikari, Y. Tang, and P. Wang. Secondary control for dc microgrids: A review. In *2016 Asian Conference on Energy, Power and Transportation Electrification (ACEPT)*, pages 1–6, 2016.

[17] V. Nasirian, S. Moayedi, A. Davoudi, and F. L. Lewis. Distributed cooperative control of dc microgrids. *IEEE Transactions on Power Electronics*, 30(4):2288–2303, 2015.

[18] P. Wang, X. Lu, X. Yang, W. Wang, and D. Xu. An improved distributed secondary control method for dc microgrids with enhanced dynamic current sharing performance. *IEEE Transactions on Power Electronics*, 31(9):6658–6673, 2016.

[19] V. Nasirian, A. Davoudi, F. L. Lewis, and J. M. Guerrero. Distributed adaptive droop control for dc distribution systems. *IEEE Transactions on Energy Conversion*, 29(4):944–956, 2014.

[20] A. Mehrizi-Sani and R. Iravani. Potential-function based control of a microgrid in islanded and grid-connected modes. *IEEE Transactions on Power Systems*, 25(4):1883–1891, 2010.

[21] J. M. Guerrero, J. C. Vasquez, J. Matas, L. G. de Vicuna, and M. Castilla. Hierarchical control of droop-controlled ac and dc microgrids-a general approach toward standardization. *IEEE Transactions on Industrial Electronics*, 58(1):158–172, 2011.

[22] M. Tucci, S. Riverso, J. C. Vasquez, J. M. Guerrero, and G. Ferrari-Trecate. A decentralized scalable approach to voltage control of dc islanded microgrids. *IEEE Transactions on Control Systems Technology*, 24(6):1965–1979, Nov 2016.

[23] M. Cucuzzella, S. Trip, C. De Persis, X. Cheng, A. Ferrara, and A. van der Schaft. A robust consensus algorithm for current sharing and voltage regulation in dc microgrids. *IEEE Transactions on Control Systems Technology*, 27(4):1583–1595, July 2019.

[24] Fei GAO, Ren KANG, Jun CAO, and Tao YANG. Primary and secondary control in dc microgrids: a review. *Journal of Modern Power Systems and Clean Energy*, 7(2):227–242, Mar 2019.

[25] Michele Tucci and Giancarlo Ferrari-Trecate. A scalable, line-independent control design algorithm for voltage and frequency stabilization in ac islanded microgrids. *Automatica*, 111:108577, 2020.

[26] Jihene Ben Rejeb, Irinel-Constantin Morărescu, and Jamal Daafouz. Control design with guaranteed cost for synchronization in networks of linear singularly perturbed systems. *Automatica*, 91:89 – 97, 2018.

[27] Dan T. Ton and Merrill A. Smith. The u.s. department of energy's microgrid initiative. *The Electricity Journal*, 25(8):84 – 94, 2012.

[28] L. Meng, Q. Shafiee, G. F. Trecate, H. Karimi, D. Fulwani, X. Lu, and J. M. Guerrero. Review on control of dc microgrids and multiple microgrid clusters. *IEEE Journal of Emerging and Selected Topics in Power Electronics*, 5(3):928–948, Sept 2017.

[29] D. E. Olivares, A. Mehrizi-Sani, A. H. Etemadi, C. A. Canizares, R. Iravani, M. Kazerani, A. H. Hajimiragha, O. Gomis-Bellmunt, M. Saeedifard, R. Palma-Behnke, G. A. Jiménez-Estévez, and N. D. Hatziargyriou. Trends in microgrid control. *IEEE Transactions on Smart Grid*, 5(4):1905–1919, July 2014.

[30] A. Banerji, D. Sen, A. K. Bera, D. Ray, D. Paul, A. Bhakat, and S. K. Biswas. Microgrid: A review. In *2013 IEEE Global Humanitarian Technology Conference: South Asia Satellite (GHTC-SAS)*, pages 27–35, Aug 2013.

[31] L. Sguier J. Dulout, C. Alonso and B. Jammes. Development of a photovoltaic low voltage dc microgrid for buildings with energy storage systems. In *ELECTRIMACS. APEC '96*, page 6, 2017.

[32] T. H. Pham, I. Prodan, D. Genon-Catalot, and L. Lefèvre. Dissipated energy minimization for an electro-mechanical elevator of a dc microgrid. In *2018 European Control Conference (ECC)*, pages 1118–1123, 2018.

[33] G. Buticchi, S. Bozhko, M. Liserre, P. Wheeler, and K. Al-Haddad. On-board microgrids for the more electric aircraft-technology review. *IEEE Transactions on Industrial Electronics*, 66(7):5588–5599, July 2019.

[34] Adam Hirsch, Yael Parag, and Josep Guerrero. Microgrids: A review of technologies, key drivers, and outstanding issues. *Renewable and Sustainable Energy Reviews*, 90:402 – 411, 2018.

[35] M. Faisal, M. A. Hannan, P. J. Ker, A. Hussain, M. B. Mansor, and F. Blaabjerg. Review of energy storage system technologies in microgrid applications: Issues and challenges. *IEEE Access*, 6:35143–35164, 2018.

[36] Y. Dahmane, R. Chenouard, M. Ghanes, and M. Alvarado-Ruiz. Coordinated charging of large electric vehicle fleet in a charging station with limited transformer power. In *2020 IEEE Conference on Control Technology and Applications (CCTA)*, pages 1054–1059, 2020.

[37] N. Blin, P. Riedinger, J. Daafouz, L. Grimaud, and P. Feyel. A comparison of harmonic modeling methods with application to control of switched systems with active filtering. In *2019 18th European Control Conference (ECC)*, pages 4198–4203, 2019.

[38] A. Gutierrez, E. Marcault, C. Alonso, and D. Tremouilles. Performance analysis of rl damper in gan-based high-frequency boost converter. In *2020 22nd European Conference on Power Electronics and Applications (EPE'20 ECCE Europe)*, pages P.1–P.8, 2020.

[39] Li Fusheng, Li Ruisheng, and Zhou Fengquan. Chapter 2 - composition and classification of the microgrid. In Li Fusheng, Li Ruisheng, and Zhou Fengquan, editors, *Microgrid Technology and Engineering Application*, pages 11 – 27. Academic Press, Oxford, 2016.

[40] Adam Hirsch, Yael Parag, and Josep Guerrero. Microgrids: A review of technologies, key drivers, and outstanding issues. *Renewable and Sustainable Energy Reviews*, 90:402 – 411, 2018.

[41] Jaynendra Kumar, Anshul Agarwal, and Vineeta Agarwal. A review on overall control of dc microgrids. *Journal of Energy Storage*, 21:113 – 138, 2019.

[42] T. Dragicevic, X. Lu, J. C. Vasquez, and J. M. Guerrero. Dc microgrids-part i: A review of control strategies and stabilization techniques. *IEEE Transactions on Power Electronics*, 31(7):4876–4891, 2016.

[43] Elodie Buzaud. L'imt de grenoble devient le premier smart campus de france avec des formations dédiées, [Online; accessed June 7, 2020]. https://www.emploi-environnement.com/news/imt-grenoble-premier-smart-campus-france-411.html.

[44] DNV GL website. Powermatching city established in hoogkerk, in the dutch province of groningen, [Online; accessed May 06, 2020]. https://images.app.goo.gl/7dExVy1LDbE8J3BG8.

[45] Kythnos microgrid project, [Online; accessed May 15, 2020]. http://www.microgrids.eu/index.php?page=kythnos&id=2.

[46] H. Karimi. *Islanding Detection and Control of an Islanded Electronically-coupled Distributed Generation Unit*. Canadian theses. Library and Archives Canada = Bibliothèque et Archives Canada, 2008.

[47] Cynthia K. Veitch, Jordan M. Henry, Bryan T. Richardson, and Derek H. Hart. Microgrid cyber security reference architecture. 2015.

[48] X. Zhong, L. Yu, R. Brooks, and G. K. Venayagamoorthy. Cyber security in smart dc microgrid operations. In *2015 IEEE First International Conference on DC Microgrids (ICDCM)*, pages 86–91, 2015.

[49] Y. Simmhan, A. G. Kumbhare, B. Cao, and V. Prasanna. An analysis of security and privacy issues in smart grid software architectures on clouds. In *2011 IEEE 4th International Conference on Cloud Computing*, pages 582–589, 2011.

[50] J. Rajagopalan, K. Xing, Y. Guo, F. C. Lee, and B. Manners. Modeling and dynamic analysis of paralleled dc/dc converters with master-slave current sharing control. In *Proceedings of Applied Power Electronics Conference. APEC '96*, volume 2, pages 678–684 vol.2, 1996.

[51] S. K. Mazumder, M. Tahir, and K. Acharya. Master-slave current-sharing control of a parallel dc-dc converter system over an rf communication interface. *IEEE Transactions on Industrial Electronics*, 55(1):59–66, 2008.

[52] I. Batarseh, K. Siri, and H. Lee. Investigation of the output droop characteristics of parallel-connnected dc-dc converters. In *Proceedings of 1994 Power Electronics Specialist Conference - PESC'94*, volume 2, pages 1342–1351 vol.2, 1994.

[53] J. Perkinson. Current sharing of redundant dc-dc converters in high availability systems-a simple approach. In *Proceedings of 1995 IEEE Applied Power Electronics Conference and Exposition - APEC'95*, volume 2, pages 952–956 vol.2, 1995.

[54] Jung-Won Kim, Hang-Seok Choi, and Bo Hyung Cho. A novel droop method for converter parallel operation. *IEEE Transactions on Power Electronics*, 17(1):25–32, 2002.

[55] T. M. Haileselassie and K. Uhlen. Impact of dc line voltage drops on power flow of mtdc using droop control. *IEEE Transactions on Power Systems*, 27(3):1441–1449, 2012.

[56] F. Chen, R. Burgos, D. Boroyevich, J. C. Vasquez, and J. M. Guerrero. Investigation of nonlinear droop control in dc power distribution systems: Load sharing, voltage regulation, efficiency, and stability. *IEEE Transactions on Power Electronics*, 34(10):9404–9421, 2019.

[57] F. Chen, R. Burgos, D. Boroyevich, and W. Zhang. A nonlinear droop method to improve voltage regulation and load sharing in dc systems. In *2015 IEEE First International Conference on DC Microgrids (ICDCM)*, pages 45–50, June 2015.

[58] P. Prabhakaran, Y. Goyal, and V. Agarwal. Novel nonlinear droop control techniques to overcome the load sharing and voltage regulation issues in dc microgrid. *IEEE Transactions on Power Electronics*, 33(5):4477–4487, May 2018.

[59] X. Lu, K. Sun, J. M. Guerrero, J. C. Vasquez, and L. Huang. State-of-charge balance using adaptive droop control for distributed energy storage systems in dc microgrid applications. *IEEE Transactions on Industrial Electronics*, 61(6):2804–2815, 2014.

[60] X. Lu, K. Sun, J. M. Guerrero, J. C. Vasquez, and L. Huang. Double-quadrant state-of-charge-based droop control method for distributed energy storage systems in autonomous dc microgrids. *IEEE Transactions on Smart Grid*, 6(1):147–157, 2015.

[61] T. Morstyn, A. V. Savkin, B. Hredzak, and V. G. Agelidis. Multi-agent sliding mode control for state of charge balancing between battery energy storage systems distributed in a dc microgrid. *IEEE Transactions on Smart Grid*, 9(5):4735–4743, 2018.

[62] Tao Wu, Yanghong Xia, Liang Wang, and Wei Wei. Multiagent based distributed control with time-oriented soc balancing method for dc microgrid. *Energies*, 13(11):2793, Jun 2020.

[63] Daner Hu, Yonggang Peng, Wei Wei, and Yalong Hu. Distributed secondary control for state of charge balancing with virtual impedance adjustment in a dc microgrid. *Energies*, 13(2):408, Jan 2020.

[64] H. et al Yang. Hierarchical distributed control for decentralized battery energy storage system based on consensus algorithm with pinning node. *Prot Control Mod Power Syst*, 3(6), 2018.

[65] Pulkit Nahata, Raffaele Soloperto, Michele Tucci, Andrea Martinelli, and Giancarlo Ferrari-Trecate. A passivity-based approach to voltage stabilization in dc microgrids with zip loads. *Automatica*, 113:108770, 2020.

[66] Demetri Spanos, Reza Olfati-Saber, and Richard M. Murray. Dynamic consensus for mobile networks. 2005.

[67] Mehran Mesbahi and Magnus Egerstedt. *Graph Theoretic Methods in Multiagent Networks*. Princeton University Press, 2010.

[68] C. Godsil and G. Royle. *Algebraic Graph Theory*. Pearson education Taiwan, 2013.

[69] A. Dorri, S. S. Kanhere, and R. Jurdak. Multi-agent systems: A survey. *IEEE Access*, 6:28573–28593, 2018.

[70] POLANSZKY , NICK . Schooling fish, 2020. [Online; accessed May 15, 2020].

[71] R. Olfati-Saber, J. A. Fax, and R. M. Murray. Consensus and cooperation in networked multi-agent systems. *Proceedings of the IEEE*, 95(1):215–233, 2007.

[72] Wei Ren and Randal W. Beard. *Distributed Consensus in Multi-vehicle Cooperative Control: Theory and Applications*. Springer, 2008.

[73] Jean-Jacques E.. Slotine and Weiping Li. *Applied nonlinear control*. Pearson education Taiwan, 2005.

[74] Hassan K Khalil. *Nonlinear systems; 3rd ed.* Prentice-Hall, Upper Saddle River, NJ, 2002.

[75] C. Scherer and S. Wieland. *Linear Matrix inequalities in Control*. lecture support, DELFT University, 2004.

[76] Jan C. Willems. Dissipative dynamical systems Part II: Linear systems with quadratic supply rates. *Archive for Rational Mechanics and Analysis*, 45(5):352–393, January 1972.

[77] Weiyuan Zhang and Yajie Wang. Passivity analysis of bam nns with mixed time delays. In De-Shuang Huang and Kyungsook Han, editors, *Advanced Intelligent Computing Theories and Applications*, pages 127–135, Cham, 2015. Springer International Publishing.

[78] Michele Cucuzzella. *Design and Analysis of Sliding Mode Control Algorithms for Power Networks*. PhD thesis, University of Pavia, 2017.

[79] M. Tucci. *Scalable control of islanded microgrids*. PhD thesis, University of Pavia, 2018.

[80] F. Dorfler and F. Bullo. Kron reduction of graphs with applications to electrical networks. *IEEE Transactions on Circuits and Systems I: Regular Papers*, 60(1):150–163, 2013.

[81] J. Daafouz, P. Riedinger, and C. Iung. Stability analysis and control synthesis for switched systems: a switched lyapunov function approach. *IEEE Transactions on Automatic Control*, 47(11):1883–1887, Nov 2002.

[82] L. Maharjan, S. Inoue, H. Akagi, and J. Asakura. State-of-charge (soc)-balancing control of a battery energy storage system based on a cascade pwm converter. *IEEE Transactions on Power Electronics*, 24(6):1628–1636, June 2009.

[83] Sabine Piller, Marion Perrin, and Andreas Jossen. Methods for state-of-charge determination and their applications. *Journal of Power Sources*, 96(1):113 – 120, 2001. Proceedings of the 22nd International Power Sources Symposium.

[84] Q. Shafiee, T. Dragicevic, F. Andrade, J. C. Vasquez, and J. M. Guerrero. Distributed consensus-based control of multiple dc-microgrids clusters. In *IECON 2014 - 40th Annual Conference of the IEEE Industrial Electronics Society*, pages 2056–2062, Oct 2014.

[85] X. Lu, K. Sun, J. M. Guerrero, J. C. Vasquez, and L. Huang. Double-quadrant state-of-charge-based droop control method for distributed energy storage systems in autonomous dc microgrids. *IEEE Transactions on Smart Grid*, 6(1):147–157, 2015.

Abstract: In recent years, the power grid has undergone a rapid transformation with the massive penetration of renewable and distributed generation units. The concept of microgrids is a key element of this energy transition. Microgrids are made up of a set of several distributed generation units (DGUs), storage units (SUs) and loads interconnected by power lines. A microgrid can be installed in several locations, for example in houses, hospitals, a neighborhood or village, etc. and operates either in connected mode to the main grid or in isolated (autonomous) mode.

Microgrids are facing several challenges related to stability assurance, cyber-security, energy cost optimization, energy management, power quality, etc. In this work, we focus our attention on the control of islanded direct current microgrids. The main contribution is the design of a new $distributed$ control approach to $provably$ achieve current sharing, average voltage regulation and state-of-charge balancing simultaneously with $global\ exponential\ convergence$. The main tools are consensus in multi-agent systems, passivity, Lyapunov stability, linear matrix inequalities, etc.

The thesis is divided into three parts. The First part presents the concept of microgrids, a literature review of their control strategies and the mathematical preliminaries required throughout the manuscript.

The second part deals with the design of the proposed distributed control approach to achieve the considered objectives. The system is augmented with three distributed consensus-like integral actions. The existence of equilibrium points for the augmented system is proved and a distributed-based static state feedback control architecture is proposed. Starting from the assumption that the agents (DGUs or SUs) have the same physical parameters, we provide proof of global exponential convergence of the system state to the set of equilibria where the control objectives are achieved.

Moreover, the proposed control approach is distributed, i.e., each agent exchange relative information with only its neighbors through sparse communication networks. A leader-follower approach is used to ensure the convergence of all the state-of-charge to a common reference available only for one SU which acts as a leader. This gives the possibility for high-level monitoring of the state-of-charge through an energy management strategy. The proposed controllers do not need any information about the parameters of the power lines neither the topology of the microgrid. The control objectives are reached despite the unknown load variation.

In the third part, the proposed distributed controllers are assessed in different scenarios through Matlab/Simulink simulation and real-time Hardware-in-the-Loop implementation tests. The results show that the control objectives are successfully achieved, illustrating the effectiveness of the proposed control methodology.

Keywords: Distributed control, direct current microgrids, current sharing, average voltage regulation, state-of-charge balancing, consensus-like integral actions, real-time hardware-in-the-loop implementation.

Résumé. Au cours des dernières années, le réseau électrique connait une transformation rapide avec la pénétration massive des unités de production renouvelables et distribuées. Le concept de microgrids (micro-réseau électrique) est un élément clés de cette transition énergétique. Ces micro-réseaux sont constitués par un ensemble de plusieurs unités de production distribuées (DGUs), d'unités de stockage (SUs) et de charges interconnectées par des lignes électriques. Un microgrid peut être installé dans plusieurs endroits, par exemple dans des maisons, des hôpitaux, un quartier ou un village, etc. et fonctionne soit en mode connecté au réseau principale, soit en mode isolé (autonome).

Les microgrids sont confrontés à plusieurs défis liés à la garantie de la stabilité, la cybersécurité, l'optimisation des coûts énergétiques, la gestion de l'énergie, la qualité de l'énergie, etc. Dans ce travail, nous concentrons notre attention sur le contrôle des microgrids à courant continu en mode de fonctionnement autonome. La principale contribution de cette thèse est l'établissement de lois de commande par retour d'état distribuées assurant un partage de courant proportionnel entre les unités de production, une régulation de la tension moyenne des lignes et un équilibrage simultané des états de charge des éléments de stockage. La preuve de la convergence exponentielle et globale est donnée en l'absence d'une connaissance de la charge présente sur le réseau. Les principaux outils utilisés sont le consensus dans les systèmes multi-agents, la passivité, la stabilité de Lyapunov, les inégalités matricielles linéaires, etc.

La thèse est divisée en trois parties. La première partie présente le concept des microgrids, un état de l'art sur leurs stratégies de contrôle et les préliminaires mathématiques nécessaires tout au long du manuscrit.

La deuxième partie constitue la contribution théorique de cette thèse et aborde la synthèse de lois de contrôle distribuées, garantissant les objectifs envisagés en l'absence d'une connaissance de la charge variable sur le réseau. Cette garantie est apportée en considérant trois actions intégrales distribuées de type consensus. L'existence de points d'équilibre pour le système augmenté est alors prouvée et une commande distribuée par retour d'état statique est proposée. En partant de l'hypothèse que les agents (DGU ou SU) ont les mêmes paramètres physiques, nous apportons la preuve de la convergence exponentielle globale de l'état du système vers l'ensemble des équilibres où les objectifs de contrôle sont atteints.

De plus, l'approche de contrôle proposée est distribuée, c'est-à-dire que chaque agent n'échange que des informations relatives avec ses voisins par le biais de réseaux de communication. Une approche leader-follower est utilisée pour assurer la convergence de tous les états de charge vers une référence commune. Cela donne la possibilité d'un suivi de haut niveau de l'état de charge grâce à une stratégie de gestion de l'énergie. Les contrôleurs proposés n'ont besoin d'aucune information sur les paramètres des lignes électriques ni sur la topologie du microgrid. Les objectifs de contrôle sont atteints malgré la variation inconnue de la charge.

Dans la troisième partie, les contrôleurs distribués proposés sont évalués dans différents scénarios par le biais de simulation Matlab/Simulink et de tests Hardware-in-the-Loop (HIL) en temps réel. Les résultats montrent que les objectifs de contrôle sont atteints avec succès, ce qui illustre l'efficacité de la méthodologie de contrôle proposée.

Mots clés: Commande distribuée, microgrids à courant continu, partage du courant, régulation de la tension moyenne, équilibrage des états de charge, actions intégral, consensus, implémentation temps-réel hardware-in-the-loop.